Identification and expression analysis of *Phytophthora cinnamomi CRN* effector genes during infection of *Persea americana* (Mill.)

by

Kayla Alexis Midgley

Submitted in partial fulfilment of the requirements for the degree

Magister Scientiae

In the Faculty of Natural & Agricultural Sciences

Department of Biochemistry, Genetics and Microbiology

University of Pretoria

Pretoria

15 November 2023

Supervisor: Dr Velushka Swart

Co-supervisor: Prof. Noëlani van den Berg

UNIVERSITEIT VAN PRETORIA
UNIVERSITY OF PRETORIA
YUNIBESITHI YA PRETORIA

Declaration

I, Kayla Alexis Midgley declare that the dissertation, which I hereby submit for the degree Magister Scientiae in Genetics at the University of Pretoria, is my own work and has not previously been submitted by me for a degree at this or any other tertiary institution.

Kayla Alexis Midgley

15 November 2023

Acknowledgements

I would like to thank each of the following people and organisations that made the completion of this research project possible:

- To my primary supervisor, Dr Velushka Swart, for your guidance and support. Thank you for always being there for me and nurturing me as a young scientist. You have become like family to me, and I greatly appreciate the happy and joyful research environment you created. I would not be where I am without you, and I am eternally grateful to you.
- To Prof Noëlani van den Berg, thank you for your wisdom and your gracious heart. You have built an incredible and world-class research group that I am lucky to be a part of.
- To Dr Robert Backer, thank you for assisting me in all thing's bioinformatics - especially when I was confused and overwhelmed. Thank you for your honesty and being a source of laughter in the lab.
- To the Hans Merensky Foundation for providing the funding that made this project possible.
- To my parents, Ms Keri Midgley and Mr Alex Midgley, thank you for your unwavering support, reminding me to never give up and pushing me to be the best I can be. I hope I have made you both proud.
- To Mr Ross Massey, thank you for being my rock and never letting me down. You have watched my entire academic journey up until this point and have cheered me on every step of the way. Your support and friendship have no limit and you mean the world to me.
- To Miss Kat Baird, thank you for supporting me when experiments fail, for making sure I take lunch breaks, and for knowing when I am having a bad day and doing everything you can to make me smile. I am grateful for your friendship.
- To Mr Grant Davidson, who has stood by me through all the ups and downs of my degree. Thank you for letting me talk off your ear about my research, lifting me up when I was down, and making me believe in myself when I felt I didn't deserve to be where I am. No words could express my gratitude.
- To all my friends and colleagues in the Avocado Research Programme and in the Forestry and Agricultural Biotechnology Institute, thank you for always lending a helping hand and being a home away from home.
- Finally, to my little brothers Aidan and Andre Midgley, I hope I have inspired you to work hard and follow your passion.

Preface

Phytophthora cinnamomi Rands is a soil-borne oomycete plant pathogen of over 5000 species worldwide. *P. cinnamomi* causes Phytophthora Root Rot (PRR) in avocado (*Persea americana* Mill.), a disease which affects the fine feeder roots resulting in dieback and eventual death of the tree. PRR is the most significant yield-limiting disease to avocado worldwide and poses a challenge to the South African avocado industry. Despite the economic importance of *P. cinnamomi*, our understanding of the molecular mechanisms *P. cinnamomi* utilises to infect and cause disease in susceptible host plants is limited. Of particular interest is the molecular pathways of host programmed cell death (PCD) during *P. cinnamomi* infection. There is a complex relationship between the induction and suppression of cell death in host plants during *P. cinnamomi* infection which could either benefit the host plant or the pathogen. Numerous effectors in other *Phytophthora* species have been implicated in the manipulation of cell death during infection, of which crinkling and necrosis (CRNs) effectors have been associated with different roles in host plant cell death. Published research on *P. cinnamomi* effectors however remains lacking; the environmental and economic importance of this pathogen however necessitates a better understanding of the role that effectors play in the successful infection and colonisation of its plant host, particular in agricultural crops such as avocado.

Chapter 1 of this thesis presents a review of literature on *Phytophthora* effectors and host plant PCD, which was published in Microorganisms (https://doi.org/10.3390/microorganisms10061139). First, the current knowledge on host plant PCD is assessed. Subsequently the role of PCD in *Phytophthora* virulence is evaluated, and the function of various *Phytophthora* effectors in cell death is reviewed. Finally, the current techniques used to functionally characterise *Phytophthora* effectors are discussed.

Chapter 2 reports on the identification of CRN effector proteins from the *P. cinnamomi* transcriptome during infection of avocado, submitted for publication in BMC Genomics. Candidate *P. cinnamomi CRNs* were identified as potential cell death manipulators based on their expression profiles during infection of both a susceptible and partially resistant avocado rootstock using RNA sequence data. The genes encoding the candidate CRNs were sequenced, and the resultant protein sequences were subjected to phylogenetic analyses and protein architecture predictions. Putative functions in cell death manipulation were assigned based on expression data, phylogenetic relatedness to other functionally characterised *Phytophthora* CRNs, domain analyses and the predicted folding of the tertiary proteins.

Summary

Phytophthora cinnamomi is a hemi-biotrophic plant pathogen impacting the South African avocado industry. Like other *Phytophthora* spp., this pathogen employs a repertoire of effectors to suppress host defence mechanisms and facilitate successful infection in host plants. Because *P. cinnamomi* is a hemi-biotroph, the pathogen would benefit from the suppression of cell death during the biotrophic phase early in infection and the subsequent induction of cell death later in infection when the pathogen switches to a necrotrophic phase. *P. cinnamomi* achieves this beneficial pattern of cell death through the differential expression and delivery of effectors at different stages of infection. Multiple effectors have been shown to play a role in host cell death manipulation in *Phytophthora*, but CRNs are of ongoing interest due to their ability to both supress and induce cell death during infection.

The research in this thesis is a continuation of honours research conducted by me in 2020, where a pipeline was created to identify and validate *P. cinnamomi* CRN (PcinCRN) effector protein sequences from the *P. cinnamomi* GKB4 transcriptome. In the work conducted for this MSc degree, *P. cinnamomi CRN* expression profiles were analysed using dual RNA-seq data from *P. cinnamomi*-infected avocado rootstocks. Candidate *CRNs* were selected based on their expression profile and their coding sequences were confirmed via cloning and Sanger sequencing. Amino acid sequences of CRN candidates and their variants were extracted and compared to other *Phytophthora* CRN sequences that have been functionally characterised as cell death inducers or suppressors during infection of host plant species. Tertiary protein structures for each CRN were predicted and their domains were assessed. Putative functions in cell death manipulation during infection of avocado were assigned to *P. cinnamomi* CRNs based on expression profiles, relatedness to other *Phytophthora* CRNs, domain analyses and protein folding predictions.

From a list of 25 full-length *P. cinnamomi* CRNs, 13 *CRN* genes demonstrated expression profiles corresponding to a potential role in cell death manipulation during infection of avocado. The coding sequences of 10 candidate *CRNs* were confirmed, of which six were found to have two alleles. Additionally, one was found to have the potential to undergo alternative splicing. PcinCRN52 was molecular characterised as a cell death inducer during late infection and PcinCRN30, PcinCRN77, PcinCRN81 and PcinCRN86 were molecularly characterised as cell death suppressors during early infection. PcinCRN11, PcinCRN53, PcinCRN73, PcinCRN75 and PcinCRN95 were found to have variants that potentially play contradicting roles in cell death or where one variant may function in a different host plant species.

The findings from this study suggest that *P. cinnamomi* CRNs may function by regulating each other, to either suppress or induce cell death at appropriate stages to promote successful colonisation of avocado. This study highlights the complex and dynamic interactions between CRN effectors and their potential impact on the outcome of *P. cinnamomi* infection of the host plant.

List of abbreviations

SAR - Systemic acquired resistance

dPCD - Developmentally controlled PCD

pPCD - Pathogen-triggered PCD

TF - Transcription factor

ERF - Ethylene-responsive element-binding factor

CSD1 - Copper Zinc Superoxide Dismutase 1

SA - Salicylic acid

ET - Ethylene

JA - Jasmonic acid

PSE1 - Penetration-specific effector 1

ROS - Reactive oxygen species

SI - Self- incompatibility

NO - Nitric oxide

NLP - Nep1-like proteins

PL - Pectate lyase

GH - Glycoside hydrolase

MAMPs - Microbe-associated molecular patterns

MAPKs - Mitogen-activated protein kinases

NPP1 - Necrosis-inducing Phytophthora protein 1

cNLPs - Cytolytic Nep1-like proteins

ncNLPs - Noncytolytic Nep1-like proteins

EST - Expressed sequence tag

HR - Hypersensitive Response

PCD - Programmed Cell Death

PRR - Phytophthora root rot

CRN - Crinkling and necrosis effector (Crinkler)

PsCRN – *Phytophthora sojae* CRN

PcinCRN – *Phytophthora cinnamomi* CRN

PpCRN – *Phytophthora parasitica* CRN

PcCRN – *Phytophthora capsici* CRN

PiCRN – *Phytophthora infestans* CRN

PmCRN – *Phytophthora megakarya* CRN

PuCRN - *Pythium ultimum CRN*

HMM - Hidden Markov Model

RNA-seq - RNA-sequencing

LCR - Low complexity regions

Ubl - Ubiquitin-like domain

P-loop - Phosphate-loop

REase - Restriction endonuclease

NTPase - Nucleoside-triphosphatase

HTH - Helix-turn-helix domain

TMH – Transmembrane helix

SNP – Single nucleotide polymorphism

INDEL - Insertion or deletion

NLS – Nuclear localisation signal

PAMP - Pathogen associated molecular pattern

PTI - PAMP triggered immune response

ETI - Effector triggered immune response

HSP – Heat shock proteins

HSE – Heat shock elements

hpi – hours post-inoculation

Table of Contents

Chapter 1

Unraveling plant cell death during *Phytophthora* infection

Published in Microorganisms

https://doi.org/10.3390/microorganisms10061139

31st May 2022

microorganisms

MDPI

Review

Unraveling Plant Cell Death during *Phytophthora* Infection

Kayla A. Midgley, Noëlani van den Berg and Velushka Swart *

Department of Biochemistry, Genetics and Microbiology, Hans Merensky Chair in Avocado Research, Forestry and Agricultural Biotechnology Institute, University of Pretoria, Pretoria 0002, South Africa; kayla.midgley@fabi.up.ac.za (K.A.M.); noelani.vdberg@fabi.up.ac.za (N.v.d.B.)
* Correspondence: velushka.swart@fabi.up.ac.za

Abstract: Oomycetes form a distinct phylogenetic lineage of fungus-like eukaryotic microorganisms, of which several hundred organisms are considered among the most devastating plant pathogens—especially members of the genus *Phytophthora*. *Phytophthora* spp. have a large repertoire of effectors that aid in eliciting a susceptible response in host plants. What is of increasing interest is the involvement of *Phytophthora* effectors in regulating programed cell death (PCD)—in particular, the hypersensitive response. There have been numerous functional characterization studies, which demonstrate *Phytophthora* effectors either inducing or suppressing host cell death, which may play a crucial role in *Phytophthora's* ability to regulate their hemi-biotrophic lifestyle. Despite several advances in techniques used to identify and characterize *Phytophthora* effectors, knowledge is still lacking for some important species, including *Phytophthora cinnamomi*. This review discusses what the term PCD means and the gap in knowledge between pathogenic and developmental forms of PCD in plants. We also discuss the role cell death plays in the virulence of *Phytophthora* spp. and the effectors that have so far been identified as playing a role in cell death manipulation. Finally, we touch on the different techniques available to study effector functions, such as cell death induction/suppression.

Keywords: plant pathology; necrosis; hemi-biotroph; agroinfiltration; CRN

Citation: Midgley, K.A.; van den Berg, N.; Swart, V. Unraveling Plant Cell Death during *Phytophthora* Infection. *Microorganisms* **2022**, *10*, 1139. https://doi.org/10.3390/microorganisms10061139

Academic Editors: Teresa Lino-Neto and Paula Baptista

Received: 4 April 2022
Accepted: 30 May 2022
Published: 31 May 2022

1. Introduction

Pathogens within the oomycete genus *Phytophthora* are among some of the most destructive plant pathogens globally, causing disease and significant losses in important agricultural and forestry crops, damaging the environment, as well as impeding attempts to mitigate climate change [1–4]. One of the more well-known incidences of *Phytophthora* disease is the Irish Potato Famine in 1845. This incident was caused by *Phytophthora infestans*—the causal agent of late blight of potatoes. The disease resulted in the death of half of the potato crop that year and about three-quarters of the crop over the next seven years [3,5]. Other *Phytophthora* spp., which cause significant impact worldwide, include the causal agents of sudden oak death in California (*Phytophthora ramorum*), stem rot of soybean (*Phytophthora sojae*), black shank of tobacco *Phytophthora nicotianae*), phytophthora root rot of avocado and jarrah dieback of trees in the Jarrah Forest, both caused by *Phytophthora cinnamomi* [3,6,7]. Despite the economic and ecological relevance of *P. cinnamomi*, the mechanisms this pathogen utilizes to infect and successfully colonize its hosts are still largely unknown. *P. cinnamomi* is known to infect plants that are important for agriculture and forestry, with the most significant food losses occurring in avocados. There is little to no knowledge on how *P. cinnamomi,* a hemi-biotrophic pathogen, maintains a biotrophic lifestyle early in the infection and a necrotrophic lifestyle later in the infection.

Pathogenic lifestyles are centered around feeding on host tissue, where success is dependent on the pathogen's ability to overcome host defenses. One host defense strategy *Phytophthora* spp. must evade to sustain their biotrophic phase is the hypersensitive response (HR). The HR is a form of programed cell death (PCD) and is generally the last resort in a host plant's defense response against a pathogen. The response involves the

localized death of cells surrounding the initial site of infection to inhibit the spread of the pathogen. Later in the infection, the HR is favored during the necrotrophic phase. Studies have shown that *Phytophthora* spp. manipulate the host plant's cell death machinery to elicit a susceptible outcome [8,9].

Phytophthora spp. harbor a distinct set of genes involved in moderating host–pathogen interactions [10]. These genes encode effectors—small, secreted proteins—that interfere with host defense processes. There are two groups of effectors, cytoplasmic and apoplastic effectors, which are classified by where in the host cell they act. The most well-studied classes of *Phytophthora* cytoplasmic effectors are Crinklers (CRNs) and RxLRs (Arg-x-Leu-Arg, where x is any amino acid) [4]. Research into *Phytophthora* effectors has greatly expanded due to the availability of genomic and transcriptomic data, allowing for the prediction of putative effector homologs in *Phytophthora* spp. [11]. These valuable tools—followed by functional characterization techniques, such as transient transformation in model plants—allow for the identification of effectors that may play crucial roles during infection. However, little genomic research has been conducted on *P. cinnamomi*, which leaves a gap in knowledge on the mechanisms employed by this pathogen to successfully infect and cause disease in economically and ecologically important plants.

Due to their economic impact, *Phytophthora* spp. are some of the most studied among oomycetes [4,12]. There is, however, still limited knowledge on the mechanisms utilized to regulate cell death in host plants. It is likely these processes are determined by the delivery of functionally distinct pathogen effectors into the host cell [13]. In this review, the role of *Phytophthora* effectors in host cell death induction and suppression is discussed by reporting on forms of cell death, recent studies of *Phytophthora* effectors involved in host cell death and technological advances, which have aided in the identification and characterization of effectors.

2. Programed Cell Death in Host Plants

Plants are immobile organisms and have had to develop morphological, biochemical and physiological adaptations to survive in their environment. PCD is an important mechanism for plant development or defense and can be triggered by both abiotic and biotic stressors [9,14,15]. PCD is described as a genetically controlled process where selected cells are eliminated through a coordinated multi-step fashion [15]. This phenomenon is of considerable importance in agriculture because PCD can significantly affect plant health and subsequent yield [16,17]. Therefore, it is important to understand both the triggers and the pathways through which PCD is elucidated.

2.1. Classification of PCD

There has been some confusion regarding how different forms of PCD should be classified and how terminology should be standardized. Cell death is classified based on the morphological characteristics and, as a result, two major classes of PCD are proposed to occur in plant biology [14]. Class one is vacuolar cell death, which involves the engulfment of the cytoplasm by lytic vacuoles, uptake and degradation of portions of the cytoplasm in the vacuolar lumen and, finally, rupture of the tonoplast followed by a massive release of vacuolar hydrolases. This results in the rapid destruction of the entire protoplast—a cell whose cell wall has been removed by enzymes—or, in some cases, even the entire cell, including the cell wall (Figure 1A). Class two is necrotic cell death, which is distinguished from vacuolar cell death by mitochondrial swelling, absence of the growing lytic vacuoles and early rupture of the plasma membrane, resulting in shrinkage of the protoplast (Figure 1B). Necrosis is regarded as an acute death response, which develops rapidly, taking anywhere from several minutes to a day to complete [14]. The use of morphology to classify PCD has allowed a better understanding of how cell death manifests. Although one limitation in this is that a well-known form of PCD, known as the HR, cannot be ascribed to either class, as its development displays characteristics of both vacuolar and necrotic cell death [14,18–20].

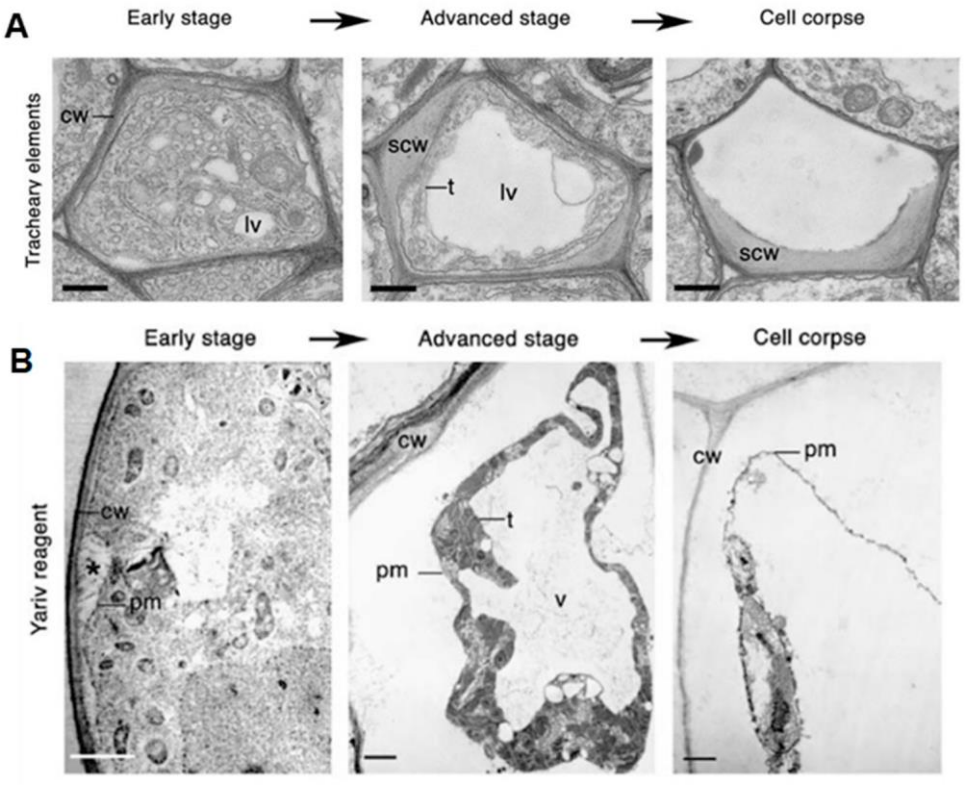

Figure 1. Classes of cell death. (**A**) Vacuolar cell death. Electron micrographs of programed cell death (PCD) in *Arabidopsis* tracheary elements. cw, cell wall; lv, lytic vacuole; n, nucleus; scw, secondary cell wall; t, tonoplast. Scale bars, 500 nm (tracheary elements). Manifests by a gradual decrease in cytoplasm volume and an increase in lytic vacuole volume. (**B**) Necrotic cell death. Electron micrographs of Yariv-reagent-induced death in the *Arabidopsis* cell culture. Asterisks denote the detachment of plasma membrane form the cell wall during early stages of cell death. c, chloroplast; cw, cell wall; pm, plasma membrane; t, tonoplast; v, vacuole. Scale bars, 2 µm. There is an absence of a growing lytic vacuole, and there is early rupture of the plasma membrane, which results in shrinkage of the protoplast. Pictures of *Arabidopsis* treachery elements were republished with authors' permission from Avci, U.; Petzold, E.; Ismail, I.O.; Beers, E.P.; Haigler, C.H. Cysteine proteases XCP1 and XCP2 aid micro-autolysis within the intact central vacuole during xylogenesis in *Arabidopsis* roots. Plant J. 2008, 56, 303–315, https://doi.org/10.1111/j.1365-313X.2008.03592.x [21] and those of the Yariv-reagent-induced cell death were republished with authors' permission from Gao, M.; Showalter, A.M.; Yariv reagent treatment induces PCD in *Arabidopsis* cell cultures and implicates arabinogalactan protein involvement. Plant J. 1999, 19, 321–331, https://doi.org/10.1046/j.1365-313X.1999.00544.x [22].

The HR is a special form of PCD, involving rapid localized cell death at the point of pathogen penetration [16,23]. The host plant utilizes HR to limit biotrophic pathogen growth and generates long-range signals for systemic acquired resistance (SAR) [24]. Thus, another PCD classification system was developed to accommodate the placement of the HR. This system classifies forms of PCD based on what functions they play in the host plant, rather than by their morphology or pathways. Two classes were described: developmentally controlled PCD (dPCD) and pathogen-triggered PCD (pPCD). During vegetative and reproductive development, dPCD occurs and is often a final differentiation step for specific cell types [25]. Conversely, pPCD is elicited in the host plant by invading agents and can benefit either the plant or pathogen, depending on the studied plant–pathogen interaction [26]. An additional class has also been proposed to describe PCD resulting from environmental stress, termed ePCD [25]. The ePCD classification includes stresses, such as temperature or irradiation, or biotic aggressors, such as pathogens [15]. pPCD

is specific to pathogen-triggered cell death, whereas ePCD includes all external stressors as PCD triggers. The use of ePCD as a classification may, however, be problematic, since different PCD pathways may be in play during both abiotic and biotic-triggered PCD.

2.2. Programed Cell Death in Host Plants

Plant PCD pathways are not as well understood as animal cell death. Animals have a core PCD machinery that is mainly regulated post-translationally [17,27], whereas it is not known whether the different forms of plant PCD share the same core machinery or whether the similarities they share were independently adopted to fulfill analogous roles for different pathways [9]. When looking at the two main plant PCD forms—dPCD and pPCD—there are marked differences as well as commonalities in their proposed pathways. For one, a vacuolar type of cell death is associated with dPCD, and features of both necrosis and vacuolar PCD are seen in pPCD [9]. There is also evidence of transcriptional regulation and signaling in both forms of plant PCD, but in different contexts. Unfortunately, there are still gaps in our knowledge regarding pPCD. This is largely due to predominance of previous dPCD-centered investigations. In addition, variability has been seen in pPCD responses to a multitude of different abiotic and biotic factors, whereas dPCD is a relatively conserved process across all plant species. This section serves to summarize our current knowledge on the transcriptional regulation, hormonal signaling and triggers involved in pPCD.

2.2.1. Transcriptional Regulation of pPCD

The stimulation and repression of cell death pathways by transcription regulators has been seen in animal PCD [28,29], and recent evidence indicates that some level of transcriptional control of PCD is also likely in plants [30–34]. Different classes of transcription factors (TFs), including members of NAC, ethylene-responsive element-binding factors (ERFs) and WRKY families, have been shown to play roles in cell fate regulation in response to different stresses. NAC TFs have been linked to the regulation of PCD triggered by both abiotic and biotic stresses [34]. One example is that of OsNAC4, which has been shown to be a key positive regulator of the HR by modulating the expression of almost 150 genes in rice, such as Copper Zinc Superoxide Dismutase 1 (*CSD1*) gene and BAX Inhibitor 1(*BI-1*) gene [35]. ERF TFs also play a role in the regulation of the HR, where the conditional expression of NbCD1—from *Nicotiana benthamiana*—in response to multiple HR elicitors is sufficient to induce the HR [30]. Numerous WRKY TFs are involved in the regulation of cell death, and they may play a role in the suppression of the HR during initial infection of the necrotrophic fungus, *Botrytis cinerea*, in *Arabidopsis* [36], through the activation or suppression of antagonistic signaling pathways, such as salicylic acid (SA), ethylene (ET) and jasmonic acid (JA) mediated pathways. Although there is a large body of research onTFs and their role in pPCD, there is still a lack of knowledge on *Phytophthora* pathogens and the involvement of TFs in eliciting or suppressing PCD during *Phytophthora* infection.

2.2.2. Phytohormone Signaling Pathways Involved in pPCD

Different phytohormones play a role in dPCD, such as JA, auxin, strigolactones and ET—ET being the most characterized dPCD hormone [37–39]. Phytohormones control the dPCD processes via transcriptional regulation of genes, such as proteases and nu- cleases, to gradually build up dPCD competence during cellular differentiation. This contrasts with pPCD, where no preparation is required, and the cells are always ready to initiate an immune response upon pathogen attack [9]. The infection strategy of a plant pathogen—whether the pathogen adopts a biotrophic, necrotrophic or hemi-biotrophic lifestyle—determines the underlying mechanism for phytohormone-regulated pPCD in the host during plant–pathogen interactions [40,41]. It has been shown that SA plays an essen- tial role in host defense response against biotrophic and the early stages of hemi-biotrophic pathogens, whereas JA and ET play an important role in the host defense response against necrotrophic and the later stages of hemi-biotrophic pathogens [41]. SA is the only phyto-

hormone shown to play an essential role in the establishment of pPCD, allowing immunity toward biotrophic pathogens and susceptibility to necrotrophic pathogens. [42,43]. It has been found that some pathogens interfere with cellular SA biosynthesis or signaling through the delivery of effector proteins. [26]. For example, penetration-specific effector 1 (PSE1) from *Phytophthora parasitica* inhibits SA-mediated cell death and increased pathogen growth by promoting auxin accumulation at infection sites [44]. Due to the importance of phytohormones in the different trophic interactions, it would be of value to investigate their roles in the maintenance and switch from the biotrophic to necrotrophic stage in hemi-biotrophic pathogens, such as *Phytophthora*. This will shed light on how *Phytophthora* is able to successfully infect a host plant and avoid the hosts' defense responses.

2.2.3. Triggers of pPCD

dPCD requires preparation before PCD can be triggered/executed. Several cytoplasmic signals are implicated in dPCD triggering, such as calcium fluxes, accumulation of reactive oxygen species (ROS) and cytoplasmic acidification [45]. During the self-incompatibility (SI) response—the inability of a plant with functional pollen to set seeds when self-pollinated—in *Papaver rhoeas*, calcium influx triggers a signaling cascade, which results in rapid PCD of the incompatible pollen tubes [46]. In contrast, pPCD requires no preparation and is only triggered upon pathogen attack. The main pPCD trigger is cytoplasmic immune receptor-mediated recognition at the site of attack [47]. Calcium influxes, as well as accumulation of SA, ROS and nitric oxides (NO), are triggered upon pathogen perception during pPCD. SA signaling subsequently amplifies the ROS burst in a positive feedback loop, creating a toxic environment [48]. Some necrotrophic pathogens have been known to 'hijack' PCD machinery, where pathogens, such as *Cochliobolus victoriae,* secrete PCD triggering toxins [49,50]. Common triggers that are recognized by host receptors are effectors. Different *Phytophthora* effectors and their role in host PCD will be discussed in a later section.

3. Cell Death and *Phytophthora* Virulence

Different forms of pPCD will benefit either the plant or pathogen, depending on the type of plant–pathogen interaction and the trophic lifestyle of the pathogen [4,9,25]. Most *Phytophthora* spp. are hemi-biotrophic pathogens, meaning they feature a biotrophic life stage during early infection followed by a switch to necrotrophy during the later stages of host tissue colonization [4,51]. As the HR is generally considered most effective against biotrophic pathogens, while potentially benefiting necrotrophic pathogens, hemi-biotrophic pathogens—such as *Phytophthora*—are at a distinct advantage [52,53]. This response is a race between the host and pathogen, where the pathogen attempts to tip the balance toward suppression of host defense, and the host tries to launch an effective defense response to prevent infection [4].

Phytophthora spp. may have developed a strategy to 'hijack' a plant's HR machinery, suppressing the HR during the biotrophic stage and inducing it during the necrotrophic stage [24,54,55]. This 'hijack' strategy is further supported by the production of haustoria that deliver defense-controlling pathogenicity factors and effectors, which function in keeping the host cell alive [56,57]. Conversely, the switch to necrotrophy, which involves the upregulation of specialized effector genes—such as Nep1-like proteins (NLPs)—aims to deliberately kill the host cell [58]. This is further supported by the similarities in metabolic enzyme expression between *P. infestans* during the necrotrophic stage and the necrotrophic pathogen *Pythium ultimum* [59]. This strategy increases the virulence of *Phytophthora* spp. through the differential expression and delivery of effectors at different stages of host plant infection and colonization [13,54,55,60–62].

4. *Phytophthora* Effectors That Induce or Suppress Cell Death

Phytophthora has a large repertoire of effector proteins that serve different functions during infection. These effectors produce metabolic or structural changes in host cells, aiding in the growth of the pathogen and disease development [63]. Effectors can be divided into two main groups, namely apoplastic and cytoplastic effectors. Cytoplastic effectors are translocated to the cell cytoplasm where they interact with host targets. Apoplastic effectors are secreted into the extracellular space between cells and interact with targets within the extracellular space, as well as on the host cell surface [4,57,63,64].

Cell death plays an important role in plant–pathogen interactions, which has driven a long-standing interest in the characterization of effectors that are able to induce/suppress plant cell death [65]. Genomic resources and methods for characterizing effector functions have allowed for a better understanding of their evolution and role in disease progression. Our understanding of the effector repertoire and their roles in infection in *Phytophthora* spp. with a broad host range, such as *P. cinnamomi*, remains limited [66].

4.1. Apoplastic Effectors

Apoplastic effectors are known to act on host targets outside of the host plant cells or on plant cell surface receptors. There has been significant progress in the identification of apoplastic effectors, which induce cell death in host plants. To date, 61 cell-death-inducing apoplastic proteins have been identified in 15 *Phytophthora* spp. (Table 1). A number of these proteins belong to the pectate lyase (PL), glycoside hydrolase (GH) and PcF toxin families. The majority of the apoplastic effectors identified are, however, elicitins and Nep1-like protein (NLPs), which will be discussed in further detail below.

Table 1. Apoplastic cell-death-inducing proteins identified in *Phytophthora* spp.

Protein Family	Plant Cell Surface Receptor	Co-Receptor	Protein	*Phytophthora* spp.	Function	References
ND	-	-	PB90	*Phytophthora boehmeriae*	Induces cell death	[67–69]
Elicitin	ELR		Cacto	*Phytophthora cactorum*	Induces cell death	[70]
			PcELL1		Induces cell death	[71]
			PcINF1		Induces cell death	[72]
		BAK1, HSP70, HSP90, NbLRK1, SGT1, SRC2-1	Capsicein	*Phytophthora capsici*	Induces cell death and increases defense against *P. nicotianae* in *Nicotiana benthamiana*	[73]
			PcINF1		Induces cell death and pepper defense response	[74,75]
			Cinnamomin	*Phytophthora cinnamomi*	Induces cell death and protects *N. benthamiana* against pathogens	[76,77]
			15-kDa glycoprotein	*Phytophthora colocasiae*	Induces cell death and SAR	[78]
			Cryptogein	*Phytophthora cryptogea*	Induces cell death, SAR and defense of *N. benthamiana* against *P. nicotianae*	[73,79–85]

Table 1. *Cont.*

Protein Family	Plant Cell Surface Receptor	Co-Receptor	Protein	*Phytophthora* spp.	Function	References
			Dreα, Dreβ	*Phytophthora drechsleri*	Induces cell death	[86]
			Hibernalin1	*Phytophthora hibernalis*	Induces cell death	[87]
			INF1	*Phytophthora infestans*	Triggers HR dependent on HSP70, HSP90 and SGT1	[88–93]
			INF2A, INF2B		INF2A-induced necrosis dependent on SGT1	[92]
			MgMα, MgMβ	*Phytophthora megasperma*	Induces cell death	[94]
			α-megaspermin, β-megaspermin, γ-megaspermin/32 kDa glycoprotein		Induces cell death, PR gene expression and SAR	[95,96]
			Palmivorein	*Phytophthora palmivora*	Induces cell death	[97]
			Parasiticein/ parA1/elicitin 310/elicitin 172	*Phytophthora parasitica*	Induces cell death	[98–101]
			Syringicin	*Phytophthora syringae*	Induces HR and electrolyte leakage in *N. benthamiana*	[102]
NLP	RLP23	BAK1, COI1, HSP90, MEK2, NPR1, SGT1, SOBIR1 and TGA2.2	PcNLP1	*P. cactorum*	Induces cell death	[71]
			Pc11951, Pc107869, Pc109174, Pc118548	*P. capsici*	Induces cell death	[103]
			PcNLP1 to 3, 6 to 10, 13 to 15		Induces cell death	[104]
			PiNPP1.1	*P. infestans*	Induces HR dependent on SGT1 and HSP90	[105]
			PpNLP/NLPPp	*P. parasitica*	Induces cell death	[106–110]
			PsojNIP	*Phytophthora sojae*	Induces cell death dependent on SGT1 and HSP90	[105,111]
			PaNie213/ NLPPya	*Phytophthora aphanidermatum*	Induces cell death	[107,108, 112]
CBM	-	-	CBEL	*P. parasitica*	Induces cell death; activates defense responses via SA, JA and ET signaling pathways	[113,114]

Table 1. *Cont.*

Protein Family	Plant Cell Surface Receptor	Co-Receptor	Protein	*Phytophthora* spp.	Function	References
PL	-	-	PcPL1, PcPL15, PcPL16, PcPL20	*P. capsici*	Induces cell death	[115]
GH12	RXEG1	BAK1, SOBIR1	XEG1	*P. sojae*	Induces cell death; associates with SOBIR1 and BAK1 complex to trigger immune responses	[116,117]
GH16	-	-	OPEL	*P. parasitica*	Induces cell death	[118]
PcF toxin	-	-	PcF	*P. cactorum*	Induces cell death and PR gene expression in *N. benthamiana*	[119]
			SCR96, SCR99, SCR121		Induces cell death	[120]
			SCR113		Induces cell death	[72]

ND, not determined; NLP, Nep1-like protein; pectate lyase (PL); CBM, carbohydrate binding module; GH, glycoside hydrolase; SAR, systemic acquired resistance.

4.1.1. Elicitins

Elicitins are a conserved class of apoplastic proteins produced by oomycetes—in particular *Phytophthora* and some *Pythium* spp. [121,122]. Elicitins are involved in binding to sterols, which is believed to serve an essential role in *Phytophthora* development and pathogenicity [123,124]. The majority of elicitins possess a signal peptide, a highly conserved 98-amino-acid domain (Pfam PF00964), and a C-terminal domain of variable length (17–291), which is usually rich in threonine, serine and proline residues (Figure 2) [122,125]. Elicitins may elicit a cell death response by their recognition as microbe-associated molecular patterns (MAMPs), resulting in triggering the HR rather than a specific necrotizing activity of the protein itself [126,127].

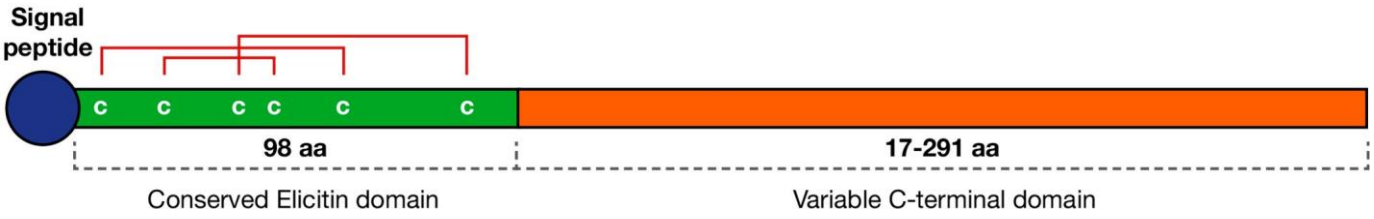

Figure 2. Structure of a *Phytophthora* elicitin. The conserved elicitin domain generally consists of 98 amino acids and contains 6 cysteine residues at conserved positions that form three disulphide bridges. The variable C-terminal tends to be rich in threonine, serine and proline residues.

It was originally believed that elicitins induced cell death via the disruption of plasma membrane integrity upon sterol binding, but *Phytophthora* mutants producing elicitins unable to bind to plant sterols still elicited cell death responses [123,128]. Studies have shown that the elicitin-induced HR involves a ROS burst. It has been proposed that mitogen-activated protein kinases (MAPKs) phosphorylate WRKY7/8/9/11 TFs, resulting in a sustained ROS burst that leads to cell death upon elicitin perception [129]. Oomycete plant pathogens, such as *Phytophthora,* are believed to have evolved an effector toolbox to modulate host responses triggered by their elicitins [126]. This is evident when considering Avr3a-KI from *P. infestans,* which suppresses the HR triggered by INF1 [130]. Additional screens have also revealed that over 30 effectors from different oomycete species suppress INF1-triggered responses [126].

4.1.2. Nep1-like Protein (NLPs)

NLPs are apoplastic effector proteins, which contain an N-terminal secretion signal peptide and a common necrosis-inducing *Phytophthora* protein 1 (NPP1) domain (Figure 3) [65]. This family of effector proteins has been found in bacteria, fungi and oomycete plant pathogens—with the genus *Phytophthora* possessing the largest NLP gene family, which is highly conserved among species [58,65,131]. NLP effectors have been shown to induce cell death and elicit strong immune responses in dicotyledonous plants [65,111,132]. NLPs can be separated into two functional classes: cytolytic (cNLPs) and noncytolytic (ncNLPs), where the specific activity of cNLPs is to cause cell death [133–136].

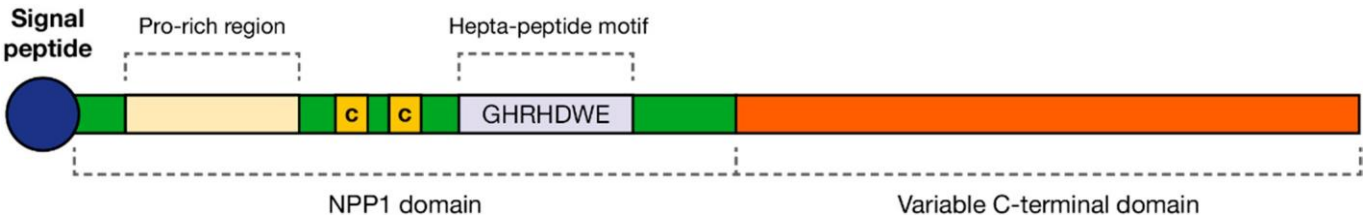

Figure 3. Structure of *Phytophthora* cNLPs. A signal peptide is present followed by a necrosis-inducing *Phytophthora* protein 1 (NPP1) domain containing a 30–45 proline rich region and a Hepta-peptide GHRHDWE motif at around 110–130 aa. In cNLPs, there are two conserved cysteines present between the Pro-rich region and Hepta-peptide motif—ncNLPs have four conserved cysteines in this region.

It has been suggested that cNLPs may play an important role in the transition of *Phytophthora* spp. from the biotrophic to necrotrophic phase [58]. This is evident by the increase in expression of *PsojNIP* and *PiNPP1*—from *P. sojae* and *P. infestans*, respectively—during the infection stages, coinciding with the transition from biotrophy to necrotrophy [105,111]. Further evidence of this role is seen in *P. capsici*, where *NLP2*, *NLP6* and *NLP14* contribute greatly to the induction of necrosis during infection—like that of *PsojNIP* [137]. Contrastingly, there have been studies reporting that ncNLP genes from *P. infestans*, *P. megakarya*, *P. capsici* and *P. cactorum* were expressed during developmental stages and the early biotrophic infection phase [71,131,137,138]. This may suggest that NLPs play additional roles in virulence, but the exact functions have yet to be resolved [4].

A *P. cinnamomi NPP1* has been reported in a study where the authors investigated the expression of the gene using RT-qPCR, both in vitro, using different carbon sources, and in vivo, during infection of *Castanea sativa* roots [139]. A decrease in *NPP1* expression was noted between 12 and 24 h post-inoculation (hpi) with a significant increase at 36 hpi, suggesting a complex host–pathogen interaction. Although this study shed light on the function of this effector during *P. cinnamomi* infection, further research is required to fully understand the mechanisms underlying the defense mechanisms against *P. cinnamomi* necrosis-inducing proteins.

4.2. Cytoplasmic Effectors

4.2.1. RxLRs

Phytophthora RxLRs are cytoplasmic effectors with a modular architecture, including an N-terminal signal peptide for protein secretion, a conserved RxLR motif to facilitate translocation into host cells and a diverse C-terminal domain executing virulence activity (Figure 4) [64,140–142]. The RxLR effector family is the largest class of translocated effectors and is specific to *Phytophthora* spp., with there being 560, 370, 390 and 238 RxLR-containing protein coding genes in the genomes of *P. infestans*, *P. ramorum*, *P. sojae* and *P. cinnamomi*, respectively [12,64,143]. These effectors localize to many subcellular organelles and structures, where they target a wide range of pathways throughout the plant cell [4,144]. A key role of RxLRs is the suppression of PAMP-triggered immunity (PTI) and effector-triggered immunity (ETI), where multiple *Phytophthora* RxLRs from different species have been reported to suppress plant cell death triggered by elicitins or other effectors [130,141,145,146].

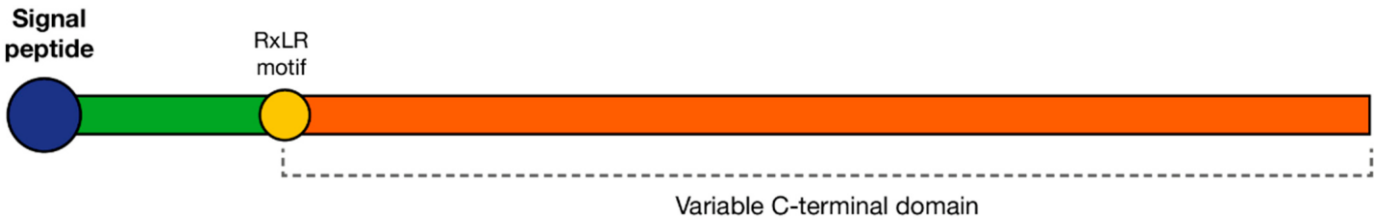

Figure 4. *Phytophthora* RxLR effector structure. Illustration of the characteristic features of *Phytophthora* RxLRs. These effectors have a signal peptide followed by a conserved RxLR (Arg-x-Leu-Arg) motif and a variable C-terminal.

RxLR effector PsAvh238 from *P. sojae* was found to either induce cell death *in planta* or suppress elicitin-induced plant cell death, depending on the different regions of Avh238 and distinct subcellular localizations [145]. The N-terminal of PsAvh238 and nuclear localization are critical to induce cell death, while the C-terminal and cytoplasmic localization are sufficient for INF1-induced cell death suppression. This illustrates how different localization can convey different RxLR functions. Interestingly, it has also been found that some RxLR effectors may alter the localization of host targets [4,146]. Another example is *P. sojae* RxLR (PsAvh52), which suppresses cell death and defense mechanisms in the early stages of infection by 'hijacking' a transacetylase enzyme (GmTAP1) [146]. PsAvh52 relocates GmTAP1 to the cell nucleus where it chemically modifies the host DNA's packaging, resulting in the activation of nearby susceptibility genes, suppressing the host plant's defense system.

Some *Phytophthora* RxLRs may also contribute to the establishment of the pathogen's necrotrophic life stage. This is seen in *P. capsici* RxLR effector PcAvh1, which triggers cell death when expressed in *N. benthamiana*, tomato and bell pepper leaves. This effector is rapidly induced during early infection stages and then exhibits a decline in expression through 3 to 24 hpi but is upregulated again at 36 and 72 hpi [147]. It has previously been proposed that *P. capsici* switches from the biotrophic to necrotrophic lifestyle sometime between 18 and 42 hpi, suggesting that PcAvh1 may help facilitate this switch. PcAvh1 may still play a role during initial infection during the biotrophic stage, but other effectors may inhibit its necrotic activity during early infection.

There have not been any functional characterization studies performed on suspected *P. cinnamomi* RxLRs. There has, however, been a study reporting to have identified and characterized the *Avr3a* gene from online genomic *P. cinnamomi* sequences by using in silico approaches alone [148]. The authors report that the gene encodes a recognized 209 amino acid protein in the host cytoplasm, where it triggers cell death. However, it should be noted that in silico analysis is not sufficient to definitively assign the function of an effector. It can be used to identify putative effectors; in vivo functional characterization is still required to confirm in silico inferences. Therefore, further in vivo techniques, such as transient transformation via *Agrobacterium,* should be used to confirm this study's findings.

4.2.2. Crinklers

CRNs are modular proteins that were first identified in *P. infestans* and classified as genes causing crinkling and necrosis [149]. These effector proteins possess a conserved N-terminal containing an LXFLAK, HVLVXXP and DWL motif, which functions in translo- cation of the CRN proteins from the apoplast into the plant cytoplasm (Figure 5) [150,151]. This is followed by a variable C-terminal, which conveys different functions, including subcellular localization required for the effector function [8,54,60,152]. *Phytophthora* spp. examined thus far have large multigene families of CRN genes, with 196 in *P. infestans*, 100 in *P. sojae* and 49 in both *P. ramorum* and *P. cinnamomi* [11,130]. Unlike RxLR effectors, CRN effectors arose early in oomycete evolution and then later diverged across plant pathogenic species, suggesting CRN effectors play an essential role in oomycete pathogenesis in plants [99,153–157].

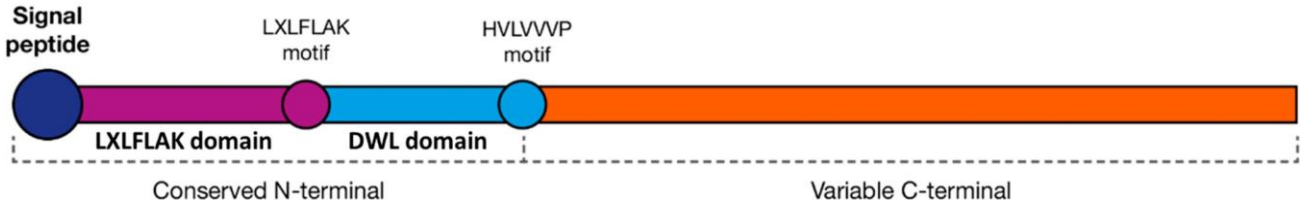

Figure 5. *Phytophthora* CRN effector structure. Diagram illustrating the LXLFLAK and DWL domains, which contains the characteristic motifs within the N-terminal and C-terminal. Featuring two conserved motifs (LXLFLAK and HVLVVP) in the N-terminal, followed by a variable C-terminal. CRNs do not always possess a signal peptide, as there are other secretion pathways.

Although CRN effectors were first noted to induce crinkling and necrosis in plant tissue, recent studies have shown that the majority of CRNs act in suppressing host cell defenses [131,138,151]. Functional characterization of *Phytophthora* CRNs has provided substantial evidence for the involvement of this class of effectors in the modulation of PCD during infection [24,54,55,60,158].

Some *Phytophthora* spp. have been shown to have at least two CRNs with contradicting functions—where one suppresses cell death, and the other induces cell death—with both required for virulence [26,54,55]. One example is that of CRN63 and CRN115 from *P. sojae*, which induce contrasting and apparently opposite responses when expressed in *N. benthamiana* [24,54]. CRN63 induces cell death, and CRN115 suppresses cell death induced by PsojNIP or CRN63; both CRNs act on catalases to alter H_2O_2 accumulation (Figure 6). The stability of catalase proteins is reduced by CRN63, which in turn enhances H_2O_2 accumulation and results in the triggering of PCD. Conversely, CRN115 suppresses PCD by inhibiting H_2O_2 accumulation induced by CRN63. This mechanism is also employed by *P. parasitica*, where CRN7 and CRN20 function analogously to *P. sojae* CRN63 and CRN115, respectively [54]. These observations are further supported by the differential expression of *CRNs* at different pathogen life stages; for example, *CRN63* shows a 2.8-times-increased expression during late stages of infection [43]. Together, these findings indicate that different CRNs have distinct functions during either the biotrophic or necrotrophic *Phytophthora* spp. life stages.

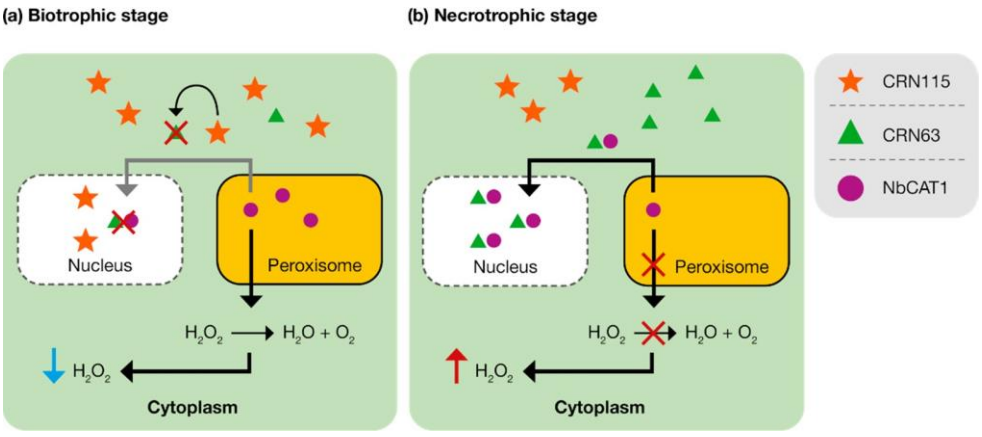

Figure 6. Schematic of how CRN63/115 modulates PCD in *Nicotiana benthamiana*. (**a**) During the early stages of infection (biotrophic stage), CRN115 inhibits the activity of CRN63, preventing the relocation and scavenging of NbCAT1. NbCAT1 is then able to convert H_2O_2 into water and oxygen. Inhibiting H_2O_2 accumulation induced by CRN63. (**b**) CRN63 is slightly induced during the late stages of infection (necrotrophic stage) and relocates NbCAT1 to the nucleus where NbCAT1 is destabilized and therefore unable to convert H_2O_2 into water and oxygen. This results in an accumulation of H_2O_2 in the cytoplasm, resulting in PCD.

Unfortunately, there has yet to be any functional characterization studies on *P. cinnamomi* CRNs. Studies such as these are of great interest, since it is suggested that these effectors play an essential role in early infection and regulating PCD [149]. Recently, there have been analyses of expression data for 49 putative *P. cinnamomi CRNs,* and it was found that 11 *CRNs* were significantly expressed, with 1 *CRN* being upregulated compared to mycelia at 120 hpi in avocado, and the remaining 10 demonstrating downregulation at the same time point [11]. This suggests that the majority of *P. cinnamomi* CRNs may function in suppressing the host defenses during the earlier stages of infection, although further expression data at earlier time points and characterization studies are required to definitively conclude the function of *P. cinnamomi* CRNs.

5. Techniques Used in the Functional Characterization of *Phytophthora* Effectors

A method commonly used in determining the function of *Phytophthora* effectors is agroinfiltration. Agroinfiltration is an *Agrobacterium tumefaciens*-based method for transient expression of genes of interest *in planta* [66]. This assay is efficient in numerous dicot plant species and is therefore broadly applied in screenings and research in molecular plant–pathogen interactions [159–162]. Agroinfiltration is also a well-established method to use for the functional characterization of pathogen effectors when that pathogen cannot be regularly transformed, as in the case of *P. cinnamomi*. This approach has been utilized in multiple studies to determine the cell death induction or suppression abilities of *Phytophthora* effectors [8,24,150,151,163]. The use of agroinfiltration coincides with the use of model plants, in particular *N. benthamiana*, which is widely used to study a variety of plant pathogens [164]. This is because *N. benthamiana* expressed sequence tags (ESTs) share similarities with important agricultural Solanaceous crops. Therefore, functional genomics research of host–pathogen interactions conducted in *N. benthamiana* will most likely reveal genes, which play similar roles in agronomically important crops.

The available genome sequences of *Phytophthora* spp. have allowed for a better understanding of the repertoire of effectors utilized by these pathogens, as well as their possible mechanisms to promote pathogen success [10,165]. Genomic and transcriptomic data allow for the prediction of putative effector homologs in *Phytophthora* spp. Tools such as RNA sequencing (RNA-Seq) are useful for gene expression profiling, which aids in identifying pathogenicity genes and predicting what functions they may have. Genome data for *Phytophthora* spp. are accumulating and have been utilized in large-scale transcriptome analyses. This will aid future research to identify key effectors, which may play a role in infection and disease development.

P. cinnamomi genomic data have been lacking. This is surprising due to the economic and ecological relevance of *P. cinnamomi* [11]. A recent study has generated a high-quality reference genome for *P. cinnamomi* using a combination of Nanopore and Illumina sequencing platforms, opening up future research on *P. cinnamomi* effectors and their functions [11]. This is an improvement on the five existing, highly fragmented draft genome sequences currently available for *P. cinnamomi* [166,167]. The assembly of the *P. cinnamomi* genome indicated that *P. cinnamomi* has a much larger genome size than what was previously estimated and has allowed better identification and characterization of various pathogenicity-related genes. Therefore, this genome serves as an important foundation for future studies.

Dual RNA-seq has enabled investigations of both host and pathogen transcriptomics simultaneously [156]. This technology allows for the detection of minute amounts of pathogen RNA, and it is more sensitive than either microarrays or northern blotting [168–170]. This tool also provides more information, as it provides a picture of global gene expression. RNA-seq data have also allowed for the identification of over 1300 putative pathogenicity genes from cyst and germinating cyst phases of *P. cinnamomi*, of which several encoded for effector proteins that served as candidates for further research [145,171]. An analysis of *P. cinnamomi* dual RNA-seq data from *Eucalyptus nitens*—5 days following inoculation with *P. cinnamomi*—revealed that a putative *P. cinnamomi CRN* effector was highly upregulated, and a pathogenicity-related (*PR-9*) gene was downregulated [156]. This and other

evidence in the study demonstrate that a *P. cinnamomi CRN* and a *E. nitens PR-9* gene may play essential roles in causing a susceptible host–pathogen interaction. RNA-seq data have also been used in a separate study to assign possible functions to three *P. cinnamomi* RxLRs [143]. However, further functional characterization is required to conclusively assign functions to any putative effector identified using gene expression data. Research aimed at characterizing effectors from different *Phytophthora* spp. has become essential to understanding the mechanisms these pathogens utilize to invoke a susceptible response in host plants. The transformation of *Phytophthora* spp. has been one method used to deduce the function of effectors; however, some species—such as *P. cinnamomi*—have had limited success in transformation [66,172,173]. The speculated reasons for these limitations are the identification of oomycete promotors and selectable markers to select for transformants [66,172]. Transformation protocols for *Phytophthora* spp., such as *P. capsici*, *P. parasitica* [174] and *P. infestans,* [175] have been successfully produced, but these protocols will not necessarily work for all *Phytophthora* spp.; notably, these protocols have not been successful in *P. cinnamomi* [66]. Although, recently, a proposed protocol has been developed using a PEG/$CaCl_2$-mediated protoplast transformation method, where three *P. cinnamomi* transformants were successfully produced in a single isolate [172]. These results have been reproduced in the same *P. cinnamomi* isolate in two separate laboratories (Nanjing Forestry University and Oregon State University). Nonetheless, this protocol still needs to be reproduced in different laboratories and using different strains before it can be validated as a standard protocol for *P. cinnamomi* transformation.

The development of efficient transformation protocols for various *Phytophthora* spp. will enable future research aimed at characterizing the effectors implicated in PCD. This, in turn, will provide some insight into how different *Phytophthora* spp. are able to maintain the biotrophic and necrotrophic stages during infection in order to achieve a susceptible outcome in host plants. Further work can also be conducted to understand the cell death pathways that may be involved and the host targets, allowing for improved screening for susceptible rootstocks to be used in agricultural practices.

6. Conclusions

PCD in plants is a complicated process with no one single mechanism, and the HR is of particular interest during the plant pathogen–host interaction. The HR can either benefit or be detrimental to host plants, depending on when it is triggered and what infection strategy is employed by the pathogen. There is evidence that *Phytophthora* effectors either directly or indirectly induce/suppress cell death, which ultimately aids in the virulence of the pathogen. This indicates that a possible infection strategy involves the 'hijacking' of the HR machinery to benefit the specific life stages of the pathogen. CRNs and NLPs may play a key role during the maintenance of the biotrophic and necrotrophic life stages and therefore require further investigation. Other *Phytophthora* spp., such as *P. cinnamomic*, which are detrimental to numerous economically important agricultural crops, should be investigated to identify effectors that may be involved in regulating host plant cell death. This will entail the development of *P. cinnamomi* transformation approaches, which will allow for better analysis of specific effectors and their functions. Until this can be performed, agroinfiltration serves as an efficient method to study effector proteins' ability to induce/suppress cell death in *Phytophthora* spp.

Funding: This research was funded by the Hans Merensky Foundation.

Conflicts of Interest: The authors declare no conflict of interest.

References

1. Kroon, L.P.N.M.; Brouwer, H.; De Cock, A.W.A.M.; Govers, F. The *Phytophthora* genus anno 2012. *Phytopathology* **2012**, *102*, 348–364. [CrossRef]
2. Lamour, K.H.; Stam, R.; Jupe, J.; Huitema, E. The oomycete broad-host-range pathogen *Phytophthora capsici*. *Mol. Plant Pathol.* **2012**, *13*, 329–337. [CrossRef] [PubMed]

3. Kamoun, S.; Furzer, O.; Jones, J.D.G.; Judelson, H.S.; Ali, G.S.; Dalio, R.J.D.; Roy, S.G.; Schena, L.; Zambounis, A.; Panabières, F.; et al. The Top 10 oomycete pathogens in molecular plant pathology. *Mol. Plant Pathol.* **2015**, *16*, 413–434. [CrossRef] [PubMed]
4. Boevink, P.C.; Birch, P.R.J.; Turnbull, D.; Whisson, S.C. Devastating intimacy: The cell biology of plant—*Phytophthora* interactions. *New Phytol.* **2020**, *228*, 445–458. [CrossRef] [PubMed]
5. Kinealy, C. *This Great Calamity: The Irish Famine 1845-52*; Gill & Macmillan Ltd.: Dublin, Ireland, 2006; pp. 10–98.
6. Batini, F.E.; Hopkins, E.R. *Phytophthora cinnamomi* Rands—a root pathogen of the Jarrah Forest. *Aust. For.* **1972**, *36*, 57–68. [CrossRef]
7. Rani, G.D. *Advances in Soil Borne Plant Diseases*; New India Publishing: New Dehli, India, 2008; pp. 371–413.
8. Mafurah, J.J.; Ma, H.; Zhang, M.; Xu, J.; He, F.; Ye, T.; Shen, D.; Chen, Y.; Rajput, N.A.; Dou, D. A virulence essential CRN effector of *Phytophthora capsici* suppresses host defense and induces cell death in plant nucleus. *PLoS ONE* **2015**, *10*, e0127965. [CrossRef]
9. Huysmans, M.; Coll, N.S.; Nowack, M.K. Dying two deaths—programmed cell death regulation in development and disease. *Curr. Opin. Plant Biol.* **2017**, *35*, 37–44. [CrossRef]
10. Tyler, B.M.; Tripathy, S.; Zhang, X.; Dehal, P.; Jiang, R.H.Y.; Aerts, A.; Arredondo, F.D.; Baxter, L.; Bensasson, D.; Beynon, J.L.; et al. *Phytophthora* genome sequences uncover evolutionary origins and mechanisms of pathogenesis. *Science* **2006**, *313*, 1261–1266. [CrossRef]
11. Engelbrecht, J.; Duong, T.A.; Prabhu, S.A.; Seedat, M.; Berg, N.V.D. Genome of the destructive oomycete *Phytophthora cinnamomi* provides insights into its pathogenicity and adaptive potential. *BMC Genom.* **2021**, *22*, 302. [CrossRef]
12. Hardham, A.R. *Phytophthora cinnamomi*. *Mol. Plant Pathol.* **2005**, *6*, 589–604. [CrossRef]
13. Koeck, M.; Hardham, A.R.; Dodds, P.N. The role of effectors of biotrophic and hemibiotrophic fungi in infection. *Cell. Microbiol.* **2011**, *13*, 1849–1857. [CrossRef] [PubMed]
14. van Doorn, W.G.; Beers, E.P.; Dangl, J.L.; E Franklin-Tong, V.; Gallois, P.; Hara-Nishimura, I.; Jones, A.M.; Kawai-Yamada, M.; Lam, E.; Mundy, J.; et al. Morphological classification of plant cell deaths. *Cell Death Differ.* **2011**, *18*, 1241–1246. [CrossRef] [PubMed]
15. Petrov, V.; Hille, J.; Mueller-Roeber, B.; Gechev, T.S. ROS-mediated abiotic stress-induced programmed cell death in plants. *Front. Plant Sci.* **2015**, *6*, 69. [CrossRef] [PubMed]
16. Mittler, R.; Blumwald, E. Genetic engineering for modern agriculture: Challenges and perspectives. *Annu. Rev. Plant Biol.* **2010**, *61*, 443–462. [CrossRef]
17. Burke, R.; Schwarze, J.; Sherwood, O.L.; Jnaid, Y.; McCabe, P.F.; Kacprzyk, J. Stressed to death: The role of transcription factors in plant programmed cell death induced by abiotic and biotic stimuli. *Front. Plant Sci.* **2020**, *11*, 1235. [CrossRef] [PubMed]
18. Kiraly, Z.; Barna, B.; Ersek, T. Hypersensitivity as a consequence, not the cause, of plant resistance to infection. *Nature* **1972**, *239*, 456–458. [CrossRef]
19. Hatsugai, N.; Kuroyanagi, M.; Yamada, K.; Meshi, T.; Tsuda, S.; Kondo, M.; Nishimura, M.; Hara-Nishimura, I. A plant vacuolar protease, VPE, mediates virus-induced hypersensitive cell death. *Science* **2004**, *305*, 855–858. [CrossRef]
20. Rojo, E.; Martín, R.; Carter, C.; Zouhar, J.; Pan, S.; Plotnikova, J.; Jin, H.; Paneque, M.; Serrano, J.J.S.; Baker, B.; et al. VPEγ exhibits a caspase-like activity that contributes to defense against pathogens. *Curr. Biol.* **2004**, *14*, 1897–1906. [CrossRef]
21. Avci, U.; Petzold, H.E.; Ismail, I.O.; Beers, E.P.; Haigler, C.H. Cysteine proteases XCP1 and XCP2 aid micro-autolysis within the intact central vacuole during xylogenesis in *Arabidopsis* roots. *Plant J.* **2008**, *56*, 303–315. [CrossRef]
22. Gao, M.; Showalter, A.M. Yariv reagent treatment induces programmed cell death in *Arabidopsis* cell cultures and implicates arabinogalactan protein involvement. *Plant J.* **1999**, *19*, 321–331. [CrossRef]
23. Mur, L.A.J.; Kenton, P.; Lloyd, A.J.; Ougham, H.; Prats, E. The hypersensitive response; the centenary is upon us but how much do we know? *J. Exp. Bot.* **2008**, *59*, 501–520. [CrossRef] [PubMed]
24. Zhang, M.; Li, Q.; Liu, T.; Liu, L.; Shen, D.; Zhu, Y.; Liu, P.; Zhou, J.-M.; Dou, D. Two cytoplasmic effectors of *Phytophthora sojae* regulate plant cell death via interactions with plant catalases. *Plant Physiol.* **2015**, *167*, 164–175. [CrossRef]
25. Daneva, A.; Gao, Z.; Van Durme, M.; Nowack, M.K. Functions and regulation of programmed cell death in plant development. *Annu. Rev. Cell Dev. Biol.* **2016**, *32*, 441–468. [CrossRef] [PubMed]
26. Mukhtar, M.S.; McCormack, M.E.; Argueso, C.T.; Pajerowska-Mukhtar, K.M. Pathogen tactics to manipulate plant cell death. *Curr. Biol.* **2016**, *26*, 608–619. [CrossRef] [PubMed]
27. Fuchs, Y.; Steller, H. Programmed cell death in animal development and disease. *Cell* **2011**, *147*, 742–758. [CrossRef] [PubMed]
28. Zhai, Z.; Ha, N.; Papagiannouli, F.; Hamacher-Brady, A.; Brady, N.; Sorge, S.; Bezdan, D.; Lohmann, I. Antagonistic regulation of apoptosis and differentiation by the Cut transcription factor represents a tumor-suppressing mechanism in *Drosophila*. *PLoS Genet.* **2012**, *8*, e1002582. [CrossRef]
29. Aubrey, B.J.; Kelly, G.L.; Janic, A.; Herold, M.J.; Strasser, A. How does p53 induce apoptosis and how does this relate to p53-mediated tumour suppression? *Cell Death Differ.* **2018**, *25*, 104–113. [CrossRef]
30. Bin Nasir, K.H.; Takahashi, Y.; Ito, A.; Saitoh, H.; Matsumura, H.; Kanzaki, H.; Shimizu, T.; Ito, M.; Fujisawa, S.; Sharma, P.C.; et al. High-throughput *in planta* expression screening identifies a class II ethylene-responsive element binding factor-like protein that regulates plant cell death and non-host resistance. *Plant J.* **2005**, *43*, 491–505. [CrossRef]
31. Xie, H.-T.; Wan, Z.-Y.; Li, S.; Zhang, Y. Spatiotemporal production of reactive oxygen species by NADPH oxidase is critical for tapetal programmed cell death and pollen development in *Arabidopsis*. *Plant Cell* **2014**, *26*, 2007–2023. [CrossRef]

32. Lee, M.H.; Jeon, H.S.; Kim, H.G.; Park, O.K. An *Arabidopsis* NAC transcription factor NAC4 promotes pathogen-induced cell death under negative regulation by microRNA164. *New Phytol.* **2017**, *214*, 343–360. [CrossRef]
33. Awwad, F.; Bertrand, G.; Grandbois, M.; Beaudoin, N. Auxin protects *Arabidopsis thaliana* cell suspension cultures from programmed cell death induced by the cellulose biosynthesis inhibitors thaxtomin A and isoxaben. *BMC Plant Biol.* **2019**, *19*, 512. [CrossRef] [PubMed]
34. Yuan, X.; Wang, H.; Cai, J.; Li, D.; Song, F. NAC transcription factors in plant immunity. *Phytopathol. Res.* **2019**, *1*, 3. [CrossRef]
35. Kaneda, T.; Taga, Y.; Takai, R.; Iwano, M.; Matsui, H.; Takayama, S.; Isogai, A.; Che, F.-S. The transcription factor OsNAC4 is a key positive regulator of plant hypersensitive cell death. *EMBO J.* **2009**, *28*, 926–936. [CrossRef] [PubMed]
36. Xu, X.; Chen, C.; Fan, B.; Chen, Z. Physical and functional interactions between pathogen-induced *Arabidopsis* WRKY18, WRKY40, and WRKY60 transcription factors. *Plant Cell* **2006**, *18*, 1310–1326. [CrossRef] [PubMed]
37. Yin, L.-L.; Xue, H.-W. The MADS29 transcription factor regulates the degradation of the nucellus and the nucellar projection during rice seed development. *Plant Cell* **2012**, *24*, 1049–1065. [CrossRef]
38. Qi, T.; Wang, J.; Huang, H.; Liu, B.; Gao, H.; Liu, Y.; Song, S.; Xie, D. Regulation of jasmonate-induced leaf senescence by antagonism between bHLH subgroup IIIe and IIId factors in *Arabidopsis*. *Plant Cell* **2015**, *27*, 1634–1649. [CrossRef]
39. Ueda, H.; Kusaba, M. Strigolactone regulates leaf senescence in concert with ethylene in *Arabidopsis*. *Plant Physiol.* **2015**, *169*, 138–147. [CrossRef]
40. Glazebrook, J. Contrasting mechanisms of defense against biotrophic and necrotrophic pathogens. *Annu. Rev. Phytopathol.* **2005**, *43*, 205–227. [CrossRef]
41. Huang, S.; Zhang, X.; Fernando, W.G.D. Directing trophic divergence in plant-pathogen interactions: Antagonistic phytohormones with no doubt? *Front. Plant Sci.* **2020**, *11*, 600063. [CrossRef]
42. Pieterse, C.M.J.; Leon-Reyes, A.; Van der Ent, S.; Van Wees, S.C.M. Networking by small-molecule hormones in plant immunity. *Nat. Chem. Biol.* **2009**, *5*, 308–316. [CrossRef]
43. Birkenbihl, R.P.; Somssich, I.E. Transcriptional plant responses critical for resistance towards necrotrophic pathogens. *Front. Plant Sci.* **2011**, *2*, 76. [CrossRef] [PubMed]
44. Kazan, K.; Lyons, R. Intervention of phytohormone pathways by pathogen effectors. *Plant Cell* **2014**, *26*, 2285–2309. [CrossRef] [PubMed]
45. Van Durme, M.; Nowack, M.K. Mechanisms of developmentally controlled cell death in plants. *Curr. Opin. Plant Biol.* **2016**, *29*, 29–37. [CrossRef] [PubMed]
46. Wilkins, K.A.; Bosch, M.; Haque, T.; Teng, N.; Poulter, N.S.; Franklin-Tong, V.E. Self-incompatibility-induced programmed cell death in field poppy pollen involves dramatic acidification of the incompatible pollen tube cytosol. *Plant Physiol.* **2015**, *167*, 766–779. [CrossRef] [PubMed]
47. Coll, N.S.; Epple, P.; Dangl, J.L. Programmed cell death in the plant immune system. *Cell Death Differ.* **2011**, *18*, 1247–1256. [CrossRef]
48. Herrera-Vāsquez, A.; Salinas, P.; Holuigue, L. Salicylic acid and reactive oxygen species interplay in the transcriptional control of defense genes expression. *Front. Plant Sci.* **2015**, *6*, 171. [CrossRef]
49. Lorang, J.; Kidarsa, T.; Bradford, C.S.; Gilbert, B.; Curtis, M.; Tzeng, S.-C.; Maier, C.S.; Wolpert, T.J. Tricking the guard: Exploiting plant defense for disease susceptibility. *Science* **2012**, *338*, 659–662. [CrossRef]
50. Lorang, J. Necrotrophic exploitation and subversion of plant defense: A lifestyle or just a phase, and implications in breeding resistance. *Phytopathology* **2019**, *109*, 332–346. [CrossRef]
51. Stam, R.; Jupe, J.; Howden, A.J.M.; Morris, J.A.; Boevink, P.C.; Hedley, P.E.; Huitema, E. Identification and characterisation CRN effectors in *Phytophthora capsici* shows modularity and functional diversity. *PLoS ONE* **2013**, *8*, e59517. [CrossRef]
52. Münch, S.; Lingner, U.; Floss, D.S.; Ludwig, N.; Sauer, N.; Deising, H.B. The hemibiotrophic lifestyle of *Colletotrichum* species. *J. Plant Physiol.* **2008**, *165*, 41–51. [CrossRef] [PubMed]
53. Jupe, J.; Stam, R.; Howden, A.J.; Morris, J.A.; Zhang, R.; Hedley, P.E.; Huitema, E. *Phytophthora capsici*-tomato interaction features dramatic shifts in gene expression associated with a hemi-biotrophic lifestyle. *Genome Biol.* **2013**, *14*, R63. [CrossRef] [PubMed]
54. Liu, T.; Ye, W.; Ru, Y.; Yang, X.; Gu, B.; Tao, K.; Lu, S.; Dong, S.; Zheng, X.; Shan, W.; et al. Two host cytoplasmic effectors are required for pathogenesis of *Phytophthora sojae* by suppression of host defenses. *Plant Physiol.* **2011**, *155*, 490–501. [CrossRef] [PubMed]
55. Maximo, H.J.; Dalio, R.O.; Litholdo, C.G.; Felizatti, H.L.; Machado, M.A. PpCRN7 and PpCRN20 of *Phythophthora parasitica* regulate plant cell death leading to enhancement of host susceptibility. *BMC Plant Biol.* **2019**, *19*, 544. [CrossRef]
56. Wang, S.; Welsh, L.; Thorpe, P.; Whisson, S.C.; Boevink, P.C.; Birch, P.R.J. The *Phytophthora infestans* haustorium is a site for secretion of diverse classes of infection-associated proteins. *MBio* **2018**, *9*, e01216-18. [CrossRef]
57. Judelson, H.S.; Ah-Fong, A.M.V. Exchanges at the plant-oomycete interface that influence disease. *Plant Physiol.* **2019**, *179*, 1198–1211. [CrossRef] [PubMed]
58. Dong, S.; Kong, G.; Qutob, D.; Yu, X.; Tang, J.; Kang, J.; Dai, T.; Wang, H.; Gijzen, M.; Wang, Y. The NLP toxin family in *Phytophthora sojae* includes rapidly evolving groups that lack necrosis-inducing activity. *Mol. Plant Microbe Interact.* **2012**, *25*, 896–909. [CrossRef]

59. Ah-Fong, A.M.V.; Shrivastava, J.; Judelson, H.S. Lifestyle, gene gain and loss, and transcriptional remodeling cause divergence in the transcriptomes of *Phytophthora infestans* and *Pythium ultimum* during potato tuber colonization. *BMC Genom.* **2017**, *18*, 764. [CrossRef]
60. Van Damme, M.; Bozkurt, T.O.; Cakir, C.; Schornack, S.; Sklenář, J.; Jones, A.M.E.; Kamoun, S. The Irish potato famine pathogen *Phytophthora infestans* translocates the CRN8 kinase into host plant cells. *PLoS Pathog.* **2012**, *8*, e1002875. [CrossRef]
61. Li, Q.; Ai, G.; Shen, D.; Zou, F.; Wang, J.; Bai, T.; Chen, Y.; Li, S.; Zhang, M.; Jing, M.; et al. A *Phytophthora capsici* effector targets ACD11 binding partners that regulate ROS-mediated defense response in Arabidopsis. *Mol. Plant* **2019**, *12*, 565–581. [CrossRef]
62. Toljamo, A.; Blande, D.; Munawar, M.; Kärenlampi, S.O.; Kokko, H. Expression of the GAF sensor, carbohydrate-active Enzymes, elicitins, and RXLRs differs markedly between two *Phytophthora cactorum* isolates. *Phytopathology* **2019**, *109*, 726–735. [CrossRef]
63. Hardham, A.R.; Blackman, L.M. *Phytophthora cinnamomi*. *Mol. Plant Pathol.* **2018**, *19*, 260–285. [CrossRef] [PubMed]
64. Kamoun, S. A catalogue of the effector secretome of plant pathogenic oomycetes. *Annu. Rev. Phytopathol.* **2006**, *44*, 41–60. [CrossRef] [PubMed]
65. Gijzen, M.; Nürnberger, T. Nep1-like proteins from plant pathogens: Recruitment and diversification of the NPP1 domain across taxa. *Phytochemistry* **2006**, *67*, 1800–1807. [CrossRef]
66. Lamour, K.; Kamoun, S. *Oomycete Genetics and Genomics: Diversity, Interactions and Research Tools*; John Wiley & Sons: Hoboken, NJ, USA, 2009; pp. 1–387.
67. Wang, Y.; Hu, D.; Zhang, Z.; Ma, Z.; Zheng, X.; Li, D. Purification and immune cytolocalization of a novel *Phytophthora boehmeriae* protein inducing the hypersensitive response and systemic acquired resistance in tobacco and Chinese cabbage. *Physiol. Mol. Plant Pathol.* **2003**, *63*, 223–232. [CrossRef]
68. Zhang, Z.-G.; Wang, Y.-C.; Li, J.; Ji, R.; Shen, G.; Wang, S.-C.; Zhou, X.; Zheng, X.-B. The role of SA in the hypersensitive response and systemic acquired resistance induced by elicitor PB90 from *Phytophthora boehmeriae*. *Physiol. Mol. Plant Pathol.* **2004**, *65*, 31–38. [CrossRef]
69. Chen, Q.; Chen, Z.; Lu, L.; Jin, H.; Sun, L.; Yu, Q.; Xu, H.; Yang, F.; Fu, M.; Li, S.; et al. Interaction between abscisic acid and nitric oxide in PB90-induced catharanthine biosynthesis of *Catharanthus roseus* cell suspension cultures. *Biotechnol. Prog.* **2013**, *29*, 994–1001. [CrossRef]
70. Huet, J.-C.; Pernollet, M.M.J.-C. Amino acid sequence of the α-elicitin secreted by *Phytophthora cactorum*. *Phytochemistry* **1993**, *34*, 1261–1264. [CrossRef]
71. Chen, X.-R.; Zhang, B.-Y.; Xing, Y.-P.; Li, Q.-Y.; Li, Y.-P.; Tong, Y.-H.; Xu, J.-Y. Transcriptomic analysis of the phytopathogenic oomycete *Phytophthora cactorum* provides insights into infection-related effectors. *BMC Genom.* **2014**, *15*, 980. [CrossRef]
72. Chen, X.R.; Huang, S.X.; Zhang, Y.; Sheng, G.L.; Zhang, B.Y.; Li, Q.Y.; Zhu, F.; Xu, J.Y. Transcription profiling and identification of infection-related genes in *Phytophthora cactorum*. *Mol. Genet. Genom.* **2017**, *293*, 541–555. [CrossRef]
73. Ricci, P.; Bonnet, P.; Huet, J.-C.; Sallantin, M.; Beauvais-Cante, F.; Bruneteau, M.; Billard, V.; Michel, G.; Pernollet, J.-C. Structure and activity of proteins from pathogenic fungi *Phytophthora* eliciting necrosis and acquired resistance in tobacco. *Eur. J. Biochem.* **1989**, *183*, 555–563. [CrossRef]
74. Liu, Z.-Q.; Qiu, A.-L.; Shi, L.-P.; Cai, J.-S.; Huang, X.-Y.; Yang, S.; Wang, B.; Shen, L.; Huang, M.-K.; Mou, S.-L.; et al. SRC2-1 is required in PcINF1-induced pepper immunity by acting as an interacting partner of PcINF1. *J. Exp. Bot.* **2015**, *66*, 3683–3698. [CrossRef] [PubMed]
75. Liu, Z.-Q.; Liu, Y.-Y.; Shi, L.-P.; Yang, S.; Shen, L.; Yu, H.-X.; Wang, R.-Z.; Wen, J.-Y.; Tang, Q.; Hussain, A.; et al. SGT1 is required in PcINF1/SRC2-1 induced pepper defense response by interacting with SRC2-1. *Sci. Rep.* **2016**, *6*, 21651. [CrossRef]
76. Billard, V.; Bruneteau, M.; Bonnet, P.; Ricci, P.; Pernollet, J.; Huet, J.; Vergne, A.; Richard, G.; Michel, G. Chromatographic purification and characterization of elicitors of necrosis on tobacco produced by incompatible *Phytophthora species*. *J. Chromatogr.* **1988**, *440*, 87–94. [CrossRef]
77. Huet, J.-C.; Pernollet, J.-C. Amino acid sequence of cinnamomin, a new member of the elicitin family, and its comparison to cryptogein and capsicein. *FEBS Lett.* **1989**, *257*, 302–306. [CrossRef]
78. Mishra, A.K.; Sharma, K.; Misra, R.S. Purification and characterization of elicitor protein from *Phytophthora colocasiae* and basic resistance in *Colocasia esculenta*. *Microbiol. Res.* **2009**, *164*, 688–693. [CrossRef]
79. Galiana, E.; Bonnet, P.; Conrod, S.; Keller, H.; Panabieres, F.; Ponchet, M.; Poupet, A.; Ricci, P. RNase activity prevents the growth of a fungal pathogen in tobacco leaves and increases upon induction of systemic acquired resistance with elicitin. *Plant Physiol.* **1997**, *115*, 1557–1567. [CrossRef]
80. Mikes, V.; Milat, M.-L.; Ponchet, M.; Ricci, P.; Blein, J.-P. The fungal elicitor cryptogein is a sterol carrier protein. *FEBS Lett.* **1997**, *416*, 190–192. [CrossRef]
81. Leborgne-Castel, N.; Lherminier, J.; Der, C.; Fromentin, J.; Houot, V.; Simon-Plas, F. The plant defense elicitor cryptogein stimulates clathrin mediated endocytosis correlated with reactive oxygen species production in bright yellow-2 tobacco cells. *Plant Physiol.* **2008**, *146*, 1255–1266. [CrossRef]
82. Coursol, S.; Fromentin, J.; Noirot, E.; Brière, C.; Robert, F.; Morel, J.; Liang, Y.; Lherminier, J.; Simon-Plas, F. Long-chain bases and their phosphorylated derivatives differentially regulate cryptogein-induced production of reactive oxygen species in tobacco (*Nicotiana tabacum*) BY-2 cells. *New Phytol.* **2015**, *205*, 1239–1249. [CrossRef]

83. Kulik, A.; Noirot, E.; Grandperret, V.; Bourque, S.; Fromentin, J.; Salloignon, P.; Truntzer, C.; Dobrowolska, G.; Simon-Plas, F.; Wendehenne, D. Interplays between nitric oxide and reactive oxygen species in cryptogein signalling. *Plant Cell Environ.* **2015**, *38*, 331–348. [CrossRef]
84. Ptáčková, N.; Klempová, J.; Obořil, M.; Nedělová, S.; Lochman, J.; Kašparovský, T. The effect of cryptogein with changed abilities to transfer sterols and altered charge distribution on extracellular alkalinization, ROS and NO generation, lipid peroxidation and LOX gene transcription in *Nicotiana tabacum*. *Plant Physiol. Biochem.* **2015**, *97*, 82–95. [CrossRef]
85. Starý, T.; Satková, P.; Piterková, J.; Mieslerová, B.; Luhová, L.; Mikulík, J.; Kašparovský, T.; Petrˇivalský, M.; Lochman, J. The elicitin β-cryptogein's activity in tomato is mediated by jasmonic acid and ethylene signalling pathways independently of elicitin-sterol interactions. *Planta* **2019**, *249*, 739–749. [CrossRef] [PubMed]
86. Huet, J.-C.; Nespoulous, C.; Pernollet, J.-C. Structures of elicitin isoforms secreted by *Phytophthora drechsleri*. *Phytochemistry* **1992**, *31*, 1471–1476. [CrossRef]
87. Capasso, R.; Di Maro, A.; Cristinzio, G.; De Martino, A.; Chambery, A.; Daniele, A.; Sannino, F.; Testa, A.; Parente, A. Isolation, characterization and structure-elicitor activity relationships of hibernalin and its two oxidized forms from *Phytophthora hibernalis*. Carne 1925. *J. Biochem.* **2008**, *143*, 131–141. [CrossRef]
88. Huet, J.; Sallé-Tourne, M.; Pernollet, J. Amino acid sequence and toxicity of the alpha elicitin secreted with ubiquitin by *Phytophthora infestans*. *Mol. Plant Microbe Interact.* **1994**, *7*, 302–304. [CrossRef] [PubMed]
89. Kamoun, S.; van West, P.; de Jong, A.J.; de Groot, K.E.; Vleeshouwers, V.G.A.A.; Govers, F. A gene encoding a protein elicitor of *Phytophthora infestans* is down-regulated during infection of potato. *Mol. Plant Microbe Interact.* **1997**, *10*, 13–20. [CrossRef]
90. Kamoun, S.; Van West, P.; Vleeshouwers, V.G.A.A.; De Groot, K.E.; Govers, F. Resistance of *Nicotiana benthamiana* to *Phytophthora infestans* is mediated by the recognition of the elicitor protein INF1. *Plant Cell* **1998**, *10*, 1413–1425. [CrossRef]
91. Kanzaki, H.; Saitoh, H.; Ito, A.; Fujisawa, S.; Kamoun, S.; Katou, S.; Yoshioka, H.; Terauchi, R. Cytosolic HSP90 and HSP70 are essential components of INF1-mediated hypersensitive response and non-host resistance to *Pseudomonas cichorii* in *Nicotiana benthamiana*. *Mol. Plant Pathol.* **2003**, *4*, 383–391. [CrossRef]
92. Huitema, E.; Vleeshouwers, V.G.; Cakir, C.; Kamoun, S.; Govers, F. Differences in intensity and specificity of hypersensitive response induction in *Nicotiana* spp. by INF1, INF2A, and INF2B of *Phytophthora infestans*. *Mol. Plant Microbe Interact.* **2005**, *18*, 183–193. [CrossRef]
93. Du, J.; Verzaux, E.; Chaparro-Garcia, A.; Bijsterbosch, G.; Keizer, L.C.P.; Zhou, J.; Liebrand, T.W.H.; Xie, C.; Govers, F.; Robatzek, S.; et al. Elicitin recognition confers enhanced resistance to *Phytophthora infestans* in potato. *Nat. Plants* **2015**, *1*, 15034. [CrossRef]
94. Huet, J.-C.; Pernollet, J.-C. Sequences of acidic and basic elicitin isoforms secreted by *Phytophthora megasperma*. *Phytochemistry* **1993**, *33*, 797–805. [CrossRef]
95. Baillieul, F.; de Ruffray, P.; Kauffmann, S. Molecular cloning and biological activity of α-, β-, and γ-megaspermin, three elicitins secreted by *Phytophthora megasperma* H20. *Plant Physiol.* **2003**, *131*, 155–166. [CrossRef] [PubMed]
96. Baillieul, F.; Genetet, I.; Kopp, M.; Saindrenan, P.; Fritig, B.; Kauffmann, S. A new elicitor of the hypersensitive response in tobacco: A fungal glycoprotein elicits cell death, expression of defence genes, production of salicylic acid, and induction of systemic acquired resistance. *Plant J.* **1995**, *8*, 551–560. [CrossRef] [PubMed]
97. Churngchow, N.; Rattarasarn, M. The elicitin secreted by *Phytophthora palmivora*, a rubber tree pathogen. *Phytochemistry* **2000**, *54*, 33–38. [CrossRef]
98. Nespoulous, C.; Huet, J.-C.; Pernollet, J.-C. Structure-function relationships of α and β elicitins, signal proteins involved in the plant-*Phytophthora* interaction. *Planta* **1992**, *186*, 551–557. [CrossRef]
99. Kamoun, S.; Klucher, K.M.; Coffey, M.D.; Tyler, B.M. A gene encoding a host-specific elicitor protein of *Phytophthora parasitica*. *Mol. Plant Microbe Interact.* **1993**, *6*, 573. [CrossRef]
100. Mouton-Perronnet, F.; Bruneteau, M.; Denoroy, L.; Bouliteau, P.; Ricci, P.; Bonnet, P.; Michel, G. Elicitin produced by an isolate of *Phytophthora parasitica* pathogenic to tobacco. *Phytochemistry* **1995**, *38*, 41–44. [CrossRef]
101. Capasso, R.; Cristinzio, G.; Evidente, A.; Visca, C.; Ferranti, P.; Blanco, F.D.V.; Parente, A. Elicitin 172 from an isolate of *Phytophthora nicotianae* pathogenic to tomato. *Phytochemistry* **1999**, *50*, 703–709. [CrossRef]
102. Capasso, R.; Cristinzio, G.; Di Maro, A.; Ferranti, P.; Parente, A. Syringicin, a new α-elicitin from an isolate of *Phytophthora syringae*, pathogenic to citrus fruit. *Phytochemistry* **2001**, *58*, 257–262. [CrossRef]
103. Chen, X.-R.; Huang, S.-X.; Zhang, Y.; Sheng, G.-L.; Li, Y.-P.; Zhu, F. Identification and functional analysis of the NLP-encoding genes from the phytopathogenic oomycete *Phytophthora capsici*. *Mol. Genet. Genom.* **2018**, *293*, 931–943. [CrossRef]
104. Feng, B.-Z.; Zhu, X.-P.; Fu, L.; Lv, R.-F.; Storey, D.; Tooley, P.; Zhang, X.-G. Characterization of necrosis-inducing NLP proteins in *Phytophthora capsici*. *BMC Plant Biol.* **2014**, *14*, 126. [CrossRef]
105. Kanneganti, T.-D.; Huitema, E.; Cakir, C.; Kamoun, S. Synergistic interactions of the plant cell death pathways induced by *Phytophthora infestans* Nep1-like protein PiNPP1.1 and INF1 elicitin. *Mol. Plant Microbe Interact.* **2006**, *19*, 854–863. [CrossRef] [PubMed]
106. Fellbrich, G.; Romanski, A.; Varet, A.; Blume, B.; Brunner, F.; Engelhardt, S.; Felix, G.; Kemmerling, B.; Krzymowska, M.; Nürnberger, T. NPP1, a *Phytophthora*-associated trigger of plant defense in parsley and *Arabidopsis*. *Plant J.* **2002**, *32*, 375–390. [CrossRef]

107. Qutob, D.; Kemmerling, B.; Brunner, F.; Kufner, I.; Engelhardt, S.; Gust, A.A.; Luberacki, B.; Seitz, H.U.; Stahl, D.; Rauhut, T.; et al. Phytotoxicity and innate immune responses induced by Nep1-like proteins. *Plant Cell* **2006**, *18*, 3721–3744. [CrossRef] [PubMed]
108. Ottmann, C.; Luberacki, B.; Küfner, I.; Koch, W.; Brunner, F.; Weyand, M.; Mattinen, L.; Pirhonen, M.; Anderluh, G.; Seitz, H.U.; et al. A common toxin fold mediates microbial attack and plant defense. *Proc. Natl. Acad. Sci. USA* **2009**, *106*, 10359–10364. [CrossRef] [PubMed]
109. Böhm, H.; Albert, I.; Oome, S.; Raaymakers, T.M.; Van Den Ackerveken, G.; Nürnberger, T. A conserved peptide pattern from a widespread microbial virulence factor triggers pattern-induced immunity in *Arabidopsis*. *PLoS Pathog.* **2014**, *10*, e1004491. [CrossRef] [PubMed]
110. Albert, I.; Böhm, H.; Albert, M.; Feiler, C.E.; Imkampe, J.; Wallmeroth, N.; Brancato, C.; Raaymakers, T.M.; Oome, S.; Zhang, H.; et al. An RLP23-SOBIR1-BAK1 complex mediates NLP triggered immunity. *Nat. Plants.* **2015**, *1*, 15140. [CrossRef]
111. Qutob, D.; Kamoun, S.; Gijzen, M. Expression of a *Phytophthora sojae* necrosis-inducing protein occurs during transition from biotrophy to necrotrophy. *Plant J.* **2002**, *32*, 361–373. [CrossRef]
112. Veit, S.; Wörle, J.M.; Nürnberger, T.; Koch, W.; Seitz, H.U. A novel protein elicitor (PaNie) from *Pythium aphanidermatum* induces multiple defense responses in carrot, *Arabidopsis*, and tobacco. *Plant Physiol.* **2001**, *127*, 832–841. [CrossRef]
113. Mateos, F.V.; Rickauer, M.; Esquerré-Tugayé, M.-T. Cloning and characterization of a cDNA encoding an elicitor of *Phytophthora parasitica var. nicotianae* that shows cellulose-binding and lectin-like activities. *Mol. Plant Microbe Interact.* **1997**, *10*, 1045–1053. [CrossRef]
114. Khatib, M.; Lafitte, C.; Esquerré-Tugayé, M.; Bottin, A.; Rickauer, M. The CBEL elicitor of *Phytophthora parasitica var. nicotianae* activates defence in *Arabidopsis thaliana* via three different signalling pathways. *New Phytol.* **2004**, *162*, 501–510. [CrossRef]
115. Fu, L.; Zhu, C.; Ding, X.; Yang, X.; Morris, P.F.; Tyler, B.M.; Zhang, X. Characterization of cell-death-inducing members of the pectate lyase gene family in *Phytophthora capsici* and their contributions to infection of pepper. *Mol. Plant Microbe Interact.* **2015**, *28*, 766–775. [CrossRef] [PubMed]
116. Ma, Z.; Song, T.; Zhu, L.; Ye, W.; Wang, Y.; Shao, Y.; Dong, S.; Zhang, Z.; Dou, D.; Zheng, X.; et al. A *Phytophthora sojae* glycoside hydrolase 12 protein is a major virulence factor during soybean infection and is recognized as a PAMP. *Plant Cell* **2015**, *27*, 2057–2072. [CrossRef]
117. Wang, Y.; Xu, Y.; Sun, Y.; Wang, H.; Qi, J.; Wan, B.; Ye, W.; Lin, Y.; Shao, Y.; Dong, S.; et al. Leucine rich repeat receptor-like gene screen reveals that *Nicotiana* RXEG1 regulates glycoside hydrolase 12 MAMP detection. *Nat. Commun.* **2018**, *9*, 594. [CrossRef] [PubMed]
118. Chang, Y.-H.; Yan, H.-Z.; Liou, R.-F. A novel elicitor protein from *Phytophthora parasitica* induces plant basal immunity and systemic acquired resistance. *Mol. Plant Pathol.* **2015**, *16*, 123–136. [CrossRef] [PubMed]
119. Orsomando, G.; Lorenzi, M.; Raffaelli, N.; Rizza, M.D.; Mezzetti, B.; Ruggieri, S. Phytotoxic protein PcF, purification, characterization, and cDNA sequencing of a novel hydroxyproline-containing factor secreted by the strawberry pathogen *Phytophthora cactorum*. *J. Biol. Chem.* **2001**, *276*, 21578–21584. [CrossRef]
120. Chen, X.-R.; Li, Y.-P.; Li, Q.-Y.; Xing, Y.-P.; Liu, B.-B.; Tong, Y.-H.; Xu, J.-Y. SCR96, a small cysteine-rich secretory protein of *Phytophthora cactorum*, can trigger cell death in the *Solanaceae* and is important for pathogenicity and oxidative stress tolerance. *Mol. Plant Pathol.* **2016**, *17*, 577–587. [CrossRef]
121. Duclos, J.; Fauconnier, A.; Coelho, A.-C.; Bollen, A.; Cravador, A.; Godfroid, E. Identification of an elicitin gene cluster in *Phytophthora cinnamomi*. *DNA Seq.* **1998**, *9*, 231–237. [CrossRef]
122. Jiang, R.H.Y.; Tyler, B.M.; Whisson, S.C.; Hardham, A.R.; Govers, F. Ancient origin of elicitin gene clusters in *Phytophthora* genomes. *Mol. Biol. Evol.* **2006**, *23*, 338–351. [CrossRef]
123. Osman, H.; Vauthrin, S.; Mikes, V.; Milat, M.-L.; Panabières, F.; Marais, A.; Brunie, S.; Maume, B.; Ponchet, M.; Blein, J.-P. Mediation of elicitin activity on tobacco is assumed by elicitin-sterol complexes. *Mol. Biol. Cell* **2001**, *12*, 2825–2834. [CrossRef]
124. Rodrigues, M.L.; Archer, M.; Martel, P.; Miranda, S.; Thomaz, M.; Enguita, F.J.; Baptista, R.P.; e Melo, E.P.; Sousa, N.; Cravador, A.; et al. Crystal structures of the free and sterol-bound forms of β-cinnamomin. *Biochim. Biophys. Acta Proteins Proteom.* **2006**, *1764*, 110–121. [CrossRef] [PubMed]
125. Boissy, G.; de La Fortelle, E.; Kahn, R.; Huet, J.-C.; Bricogne, G.; Pernollet, J.-C.; Brunie, S. Crystal structure of a fungal elicitor secreted by *Phytophthora cryptogea*, a member of a novel class of plant necrotic proteins. *Structure* **1996**, *4*, 1429–1439. [CrossRef]
126. Derevnina, L.; Dagdas, Y.F.; De la Concepcion, J.C.; Białas, A.; Kellner, R.; Petre, B.; Domazakis, E.; Du, J.; Wu, C.-H.; Lin, X.; et al. Nine things to know about elicitins. *New Phytol.* **2016**, *212*, 888–895. [CrossRef]
127. Nie, J.; Yin, Z.; Li, Z.; Wu, Y.; Huang, L. A small cysteine-rich protein from two kingdoms of microbes is recognized as a novel pathogen-associated molecular pattern. *New Phytol.* **2019**, *222*, 995–1011. [CrossRef]
128. Dokládal, L.; Obořil, M.; Stejskal, K.; Zdráhal, Z.; Ptáčková, N.; Chaloupková, R.; Damborský, J.; Kašparovský, T.; Jeandroz, S.; Žďárská, M.; et al. Physiological and proteomic approaches to evaluate the role of sterol binding in elicitin-induced resistance. *J. Exp. Bot.* **2012**, *63*, 2203–2215. [CrossRef] [PubMed]
129. Adachi, H.; Nakano, T.; Miyagawa, N.; Ishihama, N.; Yoshioka, M.; Katou, Y.; Yaeno, T.; Shirasu, K.; Yoshioka, H. WRKY transcription factors phosphorylated by MAPK regulate a plant immune NADPH oxidase in *Nicotiana benthamiana*. *Plant Cell* **2015**, *27*, 2645–2663. [CrossRef]

130. Bos, J.I.B.; Kanneganti, T.-D.; Young, C.; Cakir, C.; Huitema, E.; Win, J.; Armstrong, M.R.; Birch, P.R.J.; Kamoun, S. The C-terminal half of *Phytophthora infestans* RXLR effector AVR3a is sufficient to trigger R3a-mediated hypersensitivity and suppress INF1-induced cell death in *Nicotiana benthamiana*. *Plant J.* **2006**, *48*, 165–176. [CrossRef]
131. Haas, B.J.; Kamoun, S.; Zody, M.C.; Jiang, R.H.Y.; Handsaker, R.E.; Cano, L.M.; Grabherr, M.; Kodira, C.D.; Raffaele, S.; Torto-Alalibo, T.; et al. Genome sequence and analysis of the Irish potato famine pathogen *Phytophthora infestans*. *Nature* **2009**, *461*, 393–398. [CrossRef]
132. Masago, H. Selective inhibition of *Pythium* spp. on a medium for direct isolation of *Phytophthora* spp. from soils and plants. *Phytopathology* **1977**, *67*, 425–428. [CrossRef]
133. Cabral, A.; Oome, S.; Sander, N.; Küfner, I.; Nürnberger, T.; Van den Ackerveken, G. Nontoxic Nep1-like proteins of the downy mildew pathogen *Hyaloperonospora arabidopsidis*: Repression of necrosis-inducing activity by a surface-exposed region. *Mol. Plant Microbe Interact.* **2012**, *25*, 697–708. [CrossRef]
134. Oome, S.; Van den Ackerveken, G. Comparative and functional analysis of the widely occurring family of Nep1-like proteins. *Mol. Plant Microbe Interact.* **2014**, *27*, 1081–1094. [CrossRef] [PubMed]
135. Lenarčič, T.; Albert, I.; Böhm, H.; Hodnik, V.; Pirc, K.; Zavec, A.B.; Podobnik, M.; Pahovnik, D.; Žagar, E.; Pruitt, R.; et al. Eudicot plant-specific sphingolipids determine host selectivity of microbial NLP cytolysins. *Science* **2017**, *358*, 1431–1434. [CrossRef] [PubMed]
136. Lenarčič, T.; Pric, K.; Hodnik, V.; Albert, I.; Borišek, J.; Magistrato, A.; Nürnberger, T.; Podobnik, M.; Anderluh, G. Molecular basis for functional diversity among microbial Nep1-like proteins. *PLoS Pathog.* **2019**, *15*, e1007951. [CrossRef] [PubMed]
137. Bae, H.; Bowers, J.H.; Tooley, P.W.; Bailey, B.A. NEP1 orthologs encoding necrosis and ethylene inducing proteins exist as a multigene family in *Phytophthora megakarya*, causal agent of black pod disease on cacao. *Mycol. Res.* **2005**, *109*, 1373–1385. [CrossRef]
138. Chen, X.-R.; Xing, Y.-P.; Li, Y.-P.; Tong, Y.-H.; Xu, J.-Y. RNA-Seq reveals infection-related gene expression changes in *Phytophthora capsici*. *PLoS ONE* **2013**, *8*, e74588. [CrossRef]
139. Martins, I.M.; Meirinho, S.; Costa, R.; Cravador, A.; Choupina, A. Cloning, characterization, in vitro and *in planta* expression of a necrosis-inducing *Phytophthora* protein 1 gene npp1 from *Phytophthora cinnamomi*. *Mol. Biol. Rep.* **2019**, *46*, 6453–6462. [CrossRef]
140. Win, J.; Morgan, W.; Bos, J.; Krasileva, K.; Cano, L.M.; Chaparro-Garcia, A.; Ammar, R.; Staskawicz, B.J.; Kamoun, S. Adaptive evolution has targeted the C-terminal domain of the RXLR effectors of plant pathogenic oomycetes. *Plant Cell* **2007**, *19*, 2349–2369. [CrossRef]
141. Dou, D.; Kale, S.D.; Wang, X.; Jiang, R.H.; Bruce, N.A.; Arredondo, F.D.; Zhang, X.; Tyler, B.M. RXLR-mediated entry of *Phytophthora sojae* effector Avr1b into soybean cells does not require pathogen-encoded machinery. *Plant Cell* **2008**, *20*, 1930–1947. [CrossRef]
142. Kale, S.D.; Gu, B.; Capelluto, D.G.; Dou, D.; Feldman, E.; Rumore, A.; Arredondo, F.D.; Hanlon, R.; Fudal, I.; Rouxel, T.; et al. External lipid PI3P mediates entry of eukaryotic pathogen effectors into plant and animal host cells. *Cell* **2010**, *142*, 284–295. [CrossRef]
143. Joubert, M.; Backer, R.; Engelbrecht, J.; Berg, N.V.D. Expression of several *Phytophthora cinnamomi* putative RxLRs provides evidence for virulence roles in avocado. *PLoS ONE* **2021**, *16*, e0254645. [CrossRef]
144. Wang, S.; McLellan, H.; Bukharova, T.; He, Q.; Murphy, F.; Shi, J.; Sun, S.; van Weymers, P.; Ren, Y.; Thilliez, G.; et al. *Phytophthora infestans* RXLR effectors act in concert at diverse subcellular locations to enhance host colonization. *J. Exp. Bot.* **2019**, *70*, 343–356. [CrossRef]
145. Yang, B.; Wang, Q.; Jing, M.; Guo, B.; Wu, J.; Wang, H.; Wang, Y.; Lin, L.; Ye, W.; Dong, S.; et al. Distinct regions of the *Phytophthora* essential effector Avh238 determine its function in cell death activation and plant immunity suppression. *New Phytol.* **2017**, *214*, 361–375. [CrossRef] [PubMed]
146. Li, H.; Wang, H.; Jing, M.; Zhu, J.; Guo, B.; Wang, Y.; Lin, Y.; Chen, H.; Kong, L.; Ma, Z.; et al. A *Phytophthora* effector recruits a host cytoplasmic transacetylase into nuclear speckles to enhance plant susceptibility. *eLife* **2018**, *7*, e40039. [CrossRef] [PubMed]
147. Chen, X.-R.; Zhang, Y.; Li, H.-Y.; Zhang, Z.-H.; Sheng, G.-L.; Li, Y.-P.; Xing, Y.-P.; Huang, S.-X.; Tao, H.; Kuan, T.; et al. The RXLR effector PcAvh1 is required for full virulence of *Phytophthora capsici*. *Mol. Plant Microbe Interact.* **2019**, *32*, 986–1000. [CrossRef]
148. Branco, I.; Choupina, A. In Silico characterization of the Phytopathogenic efector, Avr3a, from *Phytophthora cinnamomi*. *J. Basic Appl. Sci.* **2020**, *16*, 20–30. [CrossRef]
149. Torto, T.A.; Li, S.; Styler, A.; Huitema, E.; Testa, A.; Gow, N.A.R.; van West, P.; Kamoun, S. EST mining and functional expression assays identify extracellular effector proteins from the plant pathogen *Phytophthora*. *Genome Res.* **2003**, *13*, 1675–1685. [CrossRef] [PubMed]
150. Schornack, S.; van Damme, M.; Bozkurt, T.O.; Cano, L.M.; Smoker, M.; Thines, M.; Gaulin, E.; Kamoun, S.; Huitema, E. Ancient class of translocated oomycete effectors targets the host nucleus. *Proc. Natl. Acad. Sci. USA* **2010**, *107*, 17421–17426. [CrossRef] [PubMed]
151. Stam, R.; Howden, A.J.M.; Delgado-Cerezo, M.; Amaro, T.M.M.M.; Motion, G.B.; Pham, J.; Huitema, E. Characterization of cell death inducing *Phytophthora capsici* CRN effectors suggests diverse activities in the host nucleus. *Front. Plant Sci.* **2013**, *4*, 387. [CrossRef] [PubMed]
152. Amaro, T.M.M.M.; Thilliez, G.J.A.; Motion, G.B.; Huitema, E. A perspective on CRN Proteins in the genomics age: Evolution, classification, delivery and function revisited. *Front. Plant Sci.* **2017**, *8*, 99. [CrossRef]

153. Cheung, F.; Win, J.; Lang, J.M.; Hamilton, J.; Vuong, H.; Leach, J.E.; Kamoun, S.; Lévesque, C.A.; Tisserat, N.; Buell, C.R. Analysis of the *Pythium ultimum* transcriptome using Sanger and pyrosequencing approaches. *BMC Genom.* **2008**, *9*, 542. [CrossRef]
154. Gaulin, E.; Madoui, M.-A.; Bottin, A.; Jacquet, C.; Mathé, C.; Couloux, A.; Wincker, P.; Dumas, B. Transcriptome of *Aphanomyces euteiches*: New oomycete putative pathogenicity factors and metabolic pathways. *PLoS ONE* **2008**, *3*, e1723. [CrossRef] [PubMed]
155. Lévesque, C.A.; Brouwer, H.; Cano, L.; Hamilton, J.P.; Holt, C.; Huitrma, E.; Raffaele, S.; Robideau, G.P.; Thines, M.; Win, J.; et al. Genome sequence of the necrotrophic plant pathogen *Pythium ultimum* reveals original pathogenicity mechanisms and effector repertoire. *Genome Biol.* **2010**, *11*, R73. [CrossRef] [PubMed]
156. Meyer, F.E.; Shuey, L.S.; Naidoo, S.; Mamni, T.; Berger, D.K.; Myburg, A.A.; Berg, N.V.D.; Naidoo, S. Dual RNA-sequencing of *Eucalyptus nitens* during *Phytophthora cinnamomi* challenge reveals pathogen and host factors influencing compatibility. *Front. Plant Sci.* **2016**, *7*, 191. [CrossRef] [PubMed]
157. Zhang, D.; Burroughs, A.M.; Vidal, N.D.; Iyer, L.M.; Aravind, L. Transposons to toxins: The provenance, architecture and diversification of a widespread class of eukaryotic effectors. *Nucleic Acids Res.* **2016**, *44*, 3513–3533. [CrossRef]
158. Li, Q.; Zhang, M.; Shen, D.; Liu, T.; Chen, Y.; Zhou, J.M.; Dou, D. A *Phytophthora sojae* effector PsCRN63 forms homo-/hetero-dimers to suppress plant immunity via an inverted association manner. *Sci. Rep.* **2016**, *6*, 26951. [CrossRef]
159. Bendahmane, A.; Querci, M.; Kanyuka, K.; Baulcombe, D.C. Agrobacterium transient expression system as a tool for the isolation of disease resistance genes: Application to the Rx2 locus in potato. *Plant J.* **2000**, *21*, 73–81. [CrossRef]
160. Van der Hoorn, R.A.L.; Laurent, F.; Roth, R.; De Wit, P.J.G.M. Agroinfiltration is a versatile tool that facilitates comparative analyses of Avr 9/Cf-9-induced and Avr4/Cf-4-induced necrosis. *Mol. Plant Microbe Interact.* **2000**, *13*, 439–446. [CrossRef]
161. Wroblewski, T.; Tomczak, A.; Michelmore, R. Optimization of Agrobacterium-mediated transient assays of gene expression in lettuce, tomato and *Arabidopsis*. *Plant Biotechnol. J.* **2005**, *3*, 259–273. [CrossRef]
162. Lee, M.W.; Yang, Y. Transient expression assay by agroinfiltration of leaves. In *Arabidopsis Protocols*; Springer: New York, NY, USA, 2006; pp. 225–229.
163. Ramirez-Garcés, D.; Camborde, L.; Pel, M.J.C.; Jauneau, A.; Martinez, Y.; Néant, I.; Leclerc, C.; Moreau, M.; Dumas, B.; Gaulin, E. CRN 13 candidate effectors from plant and animal eukaryotic pathogens are DNA-binding proteins which trigger host DNA damage response. *New Phytol.* **2016**, *210*, 602–617. [CrossRef]
164. Goodin, M.M.; Zaitlin, D.; Naidu, R.A.; Lommel, S.A. *Nicotiana benthamiana*: Its history and future as a model for plant–pathogen interactions. *Mol. Plant Microbe Interact.* **2008**, *21*, 1015–1026. [CrossRef]
165. Kamoun, S.; Goodwin, S.B. Fungal and oomycete genes galore. *New Phytol.* **2007**, *174*, 713–717. [CrossRef] [PubMed]
166. Studholme, D.; McDougal, R.; Sambles, C.; Hansen, E.; Hardy, G.; Grant, M.; Ganley, R.J.; Williams, N.M. Genome sequences of six *Phytophthora* species associated with forests in New Zealand. *Genom. Data* **2016**, *7*, 54–56. [CrossRef] [PubMed]
167. Langmuir, A.L.; Beech, P.L.; Richardson, M.F. Draft genomes of two Australian strains of the plant pathogen, *Phytophthora cinnamomi*. *F1000Research* **2017**, *6*, 1972. [CrossRef]
168. Kunjeti, S.G.; Evans, T.A.; Marsh, A.G.; Gregory, N.F.; Kunjeti, S.; Meyers, B.C.; Kalavacharla, V.S.; Donofrio, N.M. RNA-Seq reveals infection-related global gene changes in *Phytophthora phaseoli*, the causal agent of lima bean downy mildew. *Mol. Plant Pathol.* **2012**, *13*, 454–466. [CrossRef]
169. Westermann, A.J.; Gorski, S.A.; Vogel, J. Dual RNA-seq of pathogen and host. *Nat. Rev. Microbiol.* **2012**, *10*, 618–630. [CrossRef]
170. Hayden, K.J.; Garbelotto, J.M.; Knaus, B.J.; Cronn, R.C.; Wright, J.W. Dual RNA-seq of the plant pathogen *Phytophthora ramorum* and its tanoak host. *Tree Genet. Genomes* **2014**, *10*, 489–502. [CrossRef]
171. Reitmann, A.; Berger, D.K.; Berg, N.V.D. Putative pathogenicity genes of *Phytophthora cinnamomi* identified via RNA-Seq analysis of pre-infection structures. *Eur. J. Plant Pathol.* **2017**, *147*, 211–228. [CrossRef]
172. Judelson, H.S. Recent advances in the genetics of oomycete plant pathogens. *Mol. Plant Microbe Interact.* **1996**, *9*, 443–449. [CrossRef]
173. Dai, T.; Xu, Y.; Yang, X.; Jiao, B.; Qiu, M.; Xue, J.; Arredondo, F.; Tyler, B.M. An improved transformation system for *Phytophthora cinnamomi* using green fluorescent protein. *Front. Microbiol.* **2021**, *12*, 682754. [CrossRef]
174. Bailey, A.M.; Mena, G.L.; Herrera-Estrella, L.R. Genetic transformation of the plant pathogens *Phytophthora capsici* and *Phytophthora parasitica*. *Nucleic Acids Res.* **1991**, *19*, 4273–4278. [CrossRef]
175. Judelson, H.S.; Tyler, B.M.; Michelmore, R.W. Transformation of the oomycete pathogen, *Phytophthora infestans*. *Mol. Plant-Microbe Interact.* **1991**, *4*, 602–607. [CrossRef] [PubMed]

Chapter 2

Identification of *Phytophthora cinnamomi* CRN effectors and their roles in manipulating cell death during *Persea americana* infection

In review with BMC Genomics

4th October 2023

Identification of *Phytophthora cinnamomi* CRN effectors and their roles in manipulating cell death during *Persea americana* infection

Kayla A. Midgley, Noëlani van den Berg, Robert Backer and Velushka Swart*

Hans Merensky Chair in Avocado Research, Department of Biochemistry; Genetics and Microbiology; Forestry and Agricultural Biotechnology Institute; University of Pretoria; Pretoria 0002; South Africa

Keywords: Plant-pathogen interactions, Crinkler effectors, molecular characterisation, *in silico*, protein prediction, alleles, *Phytophthora*, hemibiotroph.

*** Correspondence:**

Velushka Swart: velushka.swart@fabi.up.ac.za

Abstract

The oomycete *Phytophthora cinnamomi* is a devastating plant pathogen with a notably broad host range. It is the causal agent of Phytophthora root rot (PRR), arguably the most economically important yield-limiting disease in *Persea americana* (avocado). Despite this, our understanding of the mechanisms *P. cinnamomi* employs to infect and successfully colonise avocado remains limited, particularly regarding the pathogen's ability to maintain its biotrophic and necrotrophic lifestyles during infection. The pathogen utilises a large repertoire of effector proteins which function in facilitating and establishing disease in susceptible host plants. Crinkling and necrosis effectors (CRN/Crinklers) are suspected of manipulating cell death to aid in maintenance of the pathogens biotrophic and necrotrophic lifestyles during different stages of infection. The current study identified 25 *P. cinnamomi CRN* effectors from the GKB4 genome using an HMM profile and assigned putative function to them as either cell death inducers or suppressors. Function was assigned to 10 PcinCRNs by analysing their RNA-seq expression profiles, relatedness to other functionally characterised *Phytophthora* CRNs and tertiary protein predictions. The full-length coding sequences for these *PcinCRNs* were confirmed by Sanger sequencing. Six of which were found to have two alleles, potentially indicating that the proteins encoded by these alleles may perform contradicting functions in cell death manipulation, or function in different host plant species. Overall, this study provides a foundation for future research on *P. cinnamomi* infection and cell death manipulation mechanisms.

Background

Phytophthora cinnamomi (Rands.) is a soil-borne, hemi-biotrophic oomycete. This pathogen is most often associated with root rot diseases, interfering with water uptake and transport to shoots, which subsequently causes leaf wilting, chlorosis and plant death (1). Due to the pathogens' extensive host range (known to infect more than 5000 plant species) (1), *P. cinnamomi* is regarded as one of the most devastating plant pathogens worldwide and causes significant losses to both agricultural and forestry crops with the most significant food losses occurring in avocados (*Persea americana* (Mill.)) (2-8). The pathogen is also known for damaging the environment and impeding attempts to mitigate climate change, where diseases caused by *P. cinnamomi* could become more severe in regions where the pathogen is already present (3-6, 9, 10).

Despite the economic and ecological relevance of this pathogen, the mechanisms *P. cinnamomi* utilises to infect and successfully colonise host plants are still largely unknown. In particular, there is little to no knowledge on how *P. cinnamomi* maintains a biotrophic lifestyle early in infection, or switches to a necrotrophic lifestyle later during infection (11). A likely mechanism utilised to promote biphasic infection would be suppression of the hypersensitive response (HR) during the biotrophic phase and subsequent promotion during the necrotrophic phase (11-14). The HR is a specialised form of programmed cell death (PCD), involving rapid localised cell death at the site of pathogen penetration and is often associated with disease resistance (15, 16). This phenomenon can however benefit either the pathogen or the host plant, depending on the lifestyle the pathogen adopts (17). *P. cinnamomi*, like other *Phytophthora* spp., has likely developed strategies to 'hijack' the host plant's cell death machinery/pathway, causing HR suppression or induction at inappropriate stages of infection (3, 13-15, 18, 19). This could be accomplished through the differential expression and delivery of cell death-manipulating effectors at different infection stages. During the necrotrophic phase of the pathogen, effector proteins that promote cell death would be expressed, while effectors that suppress cell death would be expressed during the biotrophic phase. The functional characterisation of *Phytophthora* effectors has revealed numerous effectors that function in the manipulation of HR (3, 14).

One class of *Phytophthora* effectors that have been repeatedly implicated in cell death suppression and induction are the crinkling and necrosis effectors (CRN/Crinklers). In *Phytophthora* spp., *CRNs* are composed of large multi-gene families that encode cytoplasmic effector proteins (20). CRN protein sequences possess a highly conserved N-terminal domain containing the LXLFLAK and HVLVXXP motifs, followed by a variable C-terminal. These effectors were originally identified by their ability to induce crinkling and necrosis in plant tissue, but research has revealed CRNs also function in targeting host factors to suppress plant defences and play important roles in cell death (12, 13, 18-24). A dual RNA-sequencing (RNA-seq) experiment of the compatible interaction between *Eucalyptus nitens* and *P. cinnamomi* found that the most abundantly expressed *P. cinnamomi* gene was a putative *CRN* effector (25). This same CRN from *P. cinnamomi* was found

to be closely related to CRN1 from *Phytophthora infestans*, an effector that induces necrosis in host plants. Suggesting that the CRN from *P. cinnamomi* may play a similar role in inducing cell death (20).

Some *Phytophthora* spp. have been shown to have at least two CRNs with contradicting functions - where one suppresses and the other induces cell death - with both effectors being essential for virulence (11, 12, 18). Computational and functional genomic approaches were used to study two *Phytophthora sojae* CRN effectors - PsCRN63 and PsCRN115 (18). This work was later supplemented with characterisation using *Agrobacterium tumefaciens* infiltration assays in *Nicotiana benthamiana* were performed to reveal the function of these PsCRNs. The study found that PsCRN63 induced cell death and PsCRN115 suppressed cell death while subsequent silencing of one or both *PsCRN*s revealed that both were required for virulence. Similar results were found in PpCRN7 and PpCRN20 from *Phytophthora parasitica* (12). *A. tumefaciens* infiltration assays in *N. benthamiana* were also conducted using these two PpCRNs, which showed that PpCRN7 increased HR through an additive effect while PpCRN20 suppressed HR. Despite the contradicting functions of PpCRN7 and PpCRN20 in cell death, both effectors were found to increase *N. benthamiana* susceptibility to *P. parasitica*. These examples indicate there is a complex relationship between *Phytophthora* CRNs and the cell death pathways within host plant cells, making them important targets for further research.

Our research identified *P. cinnamomi* CRN (PcinCRN) effectors and assigned putative functions in cell death manipulation during *P. americana* infection. PcinCRNs were identified by searching the *P. cinnamomi* GKB4 genome using a Hidden Markov model (HMM). Putative functions were assigned through analysing *PcinCRN* expression profiles during *P. americana* infection, Sanger sequencing data, phylogenetic comparison to other functionally characterised *Phytophthora* CRNs and protein folding predictions. This study identified 10 PcinCRNs with putative roles in cell death manipulation, and *PcinCRN* alleles that provide contradicting evidence to functions in cell death manipulation.

Results

Identification and validation of full-length PcinCRN effectors

A repertoire of 25 PcinCRN effectors were identified and validated as 'true' PcinCRN effector proteins (Table 1 and Figure 1) - by the presence of two conserved motifs in the N-terminal (LXLFLAK and HVLVXXP) and the absence of a TMH – out of a list of 46 putative PcinCRNs generated from the *P. cinnamomi* GKB4 genome (Supplementary Table 1 and 2). A partial/CRN-like sequence (PcinCRNpartial1) was also identified from the list of putative PcinCRNs - but was excluded from subsequent analyses. A phylogenetic analysis revealed that all 25 PcinCRNs had homology to CRNs from other *Phytophthora* spp. with posterior probabilities > 0.5, supporting their designation as 'true' CRNs (Supplementary Figure 1).

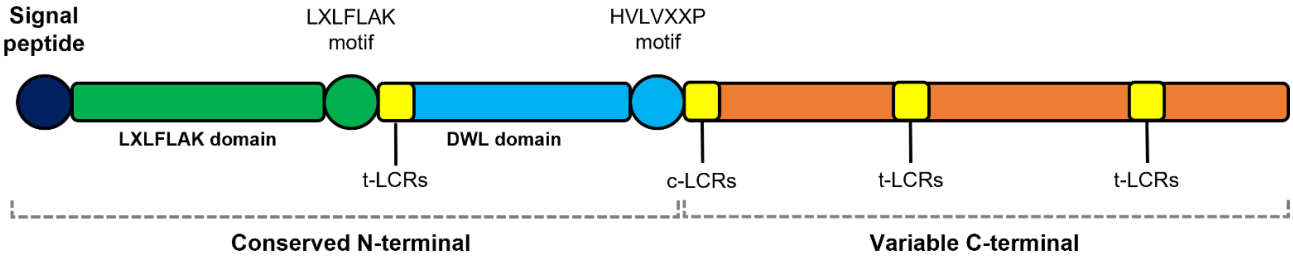

Figure 1. Schematic of a 'true' *Phytophthora* CRN effector protein. The characteristic *Phytophthora cinnamomi* crinkling and necrosis (PcinCRN) architecture includes a highly conserved N-terminal with two conserved motifs (LXLFLAK and HVLVXXP), within the LXLFLAK and DWL domains which function in the translocation of the effector from the apoplast into the host plants' cytoplasm. This is followed by a variable C-terminal that conveys various functions. CRNs do not always contain a signal peptide due to the existence of alternative secretion pathways. Yellow regions indicate regions where terminal and central low complexity regions (t-LCRs and c-LCRs, respectively) can be found. Figure adapted from Midgley *et al* (2022) (14).

Table 1: List of 25 full-length PcinCRN effector proteins. The crinkling and necrosis (PcinCRN) effector architecture of all 25 PcinCRNs identified and validated as 'true' full-length *Phytophthora cinnamomi* CRN effector proteins. A PcinCRN was validated as a 'true' *Phytophthora* CRN if the sequence contained both the LXLFLAK and HVLVXXP motifs and did not contain a trans membrane helix (TMH). The presence/absence of a signal peptide, TMH, low complexity regions (LCR's), LXLFLAK and HVLVXXP motif are indicated.

Sequence ID	Signal peptide	TMH	LXLFLAK motif	HVLVXXP motif	Low Complexity regions (LCR's)
PcinCRN11	Yes	No	Yes[1]	Yes	Central & terminal LCR
PcinCRN25	Yes	No	Yes[1]	Yes	Terminal LCR
PcinCRN29	Yes	No	Yes[1]	Yes[2]	None
PcinCRN30	Yes	No	Yes	Yes	Central LCR
PcinCRN31	Yes	No	Yes	Yes[2]	Terminal LCR
PcinCRN33	No	No	Yes	Yes[1]	Central LCR
PcinCRN35	Yes	No	Yes[1]	Yes[1]	None
PcinCRN47	No	No	Yes	Yes[1]	Central & terminal LCR
PcinCRN50	Yes	No	Yes[1]	Yes	Terminal LCR
PcinCRN51	No	No	Yes[1]	Yes	None
PcinCRN52	No	No	Yes	Yes	Central LCR
PcinCRN53	No	No	Yes	Yes	None
PcinCRN56	No	No	Yes	Yes[2]	Central & terminal LCR
PcinCRN57	No	No	Yes[1]	Yes[1]	None
PcinCRN73	Yes	No	Yes	Yes[1]	None
PcinCRN74	No	No	Yes	Yes	Central LCR
PcinCRN75	Yes	No	Yes	Yes	None
PcinCRN77	Yes	No	Yes	Yes[1]	None
PcinCRN79	Yes	No	Yes	Yes	None
PcinCRN81	Yes	No	Yes	Yes[2]	Central & terminal LCR
PcinCRN83	Yes	No	Yes	Yes[2]	None
PcinCRN86	Yes	No	Yes[1]	Yes[1]	Terminal LCR
PcinCRN87	Yes	No	Yes	Yes	Terminal LCR
PcinCRN90	Yes	No	Yes	Yes[2]	None
PcinCRN95	No	No	Yes	Yes	Central LCR

[1] The motif differs by a single amino acid; [2] The sequence was manually annotated in Integrated Genome Viewer 2.7.2.

The repertoire generated in this study was compared to the results of putative PcinCRN identified by Hardham and Blackman (1) and Engelbrecht *et al.* (26) in previous studies (Figure 2, Supplementary Table 3A and 3B). Hardham and Blackman (1) identified 49 putative PcinCRN sequences; but we validated only 10 as 'true' PcinCRN effectors and two as partial/CRN-like sequences. Eight of these 'true' PcinCRNs were present in the current studies PcinCRN repertoire. Additionally, we determined that twenty-four of the 49 putative PcinCRN sequences identified by Engelbrecht *et al.* (26) were 'true' PcinCRN effectors. All 'true' PcinCRNs from Engelbrecht *et al.* (26) were present in the repertoire identified by the current study.

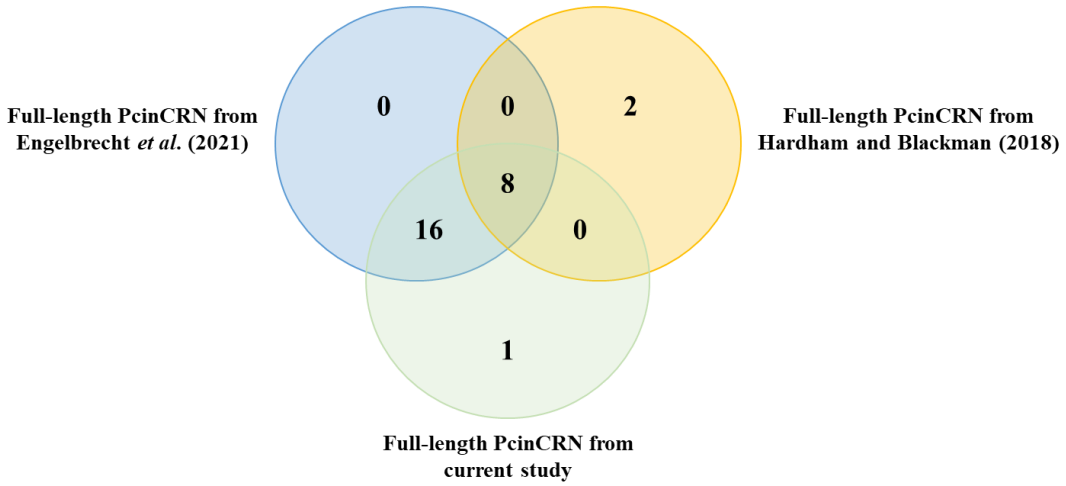

Figure 2. Comparison of *Phytophthora cinnamomi* CRN repertoires from three studies. Venn diagram illustrating the comparison of full-length 'true' *Phytophthora cinnamomi* crinkling and necrosis (PcinCRN) effectors identified from Hardham and Blackman (2018) (1), Engelbrecht *et al.* (2021) (26) and the current study. There are 10 'true' PcinCRNs in the repertoire from Hardham and Blackman (2018) (1), 24 in the repertoire from Engelbrecht *et al.* (2021) (26) and 25 from the current studies repertoire list. Eight PcinCRNs from Hardham and Blackman (2018) (1) are shared among the PcinCRNs from Engelbrecht *et al.* (2021) (26) and the current study Sixteen PcinCRNs from Engelbrecht *et al.* (2021) (26) was shared the PcinCRNs from the current study. The current study identified one PcinCRN which was unique.

Expression analyses of *PcinCRNs* during infection of avocado

During infection of the susceptible avocado rootstock (R0.12), the expression of *PcinCRNs* genes were compared to mycelia at 6-, 12-, 24-, and 120 hpi (Figure 3A, Supplementary Table 4). In comparison to mycelia, 18 *PcinCRNs* were significantly differentially expressed at one or more time points. Nine of these *PcinCRNs* were significantly downregulated during the biotrophic (6-, 12-, and 24 hpi) and necrotrophic (120 hpi) stages compared to mycelia. *PcinCRN29, PcinCRN31, PcinCRN35, PcinCRN83, PcinCRN86* and *PcinCRN87* were significantly downregulated by more than 4-fold (*p*adj <0.05) only during the necrotrophic stage compared to the mycelial control. *PcinCRN74* expression was significantly downregulated by more than 3-fold (*p*adj < 0.05) only during the biotrophic phase at 6-, 12-, and 24 hpi. *PcinCRN90* expression was significantly 2.53-fold downregulated (*p*adj < 0.05) compared to mycelial expression, during the early stage of the biotrophic stage at 6 hpi During the necrotrophic stage, *PcinCRN52* expression was 4.82-fold upregulated (*p*adj < 0.05) compared to the mycelial control.

During infection of the partially resistant avocado rootstock (Dusa®), the expression of *PcinCRNs* genes were compared to mycelia at 6-, 12-, 24-, and 120 hpi (Figure 3B, Supplementary Table 5). A total of 19 *PcinCRNs* were found to be significantly differentially expressed at one or more time points compared to mycelia. Twelve of these *PcinCRNs* were significantly downregulated during the biotrophic (6-, 12-, and 24 hpi) and necrotrophic (120 hpi) stages compared to mycelia. *PcinCRN29, PcinCRN83,* and *PcinCRN86* were significantly downregulated by more than 2-fold (*p*adj < 0.10 and

< 0.05, respectively) only during the necrotrophic stage compared to the mycelial control. The expression of *PcinCRN30* and *PcinCRN81* was upregulated by 20.86 and 40.00-fold, respectively (*p*adj <0.10), during the biotrophic stage at 12 hpi compared to the mycelial control. *PcinCRN31* and *PcinCRN95* were both upregulated by more than 5-fold (*p*adj < 0.10 and < 0.05, respectively) during the biotrophic stage compared to mycelia respectively and were subsequently downregulated by more than 35-fold during the necrotrophic stage compared to mycelia.

PcinCRN expression during infection of susceptible R0.12 was compared over time (6-, 12-, 24- and 120 hpi) (Figure 3C, Supplementary Table 6). In comparison to other time points, nine *PcinCRNs* were significantly differentially expressed at one or more time points. During the biotrophic stage, the expression of eight *PcinCRNs* (*PcinCRN11, 31, 33, 35, 73, 75, 77,* and *79*) increased by more than 2-fold (*p*adj < 0.05) compared to the necrotrophic stage (6-, 12- and 24 hpi compared to 120 hpi). Six PcinCRNs (*PcinCRN11, 33, 73, 75, 77,* and *79*) upregulated during 12- and 24 hpi (compared to 120 hpi) of the biotrophic stage were found to be downregulated by more than 4-fold (padj < 0.05) during the earliest stage of infection at 6 hpi (compared to 12- and 24 hpi).

PcinCRN expression during infection of partially resistant Dusa® was also compared over time (Figure 3D). Seven *PcinCRNs* (*PcinCRN31, 35, 74, 79, 83, 86* and *95*) were significantly upregulated more than 3-fold during the biotrophic stage compared to the necrotrophic stage (*p*adj <0.1 and <0.05). One *PcinCRNs* expression (*PcinCRN74*) that was upregulated at 12 hpi (compared to 120 hpi) during the biotrophic stage was downregulated by 13.87-fold (padj < 0.1) during early infection at 6 hpi (compared to 12- and 24 hpi). *PcinCRN75* and *PcinCRN79* expression was increased by more than 3-fold during the early infection stage (6- vs 12 hpi, *p*adj <0.1). During the biotrophic stage, the expression of *PcinCRN77* was significantly reduced by more than 6-fold compared to the necrotrophic stage (*p*adj < 0.05).

Expression of *PcinCRNs* during infection of R0.12 (incompatible interaction) was compared to their expression during infection of Dusa® (compatible interaction) (Figure 3E, Supplementary Table 7). Expression of *PcinCRN11, PcinCRN33, PcinCRN53, PcinCRN75* and *77* were increased by more than 7-fold in R0.12 compared to Dusa® during the biotrophic stage (*p*adj < 0.1 and < 0.05). *PcinCRN74* expression was decreased by 4.31-fold during the biotrophic stage in R0.12 compared to Dusa® (*p*adj < 0.1).

CRN effectors are cell death manipulators and are classified as either inducers or suppressors of cell death (12, 13, 18-24). RNA-seq analysis identified 13 *PcinCRNs* as putative cell death manipulators. Of the 13, 12 demonstrated the expression patterns of a cell death suppressor (*PcinCRN11, PcinCRN30, PcinCRN31, PcinCRN33, PcinCRN53, PcinCRN73, PcinCRN75, PcinCRN77, PcinCRN81, PcinCRN83, PcinCRN86* and *PcinCRN95*) and only one as a cell death inducer (*PcinCRN52*). (Supplementary Tables 4-8). The RNA-seq expression data for four *PcinCRNs* (*PcinCRN74, PcinCRN79, PcinCRN90*, and *PcinCRN95*) were validated using RT-qPCR, at 12 and 24 hpi (Supplementary Figure 2).

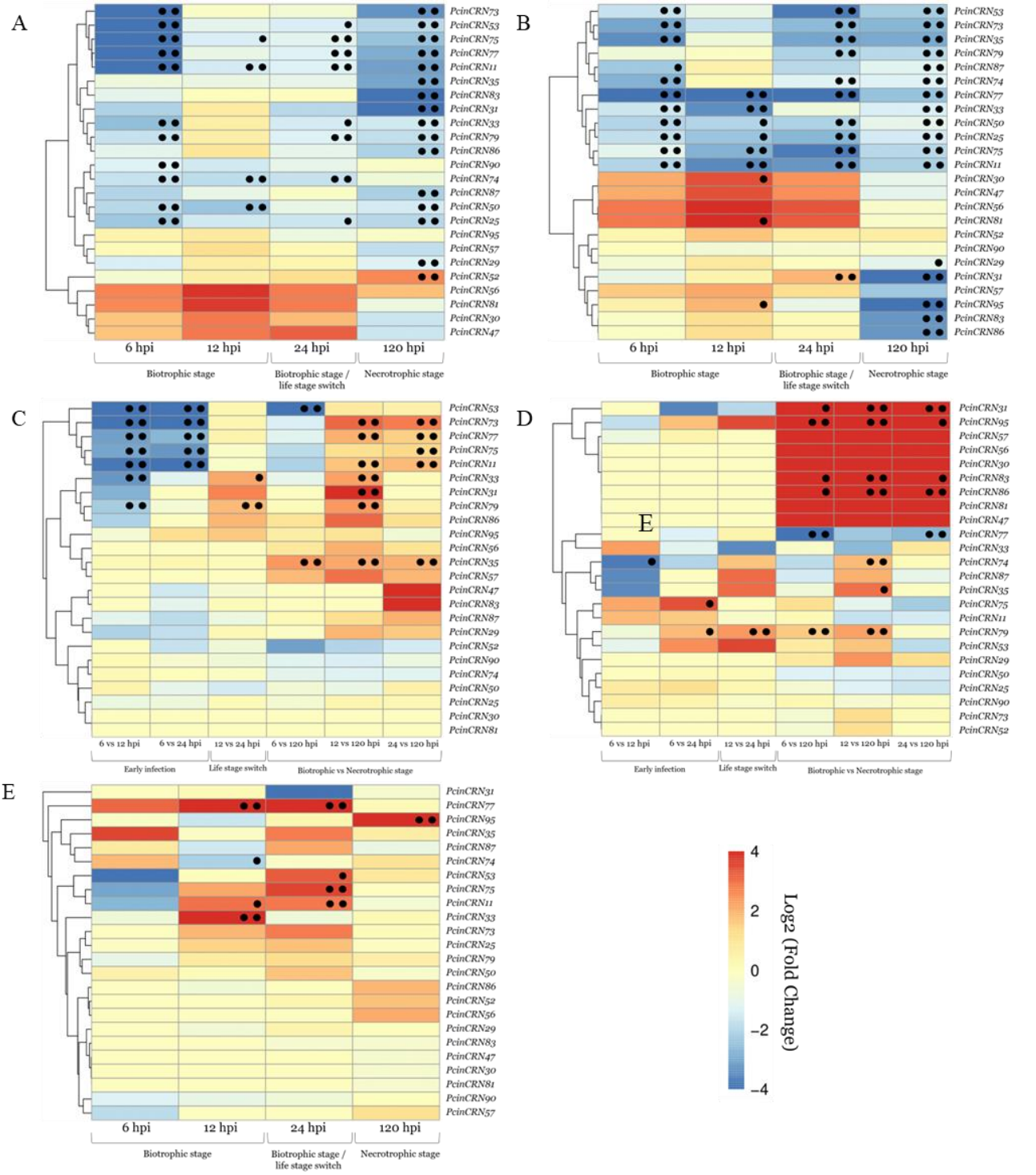

Figure 3. Heatmap depicting the expression of *PcinCRNs* during infection of R0.12 and Dusa® by *Phytophthora cinnamomi*. (A) *PcinCRN* expression during infection of R0.12 compared to mycelia. *(B) PcinCRN* expression during infection of Dusa® compared to mycelia. (C) *PcinCRN* expression during infection of R0.12. (D) Comparison of *PcinCRN* expression at different time points during infection Dusa®. (E) Comparison of *PcinCRN* expression at different time points during infection of R0.12 was compared (in-compatible interaction) to the expression in Dusa® (compatible interaction). Expression was compared at 6-, 12-, 24- and 120 hpi. The late biotrophic stage or the possible time-point where the pathogen switches over to the necrotrophic stage is considered as 24 hpi. The necrotrophic stage occurs at 120 hpi. Differential expression was visualised using Log_2 (Fold Change) and significant differentially expressed genes (DEGs) were identified as those with a Log_2 (Fold Change) ≥1 or ≤-1. Statistical significance was determined using the Benjamini-Hochberg false discovery rate (FDR) method and applying significance cut-off's (adjusted *p*-value) of < 0.1 (denoted by a single black dot) and < 0.05 (denoted by two black dots).

Confirmation of the full-length coding sequences of putative cell death manipulating *PcinCRNs*

The full-length coding sequence of 10 *PcinCRNs* were confirmed following Sanger sequencing of *P. cinnamomi* cDNA. (Table 2, Supplementary Table 9). The sequencing data demonstrated that the first 150 base pairs following the start codon of *PcinCRN77* differed from the original genome assembly annotation. Further analysis using Integrated Genome Viewer 2.7.2 (IGV) revealed that the error was likely due to the incorrect assembly of sequencing reads in this region. *PcinCRN77* was the only candidate *PcinCRN* whose nucleotide sequence differed from the original genome annotation, resulting in amino acid sequence variation. Although the amino acid sequence of PcinCRN77 was altered, both conserved CRN motifs (LXLFLAK and HVLVXXP) were present.

Table 2: Gene structure of confirmed full-length *PcinCRNs*. The full-length coding sequence was obtained for 10 *Phytophthora cinnamomi* crinkling and necrosis (*PcinCRN*) effector genes via Sanger sequencing of *P. cinnamomi* cDNA pooled from RNA isolated during infection of a susceptible *Persea americana* rootstock (R0.12) at 6, 12, 24 hpi. These data were compared to original genome annotation of the candidate *PcinCRNs* (26). Six *PcinCRNs* had alleles, of which the single nucleotide polymorphisms (SNPs), consecutive nucleotide substitutions and deletions between the alleles are indicated. *PcinCRN11* underwent alternative splicing. The presence of a nuclear localisation signal (NLS) for each PcinCRN was determined via NLStradamus using a 4 state HMM static model with a Posterior cut-off of 0.3.

PcinCRN ID	Number of introns	Consecutive nucleotide substitutions	SNPs	INDELs	Alleles	NLS
PcinCRN11	1	N/A	N/A	NO	1*	NO
PcinCRN30	0	N/A	1	NO	2	NO
PcinCRN52	1	N/A	N/A	NO	1	YES
PcinCRN53	1	N/A	9	YES	2	YES
PcinCRN73	0	7	5	YES	2	NO
PcinCRN75	0	19	15	YES	2	NO
PcinCRN77	0	N/A	N/A	NO	1	NO
PcinCRN81	0	N/A	1	NO	2	NO
PcinCRN86	0	N/A	N/A	NO	1	NO
PcinCRN95	0	N/A	11	NO	2	NO

SNPs: Single nucleotide polymorphisms; INDELS: Insertion or deletion; NLS: Nuclear localisation signal; * Alternative splicing occurs in one of the alleles, resulting in the translation of a different protein sequence.

Sequencing results revealed two alleles in the *P. cinnamomi* GKB4 genome sequence for six of the *PcinCRN* candidates (*PcinCRN30, PcinCRN53, PcinCRN73, PcinCRN75, PcinCRN81* and *PcinCRN95*). Alleles for *PcinCRN30* and *PcinCRN81* were constituted by a single nucleotide polymorphism (SNP), which resulted in a single non-synonymous amino acid change (Supplementary Figure 3). *PcinCRN95* had a total of 11 SNPs, seven of which resulted in non-

synonymous amino acid changes (*PcinCRN95_1* and *PcinCRN95_2*) (Figure 4A). The sequence of *PcinCRN53* contained nine SNPs, seven of which resulted in non-synonymous amino acid changes (*PcinCRN53_1* and *PcinCRN53_2*) (Figure 4B). Additionally, *PcinCRN53* had a 12 bp deletion that resulted in the deletion of a cysteine, glycine, arginine, and lysine from this region. Non-synonymous amino acid changes between alleles were not only the result of SNPs and nucleotide deletions, alleles of *PcinCRN73* and *PcinCRN75* demonstrated consecutive nucleotide substitutions (Figure 5).

Evidence of alternative splicing was discovered, which produced a variant of *PcinCRN11* (*PcinCRN11_2*) (Figure 6). The cDNA sequence of *PcinCRN11_1* showed no evidence of intron splicing, with the coding sequence consisting of the first of two exons and an intron containing a termination site. However, *PcinCRN11_1* is alternatively spliced to remove the intron, resulting in *PcinCRN11_2* to include both exons (Figure 6B).

To confirm the presence of all *PcinCRN* alleles, the gDNA of two additional *P. cinnamomi* isolates (Pcin_isolate129 and Pcin_isolate308) were sequenced. All the alleles for *PcinCRN53, PcinCRN75,* and *PcinCRN95* were indeed present in the genomes of both isolates, while *PcinCRN73_1* was confirmed only in Pcin_isolate129 and *PcinCRN73_2* was confirmed only in Pcin_isolate308 (Supplementary Table 10).

A PcinCRN95_ and PcinCRN95_2

```
                                20                                  40                                  60                                  80
                                |                                   |                                   |                                   |
PcinCRN95_1  MVKLFCAIVG EAGSSFSVRV DETDSVDDLK KAIKAEKMYQ FPADELQLFL AKTEGGAWLK SKDLLRMRKG EIPDEVESRY 80
PcinCRN95_2  MVKLFCAIVG EAGSSFSVRV DETDSVDDLK KAIKAEKMYQ FPADELQLFL AKTEGGAWLK SKDLLRMRKG EIPDEVESRY 80
                               100                                 120                                 140                                 160
                                |                                   |                                   |                                   |
PcinCRN95_1  MKEELDDPTD KICAKFPSTI PDGTIHVLVL VPRKSQLEWQ STQLRPHIYD PNSKYFLLEK EVMDDSGLPP SRVTLYCRPA 160
PcinCRN95_2  MKEELDDPTD KICAKFPSTI PDGTIHVLVL VPRKSQLEWQ STQLRPHIYD PNSKYFLLEK EVMDDSGLPP SRVTLYCRPA 160
                               180                                 200                                 220                                 240
                                |                                   |                                   |                                   |
PcinCRN95_1  FHMQIEFLRE RVLREGRLGW ILGPPGTGKS TTAMAFALTV DRREWVVTWI HVDTHLKWRC VRLVGGERQT RVVDITELKD 240
PcinCRN95_2  FHMQIEFLRE RVLREGRLGW ILGPPGTGKS TTAMAFALTV DRREWVVTWI HVGTHLKWRC VRLVGGERQT RVVDITELKD 240
                               260                                 280                                 300                                 320
                                |                                   |                                   |                                   |
PcinCRN95_1  VLEFGGDTKH HLVLVDGWTA AESFTNLSVM CSEWFLQKDA VMARRLAFIC SVAARGKISD NVDLLTGAME CQVWSWTLDE 320
PcinCRN95_2  VLEFGGDTKH HLVLVDGWTA AESFTNLSVI CSEWFLQKDA VMARRLAFIC SVAARGKISD NVDLLTGAME CQVWSWTLDE 320
                               340                                 360                                 380                                 400
                                |                                   |                                   |                                   |
PcinCRN95_1  YLDATTDGEF FTEVSPNLDA TVGDESAMVR TKYYYAGGSC RYMFCFNTEQ VMEKLNRAVD SLNDVAIVAT TGQRSSLSVN 400
PcinCRN95_2  YLDSTTDGEF FTEVSPNLDA TVGDESAMVR TKYYYAGGSC RYMFCFNTEQ VMEKLNRAVD SLNDVAIVAT TGQHSSLSVN 400
                               420                                 440                                 460                                 480
                                |                                   |                                   |                                   |
PcinCRN95_1  RLFAMFKRTS GVGEVSPVVS GYASATIGVR CGPEAIKMFM LTHQGDSNPA LNGWMLEMLF FSSIRNGGLD MINAAGNKIG 480
PcinCRN95_2  RLFAMFKRTS GVGEVSPVVS GYASATIGVR CGPEAIKMFM LTHQGDSNPA LNGWMLEMLF FSSIRNGGLD MINAAGNKIG 480
                               500                                 520                                 540                                 560
                                |                                   |                                   |                                   |
PcinCRN95_1  NWDEATVVVS DGIPALPPSS RVWIKPEKWN QGGYDAIMVD KKKRHVQMIQ ITSAHTHALH LNYFYLWLDA LVKSRETFEI 560
PcinCRN95_2  NWDEATVVVS DGIPVLPPSS RVWIKPEKWN QGGYDAIMVD KKKRHVQMIQ ITSAHTHTLH LNYFYLWLDA LVKSRETFEI 560
                               580                                 600
                                |                                   |
PcinCRN95_1  KLLEIIFVVE SDKLNDFSIS KVTGQGLLKP FGWKPSKELD HVKFVGIRGV FNL 613
PcinCRN95_2  KLLEIIFVVE SDKLNDFSIS TVTGQGLLKP FGWKPSKELD HVKFVGIRGV FNL 613
```

B PcinCRN53_ and PcinCRN53_2

```
                                20                                  40                                  60                                  80
                                |                                   |                                   |                                   |
PcinCRN53_1  MEQLPPGPKQ PPATCIACGA DRGGGQDVPQ VRQSDPESSG AAPPPESRVS VRRGELGSFQ TCRKCGRKFT TAASLSLHLL 80
PcinCRN53_2  MEQLPPGPKQ PPATCIACGA DRGGGQDVPQ VRQSDAESSG AAPPPESRVS VRRGELGSFH TCRK----FT TAASLSLHLL 76
                               100                                 120                                 140                                 160
                                |                                   |                                   |                                   |
PcinCRN53_1  KATPCDAPEA ARSGAFKCEN FSEKCNEVFA SARSLFAHHS RVYACDDPTR KRCAIVGQVG SSFDVEIDDG AKVSKLKKAI 160
PcinCRN53_2  KATPCDAPEA TRSGAFKCEN FSEKCNEVFV SARSLFAHHS RVYACDDPTR KRCAIVGQVG SSFDVEIDDG AKVSKLKKAI 156
                               180                                 200                                 220                                 240
                                |                                   |                                   |                                   |
PcinCRN53_1  KGEKPNDFKD IDADKLHLFL AKTEGGAWVT EADVKNGVKG ADESKALDSA GAPLKLVGLS GTDVQFTPTI EDVKAKRTPV 240
PcinCRN53_2  KGEKPNDFKD IDADKLHLFL AKTEGGAWVT EADVKNGVKG ADESNALDSA GAPLKLVGLS GTDVQFTPTI EDVKAKRTPV 236
                               260                                 280                                 300                                 320
                                |                                   |                                   |                                   |
PcinCRN53_1  HVLVVVPKQD GTSNEMSAAT TPLTVEQVEM SMNKVLRERD EKASAYSFSD LNTAMEERIV EKMRLTENIP DVKEPVNTSI 320
PcinCRN53_2  HVLVVVPKQD GTSNEMSAAT TPLTVEQVEM SMNKVLRERD EKASAYSISD LNTAMEERIV EKMRLTENIP DVKEPVNTSI 316
                               340                                 360                                 380
                                |                                   |                                   |
PcinCRN53_1  AGYSWIPKIA ESEESQRAGY MAYLQQHLKT LTDRGDFLLD DIAGDKSVLN IVDPRLPVAM KGTADV 386
PcinCRN53_2  AGYSWIPKIA ESEESQRAGY MAYLQQHLKT LTDRGDFLLD DIAGDKSVLN IVDPRLPFAM KGTADV 382
```

Figure 4. Protein sequence alignment of amino acid sequences translated from alleles of PcinCRN95 and PcinCRN53. The confirmed amino acid sequences of the *Phytophthora cinnamomi* crinkling and necrosis (PcinCRN) effectors of (A) PcinCRN95_1 and PcinCRN95_2, and (B) PcinCRN95_1 and PcinCRN95_2 were aligned using CLC Main Workbench using default parameters. *PcinCRN95_1* and *PcinCRN95_2* have 11 single nucleotide polymorphisms (SNPs) between them, with seven SNPs resulting in non-synonymous amino acid changes. *PcinCRN53_1* and *PcinCRN53_2* have nine single nucleotide polymorphisms (SNPs) between them, with seven SNPs resulting in non-synonymous amino acid changes. There is a deletion of 12 nucleotides in *PcinCRN53_2* which results in the deletion of a cysteine, glycine, arginine, and lysine from this region compared to PcinCRN53_1. The amino acids highlighted in red indicate the non-synonymous amino acid changes (Supplementary Table 9). Both alleles were confirmed in two additional *P. cinnamomi* isolates (Pcin_isolate129 and Pcin_isolate308) (Supplementary Table 10).

A PcinCRN73_ and PcinCRN73_2

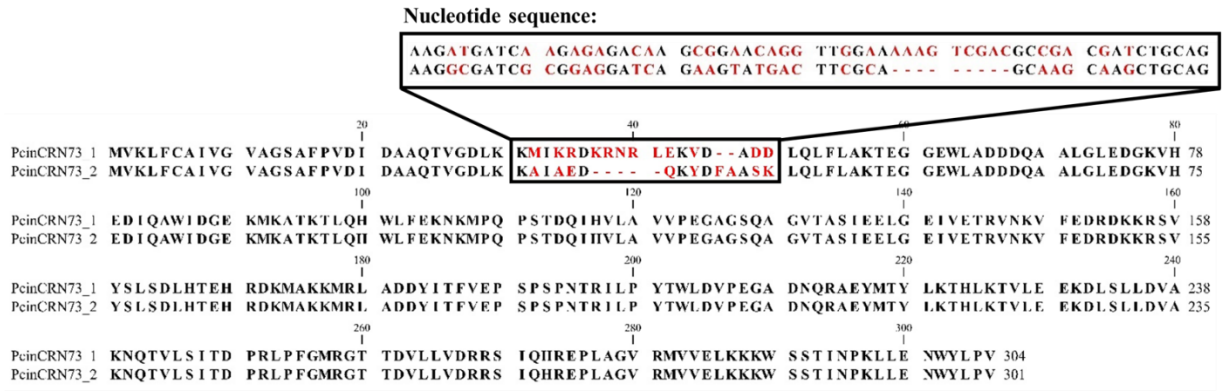

B PcinCRN75_ and PcinCRN75_2

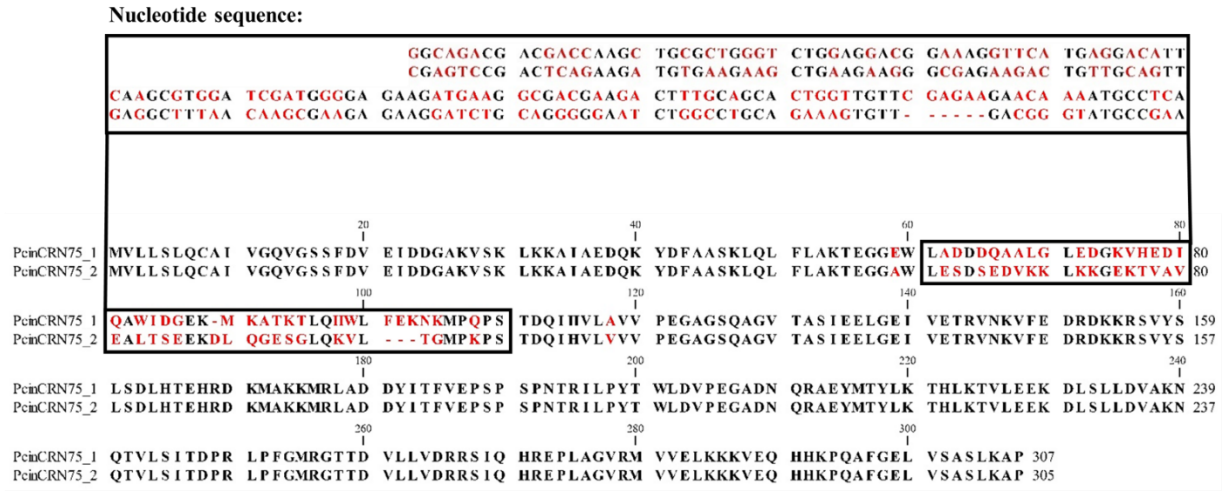

Figure 5. Protein sequence alignment of amino acid sequences translated from alleles of PcinCRN73 and PcinCRN75. The confirmed amino acid sequences of the *Phytophthora cinnamomi* crinkling and necrosis (PcinCRN) effectors of (A) PcinCRN73_1 and PcinCRN73_2, and (B) PcinCRN75_1 and PcinCRN75_2 were aligned using CLC Main Workbench using default parameters. The black box in the figure shows the nucleotide changes between alleles which results in the region of non-synonymous amino acid changes and deletions indicated in the final protein sequence. The alleles *PcinCRN73_1* and *PcinCRN73_2* have five single nucleotide polymorphisms (SNPs) between them. Numerous consecutive nucleotide substitutions of two or more nucleotides occur throughout the region, resulting in non-synonymous amino acid changes. There is a deletion of nine nucleotides in *PcinCRN73_2* which results in a shifted open reading frame (ORF) as well as amino acid deletions in this region. *PcinCRN75_1* and *PcinCRN75_2* have 15 single nucleotide polymorphisms (SNPs) between them. Numerous consecutive nucleotide substitutions of 2 or more nucleotides occur throughout the region, resulting in non-synonymous amino acid changes. There is a deletion of six nucleotides in *PcinCRN75_2* which results in a deletion of two amino acids in this region. The amino acids highlighted in red indicate the non-synonymous amino acid changes as well as the deletion of amino acids in PcinCRN73_2 (Supplementary Table 9). Both alleles were confirmed in two additional *P. cinnamomi* isolates (Pcin_isolate129 and Pcin_isolate308) (Supplementary Table 10).

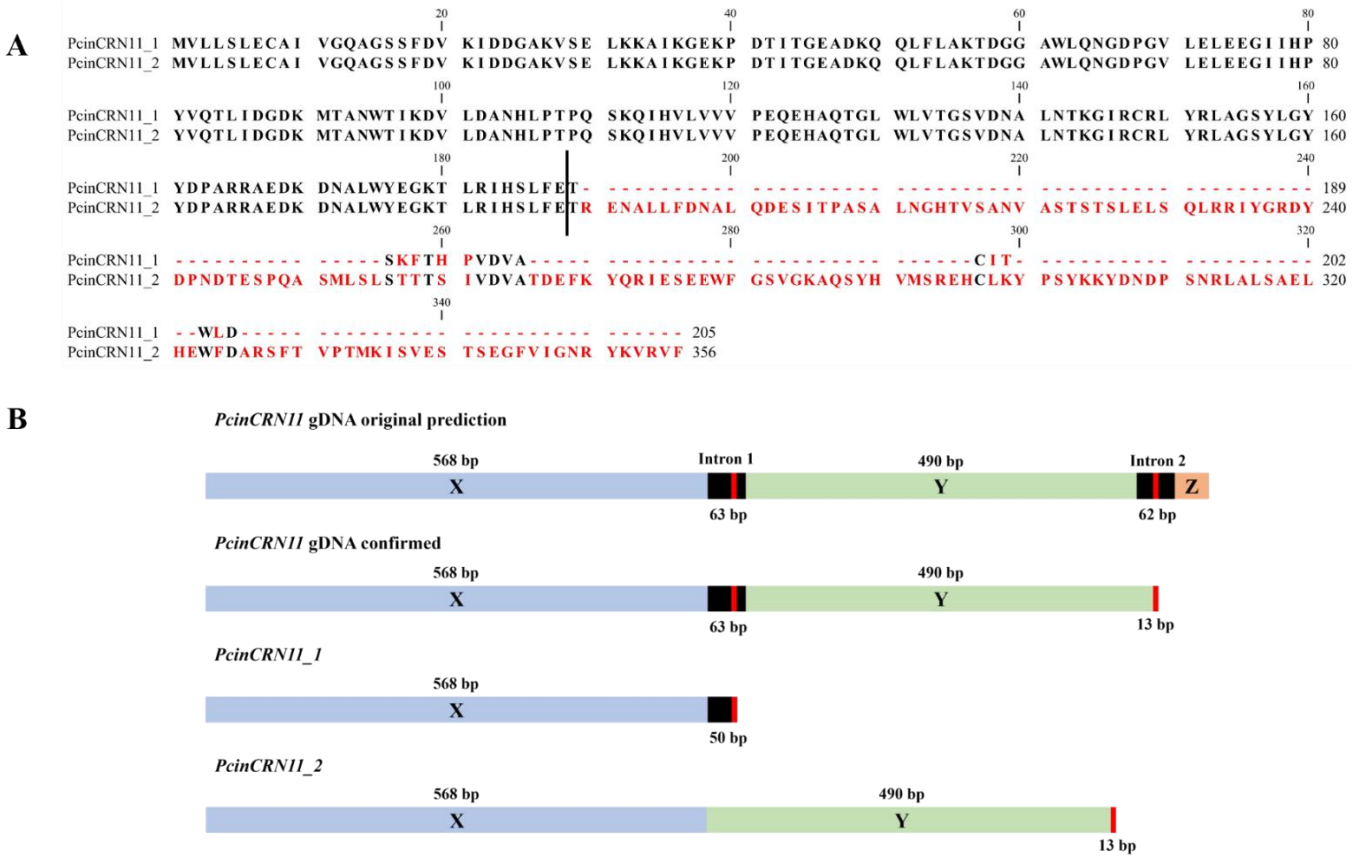

Figure 6. Protein sequence alignment and gene structure of PcinCRN11_1 and PcinCRN11_2. (A) The confirmed amino acid sequences of the *Phytophthora cinnamomi* crinkling and necrosis (PcinCRN) effectors PcinCRN11_1 and PcinCRN11_2 were aligned using CLC Main Workbench using default parameters. The black vertical line represents where the site of alternative splicing occurs, and the red amino acids represent amino acid changes because of this altered splicing. (B) Diagram illustrating the original full-length *PcinCRN11* gene prediction and the newly confirmed full-length gene sequence. The blue block labelled X and green box labelled Y represents the different exons within the transcribed region. The orange box labelled Z represents an additional exon which was thought to be in the original *PcinCRN11* gene prediction. The black boxes represent introns, and the red line within the introns represent stop codons. Splicing does not occur in *PcinCRN11_1*, resulting in the inclusion of the intron containing a stop codon. The intron is spliced out of PcinCRN11_2 allowing for the inclusion of both exon X and Y.

Phylogenetic analysis

Phylogenetic analyses revealed that the PcinCRNs and other *Phytophthora* CRNs included in the analyses formed three distinct clades (Figure 7). Each clade is represented by one or more CRNs from other *Phytophthora* spp. with previous functional characterisations in cell death manipulation. Clade 1 is comprised of PcinCRN11_1, PcinCRN11_2, PcinCRN53_1, PcinCRN53_2 PcinCRN73_1, PcinCRN73_2, PcinCRN75_1, PcinCRN75_2 and PcinCRN77. These PcinCRNs were grouped within the same clade as a *P. infestans* CRN (PiCRN1, UniprotKB ID: Q8H6Z6) and this relationship is supported by a posterior probability of 0.98, indicating good support. Clade 2 is comprised of PcinCRN30_1, PcinCRN30_2, PcinCRN52, PcinCRN81_1, PcinCRN81_2 and PcinCRN86, grouping within the same clade as *P. infestans* CRNs (PiCRN2, PiCRN15 and PiCRN16, UniprotKB ID: Q8H6Z4, Q2M3Z8 and Q2M3Z7, respectively) *P. sojae* CRNs (PsCRN63, PsCRN108, PsCRN115 and PsCRN161, UniprotKB ID: G4YRT1, A0A0M5K865, E9M7A1 and G4YUT3, respectively) and a *Phytophthora capsici* CRN (PcCRN4; UniprotKB ID: P0CV73). This relationship is supported by a posterior probability of 0.58, indicating moderate support. Within this clade, PcinCRN86 was found to be closely related to PsCRN161. PcinCRN52, was found to be closely related to PcCRN4. PcinCRN81_1 and PcinCRN81_2 were closely related to both PcCRN4 and PsCRN108. PcinCRN30_1 and PcinCRN30_2 were closely related to PsCRN108. Clade 3 is comprised of PcinCRN95_1 and PcinCRN95_2. These PcinCRNs are grouped within the same clade as two *P. infestans* CRNs (PiCRN5 and PiCRN8, UniprotKB ID: Q2M408 and Q2M405, respectively) and this relationship is moderately supported by a posterior probability of 0.56.

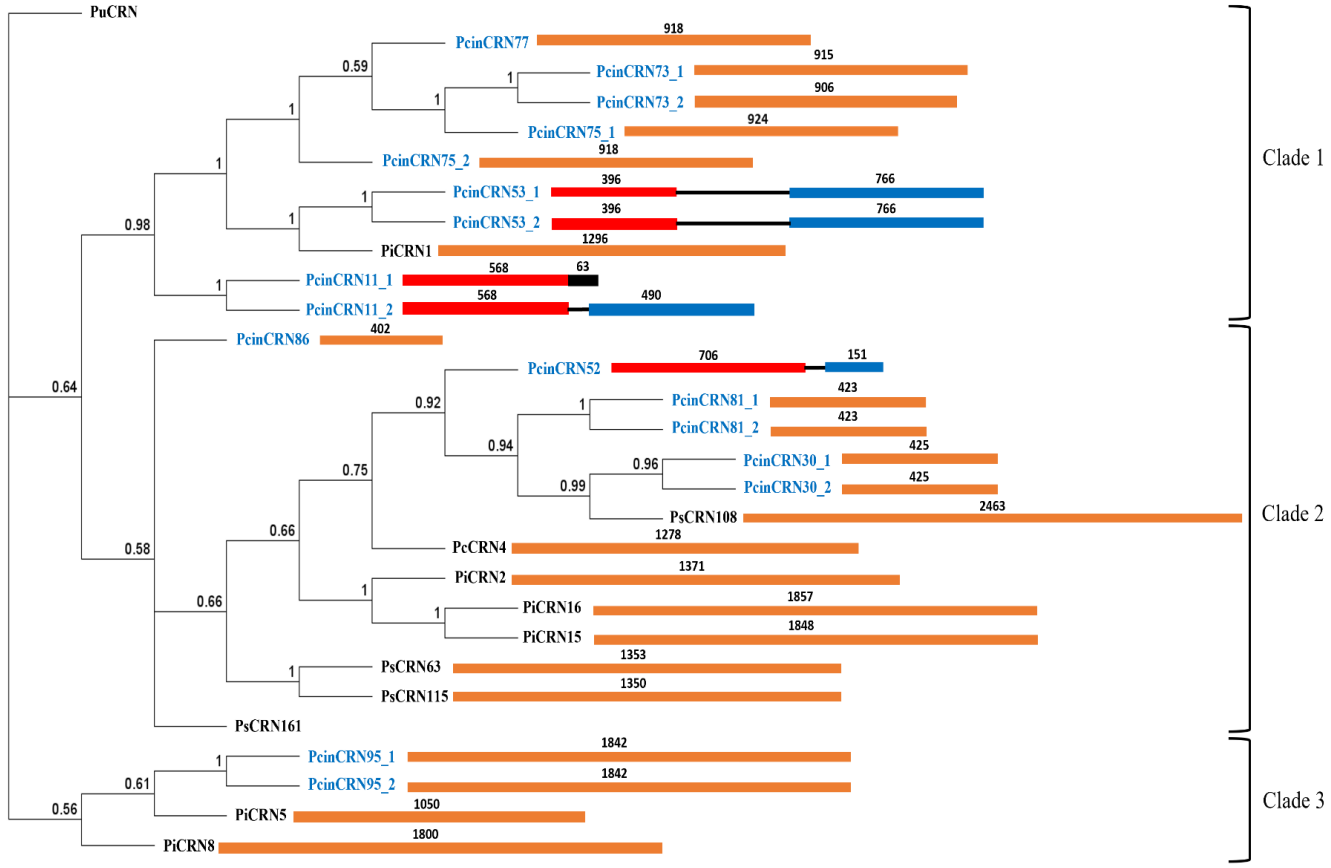

Figure 7. Evolutionary relatedness of full-length PcinCRNs to functionally characterised CRNs from other *Phytophthora* spp. Phylogenetic tree resulting from Bayesian inference analysis of the confirmed full-length *Phytophthora cinnamomi* crinkling and necrosis (PcinCRNs) effector amino acid sequences aligned with functionally characterised CRNs from other *Phytophthora* spp. (*Phytophthora infestans* CRN, PiCRN; *Phytophthora capsici*, PcCRN and *Phytophthora sojae*, PsCRN). Support for branches is indicated by posterior probability values, which are displayed for each node to the second significant digit. with a posterior probability cut-off of < 0.5. A CRN-like protein from *Pythium ultimum* was used as an outgroup (PuCRN, K3WBE4). Three distinct clades were formed. PcinCRNs are denoted in blue while CRNs from other *Phytophthora* spp. are denoted in black. The gene structures for each *CRN* are indicated next to each label. Exons are indicated in red and blue; introns are represented as black lines and genes with no introns are indicated in orange. The black in the gene structure for PcinCRN11_1, represents the predicted intron with a internal stop codon, shown to be retained by sequencing of cDNA. This intron is spliced out in PcinCRN11_2, resulting in two respective proteins of differing length. The numbers above the gene structures indicate the size of the regions in bp.

PcinCRN protein structure prediction

Domain analyses were conducted to gain further insight into the putative roles of PcinCRNs in cell death manipulation during avocado infection. Analyses of confirmed full-length PcinCRN amino acid sequences revealed that six PcinCRNs (PcinCRN11, PcinCRN 30, PcinCRN52, PcinCRN81, PcinCRN86 and PcinCRN95) possessed one or more low complexity regions (LCR's) (Table 1). PcinCRN30, PcinCRN52 and PcinCRN95 contained a central LCRs, PcinCRN86 had a terminal LCR and both PcinCRN11 and PcinCRN81 contained both a central and terminal LCR. A ubiquitin-like (Ubl) domain and a phosphate-loop (P-loop) nucleoside-triphosphatase domain (NTPase) were identified within PcinCRN95 (Figure 8).

The protein structures of PcinCRN11, PcinCRN53, PcinCRN73, PcinCRN75 and PcinCRN95 were predicted and compared. The amino acid changes resulting from SNPs, consecutive base substitutions, and deletions in the alleles of PcinCRN53, PcinCRN73 and PcinCRN75 impacted the structure of the protein (Figure 9). PcinCRN73 and PcinCRN75 allele structural variations were present in the N-terminal of the protein, rather than the functional C-terminal (Figure 9B and 9C). PcinCRN53 demonstrated an orientation shift based on the non-synonymous amino acid changes and deletions between alleles (Figure 9A). Comparison of the predicted protein structure of PcinCRN95_1 and PcinCRN95_2 showed no notable structural differences between them (Supplementary Figure 4). The predicted amino acid PcinCRN11_1 is alternatively spliced to produce PcinCRN11_2, allowing for an additional protein structure in the final tertiary structure (Figure 9C).

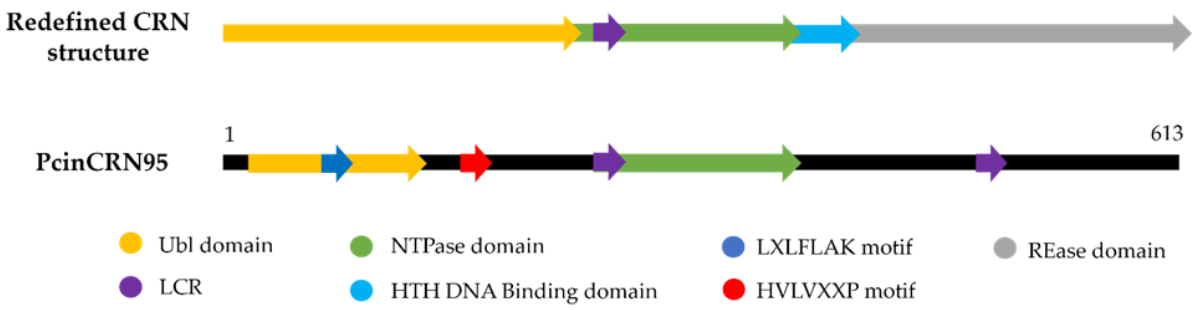

Figure 8. The protein domain architecture of PcinCRN95 closely resembles that of CRNs functioning in cell death (27). The domains in *Phytophthora cinnamomi* crinkling and necrosis effector protein 95 (PcinCRN95) are compared against the domains present in the redefined CRN architecture of a CRN functioning in the induction of cell death. There are notable similarities between the PcinCRN95 and the redefined CRN architecture, where both contain a ubiquitin-like (Ubl) domain (yellow), low complexity regions (LCR's) (purple) and a nucleoside-triphosphatase (NTPase) domain (green) providing evidence for a potentially conserved functional role.

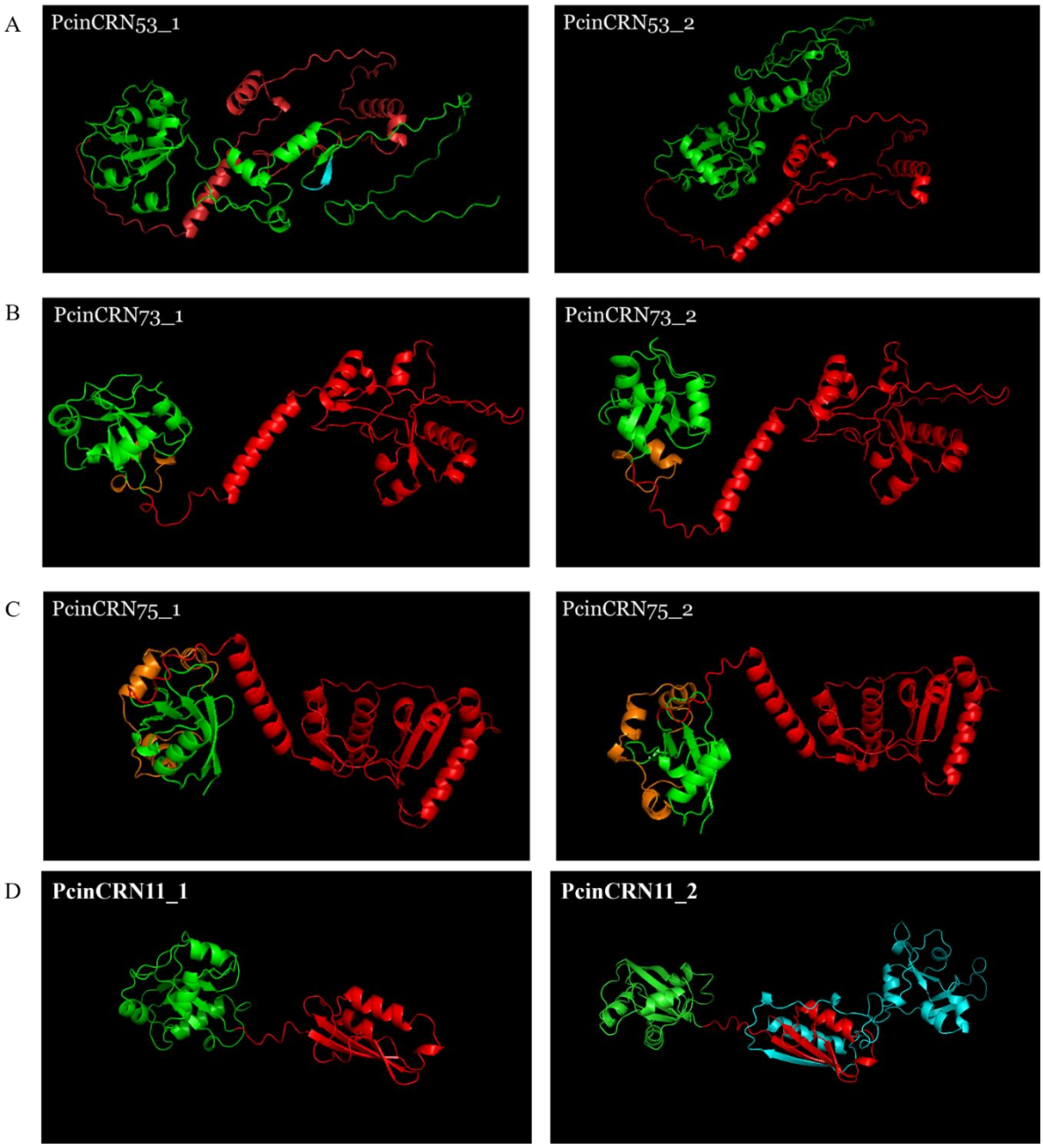

Figure 9. Predicted tertiary protein structures of the amino acid sequences encoded by the different PcinCRN alleles using AlphaFold. AlphaFold (28, 29) was used to predict the tertiary structure of *Phytophthora cinnamomi* crinkling and necrosis (PcinCRN) effector protein alleles. The predicted tertiary structures were visualised in PyMOL v2.5.5 (Schrödinger, LLC). **(A)** Tertiary protein structures of PcinCRN53_1 (pLDDT = 68.76) and PcinCRN53_2. (pLDDT = 67.05). The portion of the protein structure represented by a blue colour indicates the amino acids that are present in PcinCRN53_1 and not PcinCRN53_2. **(B)** Tertiary protein structure of PcinCRN73_1 (pLDDT = 81.70) and PcinCRN73_2 (pLDDT = 81.42). **(C)** Tertiary protein structure of PcinCRN75_1 (pLDDT = 89.02) and PcinCRN75_2 (pLDDT = 97.97). **(C)** Tertiary protein structure of PcinCRN11_1 (pLDDT = 84.52) and PcinCRN11_2 (pLDDT = 80.17). Portions of the protein structure represented by a green colour indicate the N-terminal domain up until the HVLVXXP motif. Orange coloured protein structures represent regions of amino acid variation within the N-terminal which differ between the alleles of PcinCRN73 and PcinCRN75. Portions of the proteins represented by a red colour indicate the location of the C-terminal domains. Blue labelled structure represents the additional protein structure that resulted due to the inclusion of an additional exon in PcinCRN11_2 compared to PcinCRN11_1, due to alternative splicing.

Discussion

Phytophthora effectors are known to play a role in cell death during infection of host plants by either inducing or suppressing cell death (13, 18-20, 23, 24, 30-33). Effectors such as CRNs may be utilised by *Phytophthora* spp. to manipulate the cell death pathways of the infected host plant to maintain their biotrophic and necrotrophic lifestyles, at different stages of infection (3, 13-15, 18, 19). Currently, there is a lack of functional characterisation studies on PcinCRNs. Two previous studies identified putative PcinCRN effector repertoires (1, 26), and another study revealed that a single *PcinCRN* (*CRN1*) was highly expressed during infection of *E. nitens* (25). To that end, the current study identified a repertoire of 25 full-length PcinCRNs and one partial or CRN-like sequence. Putative cell death manipulating functions were assigned to a subset of PcinCRNs based on their expression during infection of *P. americana*, Sanger Sequencing data, relatedness to other *Phytophthora* CRNs functioning in cell death manipulation, protein domain analyses, and their tertiary protein structure.

Initial work by Hardham and Blackman (1) identified 49 putative PcinCRNs due to their homology to CRNs from other *Phytophthora* spp. and the presence of a LXLFLAK and DWL motif (Figure 1). Although many PcinCRNs were identified at the time, seven were incomplete. The *P. cinnamomi* genomes used for the Hardham and Blackman (1) study were sequenced using Illumina Hi-Seq 2500 platform resulting in highly fragmented assemblies (34, 35). The most recent identification of PcinCRNs was done by Engelbrecht *et al.* (26), in which a new *P. cinnamomi* reference genome was generated using a combination of Nanopore and Illumina sequencing platforms. This approach resulted in a less fragmented genome, with 133 scaffolds vs 1314 and 10,084 scaffolds, N50 of 1.18Mb compared to 10 and 264.5 Kb, and estimated genome size of 109.7 Mb compared to 53.69 and 77.97 Mb. In their study, Engelbrecht *et al.* (26) identified 49 putative PcinCRNs, of which two were truncated.

With this, the same *P. cinnamomi* genome from Engelbrecht *et al.* (26) was used in the current study to search for putative PcinCRN effectors via a HMM profile search, in order to generate the most accurate representation of the *P. cinnamomi* CRN repertoire possible. Although this approach resulted in less putative PcinCRNs being identified compared to Hardham and Blackman (1), and Engelbrecht *et al.* (26), the number of validated 'true' PcinCRNs from the current repertoire was greater (Figure 2, Supplementary Table 3A and 3B). All 'true' PcinCRNs identified by Engelbrecht *et al.* (26), and eight of those from Hardham and Blackman (1) were among the list of 'true' PcinCRNs generated using the current studies method (Supplementary Table 3A and 3B). It was also found that two putative PcinCRNs from Hardham and Blackman (1) were not among our list of putative PcinCRNs, or that of Engelbrecht, *et al.* (26). The most likely reason for this would be an assembly-based artifact resulting from the highly fragmented genomes used in that study. Although the method utilised in the current study resulted in the identification of fewer putative PcinCRNs, a greater number of 'true' PcinCRNs, which better represent the supported characteristics of the

Phytophthora CRN effectors, were identified. Thus, based on our results we are confident that we have compiled a list of PcinCRNs which most accurately represents the true *P. cinnamomi* CRN effector repertoire.

We further assigned putative functions in cell death manipulation to PcinCRNs through multiple lines of evidence (Table 3). This included analysing *PcinCRN* expression during *P. americana* infection (Figure 3). Timepoints chosen to represent the biotrophic stage were 6- and 12 hpi, and the timepoint chosen to represent the necrotrophic stage was at 120 hpi, based on previous findings (36) (Figure 1). Based on the study by van den Berg *et al.* (35) the 24 hpi was used to represent the point at which *P. cinnamomi* was most likely transitioning from a biotrophic to a necrotrophic lifestyle (36). Expression profiles, in combination with sequencing data of PcinCRN and their alleles, relatedness to other functionally characterised *Phytophthora* CRNs and the tertiary protein predictions were used to assign function. Ultimately 10 full-length PcinCRNs were functionally characterised as either a cell death inducer, suppressors, or as having contradictory function in cell death manipulation.

Table 3. Summary of evidence supporting the assignment of putative function in cell death manipulation to 10 full-length *Phytophthora cinnamomi* crinkling and necrosis (PcinCRN) effectors. The results obtained from expression profiles, Sanger Sequencing data, phylogenetic analyses, and protein analyses for each PcinCRN were accumulated as evidence towards the classification of the PcinCRNs as either a cell death suppressor or inducer. PcinCRN alleles were classified as performing contradicting functions or functions in alternative host plant species if the evidence supports the classification of the PcinCRN as a cell death inducer and suppressor. PcinCRNs were classified as potentially playing a role in the incompatible plant-pathogen interaction if they had statistically differentiated expression during infection of R0.12 compared to Dusa®.

PcinCRN ID	Expression profile	Sanger Sequencing results	Phylogenetic relatedness	Protein analyses	Putative function
PcinCRN11	Upregulated during biotrophic stage and potential switch between lifestyles in an incompatible plant-pathogen interaction vs compatible (Figure 3C and 3E). Downregulated during initial infection in R0.12 (Figure 3C).	Alternative splicing occurs in *PcinCRN11_1* resulting in a *PcinCRN11_2* variant (Table 2, Figure 6). No alleles.	All variants form a clade with a known cell death inducer (PiCRN1) (Figure 7).	Contains both Central & Terminal LCRs (Table 1).	Cell death Inducer/suppressor. Variants may perform contradicting functions. Potentially plays a role in the incompatible interaction between avocado and *P. cinnamomi*
PcinCRN30	Upregulated during the biotrophic stage in Dusa® (Figure 3B and 3D).	Two alleles with 1 amino acid difference. (Table 2, Supplementary Figure 3B).	Both alleles have homology to a known cell death suppressor (PsCRN108) (Figure 7).	Contains Central LCR. (Table 1).	Cell death suppressor.

PcinCRN52	Upregulated during necrotrophic phase in R0.12 (Figure 3A).	No alleles.	Homology to a CRN known to induce cell death (PcCRN4) (Figure 7).	Contains a Central LCR & NLS. (Table 1).	Cell death inducer.
PcinCRN53	Upregulated during biotrophic stage or potential switch between lifestyles in an incompatible plant-pathogen interaction vs compatible (Figure 3C and 3E). Downregulated during initial stage of infection compared to the necrotrophic phase in Dusa® (Figure 5).	Two alleles with seven amino acid differences and deletion of four amino acids (Table 2, Figure 4).	Forms a clade with a known cell death inducer (PiCRN1) (Figure 7).	Demonstrates an orientation shift based on the amino acid changes and deletions between alleles which will change the function between alleles (Figure 9A). Both alleles Contain NLS (Table 2).	Cell death Inducer/suppressor. Alleles may perform contradicting functions or functions in alternative host plant species. Potentially plays a role in the incompatible interaction between plant and pathogen.
PcinCRN73	Upregulated during biotrophic phase and downregulated during necrotrophic phase in R0.12 (Figure 3A and 3C) Downregulated during initial infection at 6 hpi in R0.12 (Figure 4)	Two alleles with seven amino acid differences and deletion of two amino acids in PcinCRN73_1 and five deletions in PcinCRN73_2 (Table 2, Figure 5).	Forms a clade with a known cell death inducer (PiCRN1) (Figure 7).	Protein structure variations between alleles are within the N-terminal of the protein. (Figure 9B).	Cell death suppressor/inducer. Alleles may perform contradicting functions or functions in alternative host plant species.
PcinCRN75	Upregulated during biotrophic stage or potential switch between lifestyles in an incompatible plant-pathogen interaction vs compatible (Figure 3C and 3E). Upregulated during initial stage of infection compared to the necrotrophic phase in Dusa® (Figure 3D).	Two alleles with 34 amino acid differences and deletion of three amino acids (Table 2, Figure 5).	Forms a clade with a known cell death inducer (PiCRN1) (Figure 7).	Protein structure variations between alleles are within the N-terminal of the protein. (Figure 9C).	Cell death suppressor/inducer. Alleles may perform contradicting functions or functions in alternative host plant species. Potentially plays a role in the incompatible interaction between plant and pathogen.
PcinCRN77	Upregulated during biotrophic stage and potential switch between lifestyles in an incompatible plant-pathogen interaction vs compatible (Figure 3E).	No alleles (Table 2).	Forms a clade with a known cell death inducer (PiCRN1) (Figure 7).	N/A	Cell death suppressor. Potentially plays a role in the incompatible interaction between plant and pathogen.

PcinCRN81	Upregulated during the biotrophic stage in Dusa® (Figure 3B).	Two alleles with one amino acid difference (Table 2, Supplementary Figure 3).	Both alleles have homology to a known cell death suppressor (PsCRN108) and inducer (PcCRN4) (Figure 7).	Contains both Central & Terminal LCRs (Table 1).	Cell death suppressor.
PcinCRN86	Downregulated during necrotrophic stage of Ro.12 and Dusa® (Figure 3A and 3B). Upregulated during the biotrophic stage in Dusa® (Figure 3D).	No alleles.	Homology to a clade with a known cell death suppressor (PsCRN161) (Figure 7).	Contains Terminal LCR (Table 1).	Cell death suppressor.
PcinCRN95	Upregulated during the biotrophic phase in Dusa® (Figure 3B and 3D). Downregulated during necrotrophic phase of Dusa® (Figure 3B). Upregulated during necrotrophic stage and potential switch between lifestyles in an incompatible plant-pathogen interaction vs compatible (Figure 3E)	Two alleles with seven amino acid differences (Table 2, Figure 4).	Both alleles have homology to a CRN known to induce cell death (PiCRN5) (Figure 7).	Contains Central LCR (Table 1). Contains Ubl and P-loop NTPase domain – like redefined architecture of CRNs involved in cell death (Figure 9D).	Cell death inducer/suppressor. Alleles may perform contradicting functions or functions in alternative host plant species.

Previous research by Meyer *et al.* (25) clearly demonstrated that upregulation of *P. cinnamomi CRN1* during the late-stages of infection (120 hpi) in *E. nitens* was associated with virulence. Additionally, overexpression of *PcCRN4* in *N. benthamiana* led to induction of cell death (19). Our data demonstrated that *PcinCRN52* was significantly upregulated at 120 hpi, the timepoint considered to represent the necrotrophic phase of infection during the incompatible *P. cinnamomi-P. americana* interaction (36, 37), similar to that of *CRN1* from Meyer *et al.* (25) (Figure 3A, Table 3). PcinCRN52 was also found to be related to PcCRN4 (Figure 7, Table 3). Notably, like PcCRN4, PcinCRN52 contains a central LCR which is essential in manipulation of host translation and transcription processes (38). Additionally, PcinCRN52 contained a NLS (Table 2, Table 3) which is known to assist in the nuclear localisation of several CRNs (13, 18, 19, 21, 23); in fact, most identified cell death inducing CRNs localise to the nucleus through a NLS or alternative mechanisms, including PcCRN4 (13). This domain allows for nuclear localisation of CRNs where they enact their function and regulate the expression of cell death-related genes (11, 12, 18). Thus, our temporal expression data, structural and phylogenetic analyses would suggest that PcinCRN52 may function as a cell death inducer.

By contrast, four PcinCRNs (*PcinCRN30, PcinCRN77*, *PcinCRN81* and *PcinCRN86*) were determined to play a potential role in suppressing cell death during the biotrophic stage of infection of avocado. Notably, these PcinCRNs displayed upregulation in expression during the biotrophic stage followed by downregulation during the necrotrophic stage (Figure 3B-D, Table 3) (39). PsCRN115 is known to suppress cell death induced by other cell death inducing *Phytophthora* effectors, and this CRN is upregulated at 12 hpi (biotrophic stage) during infection of *Glycine max* (soybean) compared to later time points (18). PcinCRN30 and PcinCRN81 were found to be related to PsCRN108, and PcinCRN86 was related to PsCRN161 (Figure 7, Table 3). Both PsCRN108 and PsCRN161 suppress cell death during infection (32, 33). Although PcinCRN77 was found to be related to a PiCRN1 (20), a cell death inducer, the expression data of our study provides stronger evidence to the designation of this CRN as a cell death suppressor during infection of avocado (Figure 3C). Additionally, *PcinCRN30, PcinCRN77*, *PcinCRN81* and *PcinCRN86* did not contain a predicted NLS (Table 2). This is however not evidence that these CRNs do not localise to the nucleus, as there are various alternative methods and/or pathways for translocation into the nucleus (30, 40). Although, it is expected that these PcinCRNs do not localise to the nucleus because CRNs that function in cell death suppression often function within the cytosol (11, 40). This is because the primary targets of pathogen-associated molecular pattern (PAMP) triggered immune response (PTI) and the effector-triggered immune response (ETI) are found in the cytosol (41-43). The PTI and ETI systems influence host-pathogen interactions and involve the activation of complex signaling pathways through a repertoire of proteins in response to pathogen attack. PcinCRN30, PcinCRN77, PcinCRN81, and PcinCRN86 potentially suppress cell death by targeting PTI and ETI related proteins to prevent a mounted immune response by the host plant.

Sequencing data revealed that multiple *PcinCRN* genes (*PcinCRN53, PcinCRN73, PcinCRN75,* and *PcinCRN95*) have two alleles with more than one amino acid difference between them (Table 2, Figures 4-5). All these *PcinCRNs* exhibited the expression profile of a cell death suppressor (Figure 3A, C- E, Table 3) but PcinCRN53, PcinCRN73 and PcinCRN75 were found to be phylogenetically related to PiCRN1, and PcinCRN95 to both PiCRN5 and PiCRN8, all of which are cell death inducers from *P. infestans* (Figure 7, Table 3). Additionally, the PcinCRN95 protein architecture was indicative of a cell death inducer (Figure 8). By containing a Ubl and P-loop NTPase domain (Figure 8), PcinCRNs are similar to the redefined architecture of cell death-inducing CRNs defined by Zhang *et al.* (27). The authors reported that majority of the cell death inducing CRNs from *P. infestans* and *P. sojae* possessed a Ubl domain in the N-terminal, followed by a NTPase (Figure 7). We hypothesize that the contradicting nature of evidence, as well as the presence of alleles for *PcinCRN53, PcinCRN73, PcinCRN75,* and *PcinCRN95*, that one allele encodes for a cell death inducer and the other allele encodes a protein functioning in cell death suppression.

To illustrate that PcinCRNs with two alleles may encode proteins with contradictory function in cell death, the tertiary proteins for these alleles were predicted (Figure 9, Table 3). The predicted protein structure of PcinCRN95_1 and PcinCRN95_2 revealed no difference in protein folding due to the

amino acid changes (Supplementary Figure 4). However, this does not imply that they lack contradictory functions in cell death. For example, PsCRN63 and PsCRN115 from *P. sojae* only differ by four amino acids and they perform contradicting functions in cell death (11, 18). Investigations uncovered that PsCRN63 induces cell death and requires nuclear localisation to function. Whereas, PsCRN115 demonstrated a function in cell death suppression during the necrotrophic stage and did not require nuclear localisation to function (18). Additionally, it was determined that PsCRN115 was able to suppress the cell death induced by PsCRN63, and that silencing one or both genes negatively impacted virulence. This mechanism has also been observed in *Phytophthora parasitica,* where PpCRN7 and PpCRN20 function the same as PsCRN63 and PsCRN115, respectively (12). The interaction and manipulation observed between the two CRNs in *P. sojae* and *P. parasitica* may resemble the interaction and function of PcinCRN95_1 and PcinCRN95_2 during infection. Moreover, the tertiary protein structures between PcinCRN53_1 and PcinCRN53_2 were altered – where there is a structure deleted in the N-terminal and the orientation of the functional C-terminal is shifted (Figure 9A). Due to these changes, the different PcinCRN53 proteins could potentially play contradicting roles in cell death manipulation like that of PcinCRN95. Conversely, the changes in the folding of the tertiary protein structures potentially allow for their functionality in different host plant species or their binding to different host plant targets. This may explain why *P. cinnamomi* (~5000 host plants worldwide) has a larger host range than other *Phytophthora* spp. (7, 8). This is evident when looking at the protein predictions for the proteins encoded by different alleles of PcinCRN73 and PcinCRN75 (Figures 9B and 9C). The amino acid changes resulting between the alleles mainly occur in the N-terminal, rather than the C-terminal, indicating the changes may alter binding of the PcinCRNs to host targets (21, 44).

Confirmation of the coding sequence of *PcinCRNs* not only revealed the presence of alleles for some *PcinCRNs*, but one *PcinCRN* was demonstrated to undergo alternative splicing (*PcinCRN11*) (Table 3, Figure 6). The *PcinCRN11* gene is alternatively spliced to produce variants *PcinCRN11_1* and *PcinCRN11_2*, where PcinCRN11_2 has an additional protein structure compared to PcinCRN11_1 (Figure 9D, Table 3). This is the first evidence of a *Phytophthora* CRN gene undergoing alternative splicing. The expression of this *PcinCRN* was found to be upregulated in the susceptible rootstock (R0.12) when compared to the partially resistant rootstock (Dusa®) during the biotrophic stage, indicating this PcinCRN may serve a role in the susceptibility of host plants to *P. cinnamomi*. Although, it was shown that PcinCRN11 forms a clade with a cell death inducing *P. infestans* CRN (PiCRN1). Like other PcinCRNs, the variants of PcinCRN11 could potentially perform contradicting functions in cell death manipulation, but whether PcinCRN11_2 functions as a cell death suppressor or inducer will have to be determined.

In addition to *PcinCRN11*, other PcinCRNs were suggested to contribute to the susceptibility during a *P. cinnamomi – P. americana* incompatible interaction. A previous study was conducted by *Li* et al. (45) where the global expression profiles during a compatible and incompatible *P. infestans* - *Solanum tuberosum* interaction was investigated using dual RNA-seq. A total of five *PiCRN* genes

were found to be expressed at 24 hpi of an incompatible interaction that were not detected in the compatible interaction. Similarly, *PcinCRN11*, *PcinCRN53, PcinCRN73* and *PcinCRN75* were found to be upregulated during an incompatible interaction (R0.12) compared to the compatible interaction (Dusa®) at either or both 12- and 24 hpi (Figure 3E, Table 3). A partially resistant rootstock is defined by having minor symptoms due to a decreased pathogen load, and the HR is a plant defence response to inhibit the spread of a pathogen (15, 16). Due to *P. cinnamomi* being a hemi-biotroph, the HR would benefit the host plant during the biotrophic stage of the pathogen. Therefore, the increased expression of PcinCRNs associated with cell death suppression during the biotrophic stage of a susceptible rootstock compared to the partially resistant rootstock was expected since these PcinCRNs serve in suppressing the HR, ultimately aiding in the spread of the pathogen. Alternatively, PcinCRN95 was found to be upregulated during an incompatible interaction (R0.12) compared to a compatible interaction (Dusa®) at 120 hpi (Figure 3E, Table 3). We suggest that PcinCRN11, PcinCRN53, *PcinCRN73, PcinCRN75* and *PcinCRN95* play a role in the susceptible outcome during a *P. cinnamomi – P. americana* incompatible interaction.

Conclusion

With CRN effector proteins playing a potential role in manipulating cell death during the biotrophic and necrotrophic stages of infection by *P. cinnamomi*, the identification and characterisation of these effectors are crucial to our understanding of the infection and colonisation tactics employed by *Phytophthora* spp. We provide an up-to-date representation of the *P. cinnamomi* CRN effector protein repertoire and are the first to sequence and assign putative function in cell death manipulation to 10 PcinCRNs. With the availability of the full coding sequences of PcinCRNs and their variants, future functional characterisation studies in *P. cinnamomi* can be done. With the availability of methods such as Agroinfiltration and CRISPR-Cas knockout, the functions of the identified PcinCRN presented in this paper can be confirmed and their roles in virulence determined. This will contribute to our knowledge of *P. cinnamomi* cell death pathways and their host targets, allowing for improved screening of resistant avocado rootstocks to be used in agricultural practices.

Methods

Identification of full-length PcinCRN effector protein sequences

A pipeline was generated to identify and validate PcinCRNs as 'true' *Phytophthora* CRNs from the *P. cinnamomi* GKB4 genome (Figure 10). *Phytophthora* CRN protein sequences obtained from the NCBI database were validated by confirming the presence of the LXLFLAK and HVLVXXP motifs in the N-terminus (Supplementary Table 11), using QIAGEN CLC Main Workbench v8.0 (https://digitalinsights.qiagen.com/), and then used to generate a multiple sequence alignment. To

identify putative *P. cinnamomi* CRN (PcinCRN) protein homologs, a HMM profile was generated in HMMER v3.3.2 (http://hmmer.org/) using the multiple sequence alignment to search the full *P. cinnamomi* GKB4 protein repertoire predicted by Augustus (26). Homologous PcinCRN protein sequences identified with an E-value $>10^{-3}$ were excluded. Putative PcinCRN protein sequences were analysed for the presence of both the LXLFLAK and HVLVXXP conserved motifs in the N-terminal using CLC Main Workbench, allowing for a single amino acid difference in each motif. Putative PcinCRN sequences lacking either or both conserved motifs were excluded. The presence of TMH within the putative protein sequences was determined using TMHMM v2.0 (Technical University of Denmark) (https://services.healthtech.dtu.dk/services/TMHMM-2.0/) (46) with default parameters. Putative sequences containing a TMH were excluded. SignalPv3.0 was used to predict the presence of a signal peptide in the remaining candidate sequences. Domains within the PcinCRN protein sequences were identified using SMART (http://smart.embl-heidelberg.de/) (47). A putative CRN sequence was considered a full-length PcinCRN if the encoded amino acid sequence contained both the LXLFLAK and HVLVXXP motifs and lacked a TMH. The final list of PcinCRN protein sequences were cross-referenced against a suite of putative PcinCRN protein sequences identified in two previous studies, where the BLAST2GO method was used (1, 26). PcinCRN protein sequences from Hardham and Blackman (1), and Engelbrecht *et al.* (26) were analysed using the same method described above. In the case where the predicted protein sequences of the putative PcinCRNs were missing a HVLVXXP conserved motif, the protein sequences were manually annotated in Integrated GenomeView 2250 (IGV) (48). Of the sequences that were missing the HVLVXXP motif, the last intron was analysed to determine if the exon-intron boundaries were incorrectly predicted and if the HVLVXXP motif was present downstream of the original exon prediction. If the HVLVXXP motif was absent, the sequence was discarded.

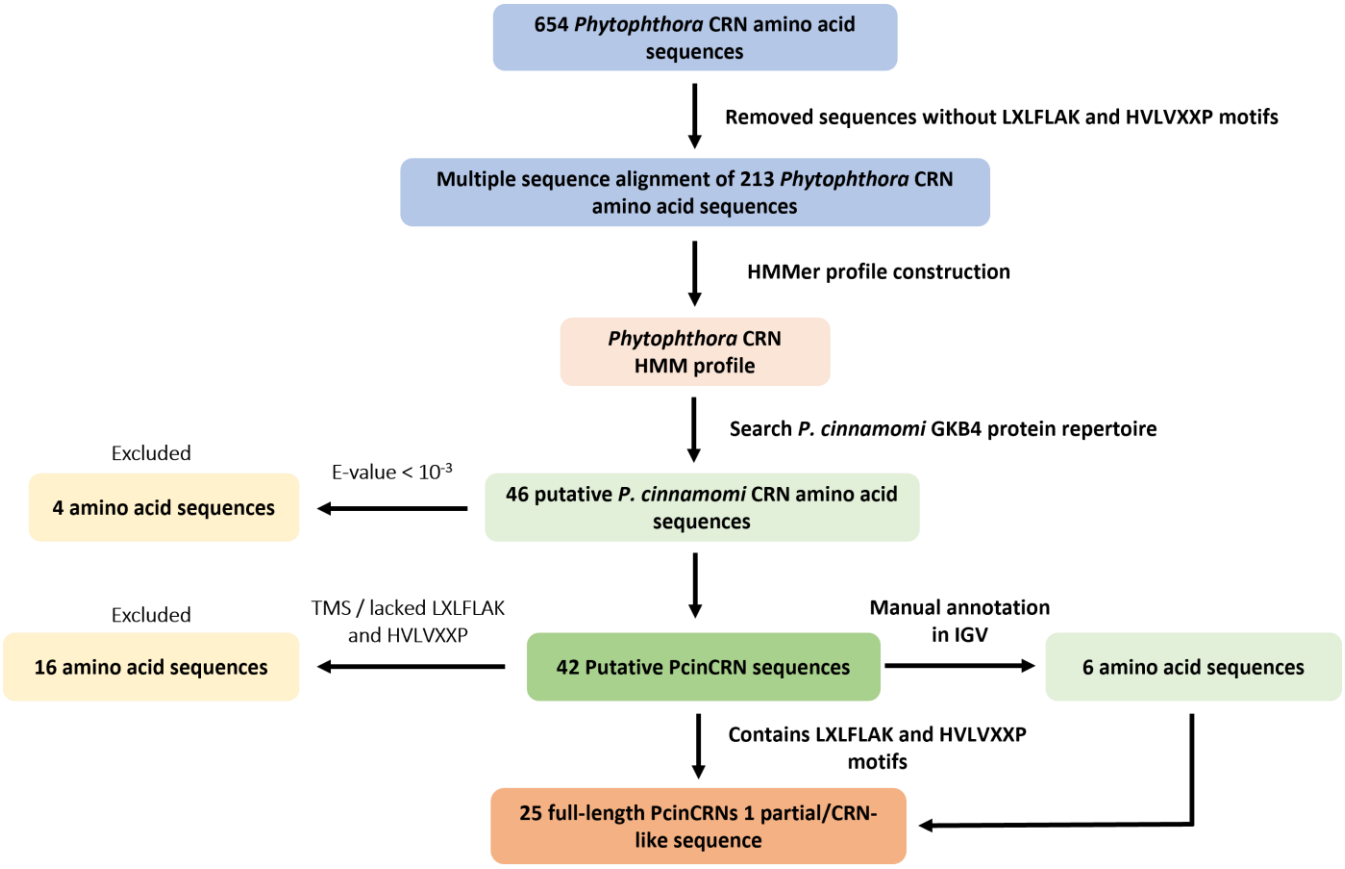

Figure 10. Schematic depicting PcinCRN identification and validation pipeline. Workflow to create a *Phytophthora* crinkling and necrosis (CRN) hidden Markov model (HMM) profile and exclusion criteria that resulted in the final repertoire of 'true' *Phytophthora cinnamomi* CRN (PcinCRN) effector proteins. A total of 213 *Phytophthora* CRN amino acid sequences were validated as 'true CRNs from a list of 654 putative *Phytophthora* CRNs, and used to generate a multiple sequence alignment which was subsequently used to construct a *Phytophthora* CRN HMM profile. The HMM profile was used to search the *P. cinnamomi* GKB4 genome, resulting in the identification of 46 putative PcinCRN amino acid sequences. Four putative PcinCRNs were excluded because of an E-value < 10^{-3}. An additional 16 putative PcinCRN sequences were excluded because they lacked one or both conserved motifs (LXLFLAK and HVLVXXP) or had a transmembrane helix (TMH). A final list of 25 full-length sequences were confirmed as 'true' *Phytophthora* CRNs and a partial/CRN-like sequence. Six of the 25 PcinCRNs were manually annotated in IGV.

Analysis of *P. cinnamomi CRN* expression profiles

The expression data of 25 *PcinCRN* effectors were obtained by previously generated dual RNA-seq data of susceptible (R0.12) and partially resistant (Dusa®) *P. americana* rootstocks inoculated with *P. cinnamomi* GKB4 (49). Briefly, RNA-seq reads were trimmed, and low-quality bases were removed using Trimmomatic v. 0.39 (50). The read quality was confirmed using FASTQC v. 0.11.9, after which the reports were summarised using MultiQC (51). RNA-seq reads were aligned to the *P. cinnamomi* genome using HISAT v. 2.0.6 (52). Transcript abundance was quantified within RNA-seq libraries across all time-points (6-, 12-, 24- and 120 hpi) using featureCounts v. 2.0.1 (53), where *P. cinnamomi* mycelia was used as a reference library. The normalisation and analysis of counts were performed using DESeq2 (54). The Wald test was used to obtain data for differentially expressed

genes (DEGs) at each time-point, and statistical significance was assigned using the Benjamini-Hochberg false discovery rate (FDR) method. Significant DEGs were identified as those with a Log_2 (Fold Change) ≥1 or ≤-1 while the statistical significance of the observations were determined using an FDR cut-off (adjusted *p*-value) of ≤ 0.05 and ≤ 0.10. Expression data for candidate *PcinCRN* genes were extracted from the output of DESeq2 using a custom R script (55). Pheatmap version 1.0.12 was used to generate heatmaps for expression data visualisation (56). The expression of each *PcinCRN* was analysed by first comparing the expression of candidate *PcinCRN* genes at 6-, 12-, 24- and 120 hpi - in both the susceptible and partially resistant rootstocks - to mycelia, and then by comparing the expression of candidate *PcinCRN* in susceptible rootstock to the expression in the partially resistant rootstock. Data comparing the expression between different time-points within each rootstock were also obtained.

Validation of *PcinCRN* expression using RT-qPCR

Reverse transcriptase (RT)- quantitative (q)PCR was used to validate the expression of four *PcinCRN* genes (*PcinCRN74, PcinCRN79, PcinCRN90*, and *PcinCRN95*). Using PrimerQuest™, primers for target *PcinCRNs* were designed (Integrated DNA Technologies, Coralville, USA). Primer sequences for candidate endogenous control genes ubiquitin-conjugated enzyme (*Ubc*), Beta-tubulin (*β-tubulin*), and *WS041* were obtained from literature (57, 58) (Supplementary Table 12A). By generating standard curves with five-fold dilutions of a *P. cinnamomi* cDNA pool, the efficiency of the respective primers was determined (Supplementary Figure 5 and 6). In the RT-qPCR reaction, 200 ng of previously prepared cDNA during *P. cinnamomi* GKB4 infection of a susceptible *P. americana* rootstock (R0.12) at 12- and 24 hpi served as the template in RT-qPCR expression analysis, while mycelia served as the control. For the RT-qPCR reactions, three biological replicates representing each time-point (12- and 24 hpi) as well as three mycelial control samples were utilised for each target and reference gene. The RT-qPCR experiment was conducted using the KAPA SYBR® FAST qPCR Master Mix (2X) Kit (Roche, Mannheim, Germany) according to the manufacturer's instructions on the BioRad CFX96 Touch™ Real-Time PCR Detection System (Bio-Rad Laboratories Inc, Hercules, United States of America (USA)). For each target and reference gene, melt curves were generated and analysed using CFX Maestro™ 1.1 (Supplementary Figure 7) (Bio-Rad Laboratories Inc). The software package qbase+ 3.2 (Biogazelle, Zwijnaarde, Belgium) was utilised for normalisation and relative quantification. Microsoft® Excel 2016 was used to calculate the Log_2 (Fold Change) for each target gene using the method described by Pfaffl (2001) (59). Microsoft® Office Excel 2016 was used to conduct a two-tailed t-test to determine statistical significance.

Amplification of *PcinCRN* coding sequences from *P. cinnamomi* cDNA

Primers were designed using PrimerQuest™ for amplification of the candidate *PcinCRN* coding sequences from *P. cinnamomi* cDNA - previously synthesised from RNA isolated during *P. cinnamomi* GKB4 infection of a susceptible *P. americana* rootstock (R0.12) at 6-, 12-, 24 hpi. Primers were designed to bind within the upstream and downstream untranslated regions and within the predicted coding sequences of each *PcinCRN* (Supplementary Table 12B). *PcinCRNs* were amplified from cDNA by PCR using Phusion Green Hot Start II High-Fidelity DNA Polymerase (Thermo Fisher Scientific, Waltham, USA). Reagent concentrations for reactions: 1X Phusion HF buffer, 200 µM dNTPs, 0.2 U Phusion Green Hot Start II High-Fidelity DNA Polymerase, 100 ng *P. cinnamomi* GKB4 cDNA and 0.5 µM of each primer. A Veriti 96 Well Thermal Cycler (Thermo Fisher Scientific) was used: initial denaturation at 98°C for 1 min, 25 cycles of 10 s denaturation at 98°C, annealing stage was omitted due to the Tm being > 69°C (except for *PcinCRN95* fragment A1, where 30 s annealing at 66°C was used) and 30 s extension at 72°C, and a final extension for 10 min at 72°C. PCR products were excised from a 2% agarose gel and purified using Zymoclean™ Gel DNA Recovery Kit (Zymo Research, USA) according to manufacturer's instructions. The concentration of each purified amplicon was determined using a NanoDrop™ 2000 Spectrophotometer (Thermo Fisher Scientific).

Cloning and sequencing of *PcinCRN* coding sequences

The *PcinCRN* amplicons were cloned using the Zero Blunt® TOPO® PCR Cloning Kit (Thermo Fisher Scientific). The cloning reaction was prepared based on the manufacturer's guidelines, where 15-30 ng of *PcinCRN* PCR product was used. The full volume of the cloning reaction was transformed into *Escherichia coli* DH5α competent cells using chemical transformation. Transformed cells were plated on LB/Kan50 agar plates (2.5% w/v LB medium, 1.5% w/v agar bacteriological, 0.1% v/v 50 µg/ml Kanamycin) and incubated overnight at 37°C. Three transformants for each *PcinCRN* amplicon were selected for plasmid extraction. Transformants were inoculated into 5 ml LB/Kan50 broth and incubated overnight at 37°C with shaking (150 rpm). Plasmids were extracted using QIAprep® Spin Miniprep Kit (QIAGEN, Hilden, Germany), with the following modifications to the manufacturer's protocol: 4 ml of overnight culture was collected by centrifugation at 13, 000 rpm for 1 min at room temperature; the PB buffer wash step was added; 30 µl of EB buffer was used to elute DNA and allowed to stand for 5 min prior to centrifugation. The concentration of the plasmid extractions was determined using a NanoDrop™ 2000 Spectrophotometer. The plasmid extractions were sequenced via Sanger sequencing using BigDye® Terminator v3.1 Cycle Sequencing Kit (Thermo Fisher Scientific) and vector specific M13 primers (Supplementary Table 12B). Each *PcinCRN* was sequenced in both the forward and the reverse orientation. Each sequencing reaction contained: 0.85 X Sequencing buffer, 4.17% v/v BigDye 3.1, 0.83 µM primer, 40-200 ng plasmid DNA. The sequencing reaction was done in the Veriti 96 Well Thermal Cycler, set for an initial

denaturation at 96°C for 5 s, followed by 25 cycles of 10 s denaturation at 96°C, 5 s annealing at 55°C and 4 min extension at 60°C.

The sequencing products were precipitated using a sodium acetate protocol, as follows: 60 µl of a precipitation mixture containing 2 µl NaOAc 3M, pH 5.2, and 50 µl 100% ethanol was added to each sequencing product. The tubes were incubated on ice for 15 min and centrifuged at 12, 000 g for 30 min. Ethanol (70% v/v) was used to clean the DNA pellet twice, each followed by centrifugation at 12, 000 g for 10 min. The supernatant was removed, and the DNA pellets were dried in a heating block set at 66 °C for 10 min. All samples were submitted to the DNA Sanger sequencing facility at the University of Pretoria for sequencing using an ABI 3500xl genetic analyser (Thermo Fisher Scientific). The presence of a NLS was determined by submitting the translated amino acid sequences of each PcinCRN through NLStradamus (60) using a 4 state HMM static model with a Posterior cut-off of 0.4.

Confirming the presence of *PcinCRN* alleles in two additional *P. cinnamomi* isolates

Genomic DNA was extracted from freeze-dried mycelia of two different *P. cinnamomi* isolates (Pcin_isolate129 and Pcin_isolate308) using CTAB extraction protocol (61). Both isolates were sampled from *P. cinnamomi* infected *P. americana* trees located in different orchards in Tzaneen, Limpopo, South Africa. The same amplification, cloning, extraction, and sequencing protocol as mentioned above was used to confirm the presence of *PcinCRN73, PcinCRN75, PcinCRN53* and *PcinCRN95* alleles.

Protein modelling of confirmed full-length PcinCRN allele amino acid sequences

AlphaFold (28, 29) was used to predict the protein structure of PcinCRN sequences shown to have more than one allele. On a scale from 0 to 100, AlphaFold generated a per-residue confidence metric: predicted local distance difference test (pLDDT). A high pLDDT score (> 80) indicates high confidence in the structure of the residue, whereas a low pLDDT score (< 50) may indicate that the residues are in intrinsically disordered protein regions. The protein structures generated were visualised using the PyMOL Molecular Graphics System, Version v.2.3.0 (Schrödinger, LLC). The protein structures for the different alleles were compared to one another to determine whether the amino acid changes resulted in protein folding differences.

Phylogenetic analysis

The amino acid sequences of putative CRNs from other *Phytophthora* spp. were obtained from the UniprotKB database (Uniprot Consortium, 2014) (Supplementary Table 13) and the full-length PcinCRN proteins identified and validated in this study were used. All sequences were trimmed after the HVLVXXP motif so that only the N-terminal was used in the alignment. The CRN amino acid sequences were aligned using MUSCLE in CLC Main Workbench. The alignment was subjected to Bayesian inference analysis using MrBayes 3.2.7a. in Geneious Prime 2022.2.2 (Biomatters, New Zealand), using the Poisson substitution model and a CRN from *Pythium ultimum* as an outgroup. In the analysis, one million generations of the Markov chain Monte Carlo (MCMC) analysis were used, with trees being sampled at every 200th generation. Following the MCMC analysis, 10% of the trees were discarded as burn-in phase, with the remaining trees being used to calculate posterior probabilities. A second phylogenetic analysis was performed using the same criteria as above, except the full-length sequences of confirmed PcinCRN amino acid sequences were compared to the full-length amino acid sequences of only functionally characterised CRNs from other *Phytophthora* spp. (Supplementary Table 14).

References

1. Hardham AR, Blackman LM. *Phytophthora cinnamomi*. Molecular Plant Pathology. 2018;19:260-85. https://doi.org/10.1111/mpp.12568.
2. Ramírez-Gil JG, Castañeda-Sánchez DA, Morales-Osorio JG. Production of avocado trees infected with *Phytophthora cinnamomi* under different management regimes. Plant Pathology. 2017;66:623-32. https://doi.org/10.1111/ppa.12620.
3. Boevink PC, Birch PR, Turnbull D, Whisson SC. Devastating intimacy: the cell biology of plant–*Phytophthora* interactions. New Phytologist. 2020;228:445-58. https://doi.org/10.1111/nph.16650.
4. Lamour KH, Stam R, Jupe J, Huitema E. The oomycete broad-host-range pathogen *Phytophthora capsici*. Molecular Plant Pathology. 2012;13:329-37. https://doi.org/10.1111/j.1364-3703.2011.00754.x.
5. Kamoun S, Furzer O, Jones JD, Judelson HS, Ali GS, Dalio RJ, et al. The Top 10 oomycete pathogens in molecular plant pathology. Molecular Plant Pathology. 2015;16:413-34. https://doi.org/10.1111/mpp.12190.
6. Kroon L, Brouwer H, De Cock A, Govers F. The *Phytophthora* genus anno 2012. Phytopathology. 2012;102:348-64. https://doi.org/10.1094/PHYTO-01-11-0025.
7. Cahill DM, Rookes JE, Wilson BA, Gibson L, McDougall KL. *Phytophthora cinnamomi* and Australia's biodiversity: impacts, predictions and progress towards control. Australian Journal of Botany. 2008;56:279-310. https://doi.org/10.1071/BT07159.
8. Jung T, Colquhoun I, Hardy GSJ. New insights into the survival strategy of the invasive soilborne pathogen *Phytophthora cinnamomi* in different natural ecosystems in Western Australia. Forest Pathology. 2013;43:266-88. https://doi.org/10.1111/efp.12025.
9. Chakraborty S, Murray G, Magarey P, Yonow T, O'Brien R, Croft B, et al. Potential impact of climate change on plant diseases of economic significance to Australia. Australasian Plant Pathology. 1998;27:15-35.
10. Hardham AR. *Phytophthora cinnamomi*. Molecular Plant Pathology. 2005;6:589-604. https://doi.org/10.1111/j.1364-3703.2005.00308.x.
11. Zhang M, Li Q, Liu T, Liu L, Shen D, Zhu Y, et al. Two cytoplasmic effectors of *Phytophthora sojae* regulate plant cell death via interactions with plant catalases. Plant Physiology. 2015;167:164-75. https://doi.org/10.1104/pp.114.252437.
12. Maximo HJ, Dalio RJ, Dias RO, Litholdo CG, Felizatti HL, Machado MA. PpCRN7 and PpCRN20 of *Phythophthora parasitica* regulate plant cell death leading to enhancement of host susceptibility. BMC Plant Biology. 2019;19:1-17. https://doi.org/10.1186/s12870-019-2129-8.
13. Stam R, Jupe J, Howden AJ, Morris JA, Boevink PC, Hedley PE, et al. Identification and characterisation CRN effectors in *Phytophthora capsici* shows modularity and functional diversity. PloS One. 2013;8:e59517. https://doi.org/10.1371/journal.pone.0059517.
14. Midgley KA, van den Berg N, Swart V. Unraveling plant cell death during *Phytophthora* infection. Microorganisms. 2022;10:1139. https://doi.org/10.3390/microorganisms10061139.
15. Huysmans M, Coll NS, Nowack MK. Dying two deaths—programmed cell death regulation in development and disease. Current Opinion in Plant Biology. 2017;35:37-44. https://doi.org/10.1016/j.pbi.2016.11.005.
16. Balint-Kurti P. The plant hypersensitive response: concepts, control and consequences. Molecular Plant Pathology. 2019;20:1163-78. https://doi.org/10.1111/mpp.12821.
17. Mukhtar MS, McCormack ME, Argueso CT, Pajerowska-Mukhtar KM. Pathogen tactics to manipulate plant cell death. Current Biology. 2016;26:R608-R19. http://dx.doi.org/10.1016/j.cub.2016.02.051.
18. Liu T, Ye W, Ru Y, Yang X, Gu B, Tao K, et al. Two host cytoplasmic effectors are required for pathogenesis of *Phytophthora sojae* by suppression of host defenses. Plant Physiology. 2011;155:490-501. https://doi.org/10.1104/pp.110.166470.
19. Mafurah JJ, Ma H, Zhang M, Xu J, He F, Ye T, et al. A virulence essential CRN effector of *Phytophthora capsici* suppresses host defense and induces cell death in plant nucleus. PLoS One. 2015;10:e0127965. https://doi.org/10.1371/journal.pone.0127965.
20. Torto TA, Li S, Styer A, Huitema E, Testa A, Gow NA, et al. EST mining and functional expression assays identify extracellular effector proteins from the plant pathogen *Phytophthora*. Genome Research. 2003;13:1675-85. 10.1101/gr.910003.

21. Stam R, Howden A, Delgado Cerezo M, Amaro T, Motion G, Pham J, et al. Characterization of cell death inducing *Phytophthora capsici* CRN effectors suggests diverse activities in the host nucleus. Frontiers in Plant Science. 2013;4:10.3389/fpls.2013.00387. https://doi.org/10.3389/fpls.2013.00387.
22. Adhikari BN, Hamilton JP, Zerillo MM, Tisserat N, Lévesque CA, Buell CR. Comparative genomics reveals insight into virulence strategies of plant pathogenic oomycetes. PloS One. 2013;8:e75072. https://doi.org/10.1371/journal.pone.0075072.
23. Schornack S, van Damme M, Bozkurt TO, Cano LM, Smoker M, Thines M, et al. Ancient class of translocated oomycete effectors targets the host nucleus. Proceedings of the National Academy of Sciences of the United States of America. 2010;107:17421-6. https://doi.org/10.1073/pnas.1008491107.
24. Van Damme M, Bozkurt TO, Cakir C, Schornack S, Sklenar J, Jones AM, et al. The Irish potato famine pathogen *Phytophthora infestans* translocates the CRN8 kinase into host plant cells. PLoS Pathog. 2012;8:e1002875. https://doi.org/10.1371/journal.ppat.1004753.
25. Meyer FE, Shuey LS, Naidoo S, Mamni T, Berger DK, Myburg AA, et al. Dual RNA-sequencing of *Eucalyptus nitens* during *Phytophthora cinnamomi* challenge reveals pathogen and host factors influencing compatibility. Frontiers in Plant Science. 2016;7:191. https://doi.org/10.3389/fpls.2016.00191.
26. Engelbrecht J, Duong TA, Prabhu SA, Seedat M, van den Berg N. Genome of the destructive oomycete *Phytophthora cinnamomi* provides insights into its pathogenicity and adaptive potential. BMC Genomics. 2021;22:1-15. https://doi.org/10.1186/s12864-021-07552-y.
27. Zhang D, Burroughs AM, Vidal ND, Iyer LM, Aravind L. Transposons to toxins: the provenance, architecture and diversification of a widespread class of eukaryotic effectors. Nucleic Acids Research. 2016;44:3513-33. https://doi.org/10.1093/nar/gkw221.
28. Varadi M, Anyango S, Deshpande M, Nair S, Natassia C, Yordanova G, et al. AlphaFold Protein Structure Database: massively expanding the structural coverage of protein-sequence space with high-accuracy models. Nucleic Acids Research. 2022;50:D439-D44. https://doi.org/10.1093/nar/gkab1061.
29. Jumper J, Evans R, Pritzel A, Green T, Figurnov M, Ronneberger O, et al. Highly accurate protein structure prediction with AlphaFold. Nature. 2021;596:583-9. https://doi.org/10.1038/s41586-021-03819-2.
30. Haas BJ, Kamoun S, Zody MC, Jiang RH, Handsaker RE, Cano LM, et al. Genome sequence and analysis of the Irish potato famine pathogen *Phytophthora infestans*. Nature. 2009;461:393-8. doi:10.1038/nature08358.
31. Li Q, Zhang M, Shen D, Liu T, Chen Y, Zhou J-M, et al. A *Phytophthora sojae* effector PsCRN63 forms homo-/hetero-dimers to suppress plant immunity via an inverted association manner. Scientific Reports. 2016;6:1-13. 10.1038/srep26951.
32. Song T, Ma Z, Shen D, Li Q, Li W, Su L, et al. An oomycete CRN effector reprograms expression of plant *HSP* genes by targeting their promoters. PLoS Pathog. 2015;11:e1005348. https://doi.org/10.1371/journal.ppat.1005348.
33. Rajput NA, Zhang M, Shen D, Liu T, Zhang Q, Ru Y, et al. Overexpression of a *Phytophthora* cytoplasmic CRN effector confers resistance to disease, salinity and drought in *Nicotiana benthamiana*. Plant and Cell Physiology. 2015;56:2423-35. https://doi.org/10.1093/pcp/pcv164.
34. Studholme D, McDougal R, Sambles C, Hansen E, Hardy G, Grant M, et al. Genome sequences of six *Phytophthora* species associated with forests in New Zealand. Genomics Data. 2016;7:54-6. https://doi.org/10.1016/j.gdata.2015.11.015.
35. Longmuir AL, Beech PL, Richardson MF. Draft genomes of two Australian strains of the plant pathogen, *Phytophthora cinnamomi*. F1000Research. 2017;6:1972. https://doi.org/10.12688%2Ff1000research.12867.2.
36. Backer R, Mahomed W, Reeksting BJ, Engelbrecht J, Ibarra-Laclette E, van den Berg N. Phylogenetic and expression analysis of the *NPR1*-like gene family from *Persea americana* (Mill.). Frontiers in Plant Science. 2015;6:10.3389/fpls.2015.00300. https://doi.org/10.3389/fpls.2015.00300.
37. Kanneganti T-D, Huitema E, Cakir C, Kamoun S. Synergistic interactions of the plant cell death pathways induced by *Phytophthora infestans* Nep1-like protein PiNPP1. 1 and INF1 elicitin. Molecular Plant-Microbe Interactions. 2006;19:854-63. https://doi.org/10.1094/MPMI-19-0854.
38. Kunjeti SG, Evans TA, Marsh AG, Gregory NF, Kunjeti S, Meyers BC, et al. RNA-Seq reveals infection-related global gene changes in *Phytophthora phaseoli*, the causal agent of lima bean downy mildew. Molecular Plant Pathology. 2012;13:454-66. https://doi.org/10.1111/j.1364-3703.2011.00761.x.

39. Kelley BS, Lee SJ, Damasceno CM, Chakravarthy S, Kim BD, Martin GB, et al. A secreted effector protein (SNE1) from *Phytophthora infestans* is a broadly acting suppressor of programmed cell death. The Plant Journal. 2010;62:357-66. https://doi.org/10.1111/j.1365-313X.2010.04160.x.
40. Amaro TMMM, Thilliez GJA, Motion GB, Huitema E. A perspective on CRN Proteins in the genomics age: evolution, classification, delivery and function revisited. Frontiers in Plant Science. 2017;8. https://doi.org/10.3389/fpls.2017.00099.
41. Dangl JL, Jones JD. Plant pathogens and integrated defence responses to infection. Nature. 2001;411:826-33.
42. Naveed ZA, Wei X, Chen J, Mubeen H, Ali GS. The PTI to ETI continuum in *Phytophthora*-plant interactions. Frontiers in Plant Science. 2020;11:593905. https://doi.org/10.3389/fpls.2020.593905.
43. Fick A, Swart V, Backer R, Bombarely A, Engelbrecht J, Van den Berg N. Partially resistant avocado rootstock Dusa® shows prolonged upregulation of *nucleotide binding-Leucine rich repeat* genes in response to *Phytophthora cinnamomi* infection. Frontiers in Plant Science. 2022;13. https://doi.org/10.3389%2Ffpls.2022.793644.
44. Sun F, Kale SD, Azurmendi HF, Li D, Tyler BM, Capelluto DG. Structural basis for interactions of the *Phytophthora sojae* RxLR effector Avh5 with phosphatidylinositol 3-phosphate and for host cell entry. Molecular Plant-Microbe Interactions. 2013;26:330-44. https://doi.org/10.1094/MPMI-07-12-0184-R.
45. Li H, Hu R, Fan Z, Chen Q, Jiang Y, Huang W, et al. Dual RNA sequencing reveals the genome-wide expression profiles during the compatible and incompatible interactions between *Solanum tuberosum* and *Phytophthora infestans*. Frontiers in Plant Science. 2022;13:817199. https://doi.org/10.3389/fpls.2022.817199.
46. Krogh A, Larsson B, Von Heijne G, Sonnhammer EL. Predicting transmembrane protein topology with a hidden Markov model: application to complete genomes. Molecular Biology. 2001;305:567-80. https://doi.org/10.1006/jmbi.2000.4315.
47. Letunic I, Khedkar S, Bork P. SMART: recent updates, new developments and status in 2020. Nucleic Acids Research. 2021;49:D458-D60. https://doi.org/10.1093/nar/gkaa937.
48. Abeel T, Van Parys T, Saeys Y, Galagan J, Van de Peer Y. GenomeView: a next-generation genome browser. Nucleic Acids Research. 2012;40:e12-e. https://doi.org/10.1093/nar/gkr995.
49. Backer R, Engelbrecht J, van den Berg N. Differing responses to *Phytophthora cinnamomi* infection in susceptible and partially resistant *Persea americana* (Mill.) rootstocks: A case for the role of receptor-like kinases and apoplastic proteases. Frontiers in Plant Science. 2022;13:928176. https://doi.org/10.3389/fpls.2022.928176.
50. Bolger AM, Lohse M, Usadel B. Trimmomatic: a flexible trimmer for Illumina sequence data. Bioinformatics. 2014;30:2114-20. https://doi.org/10.1093/bioinformatics/btu170.
51. Ewels P, Magnusson M, Lundin S, Käller M. MultiQC: summarize analysis results for multiple tools and samples in a single report. Bioinformatics. 2016;32:3047-8. https://doi.org/10.1093/bioinformatics/btw354.
52. Kim D, Langmead B, Salzberg SL. HISAT: a fast spliced aligner with low memory requirements. Nature Methods. 2015;12:357-60.
53. Liao Y, Smyth GK, Shi W. featureCounts: an efficient general purpose program for assigning sequence reads to genomic features. Bioinformatics. 2013;30:923-30. https://doi.org/10.1093/bioinformatics/btt656.
54. Love MI, Huber W, Anders S. Moderated estimation of fold change and dispersion for RNA-seq data with DESeq2. Genome Biology. 2014;15:550. 10.1186/s13059-014-0550-8.
55. A language and environment for statistical computing [Internet]. 2020. Available from: https://www.R-project.org/.
56. Kolde R. Pheatmap: pretty Heatmaps. . R package v 10 8. 2015;7:790.
57. King M, Reeve W, Van der Hoek MB, Williams N, McComb J, O'Brien PA, et al. Defining the phosphite-regulated transcriptome of the plant pathogen *Phytophthora cinnamomi*. Molecular Genetics and Genomics 2010;284:425-35. 10.1007/s00438-010-0579-7.
58. Narayan RD, Blackman LM, Shan W, Hardham AR. *Phytophthora nicotianae* transformants lacking dynein light chain 1 produce non-flagellate zoospores. Fungal Genetics and Biology. 2010;47:663-71. https://doi.org/10.1016/j.fgb.2010.04.008.
59. Pfaffl MW. A new mathematical model for relative quantification in real-time RT–PCR. Nucleic Acids Research. 2001;29:e45-e. https://doi.org/10.1093/nar/29.9.e45.

60. Nguyen Ba AN, Pogoutse A, Provart N, Moses AM. NLStradamus: a simple Hidden Markov Model for nuclear localization signal prediction. BMC Bioinformatics. 2009;10:1-11. 10.1186/1471-2105-10-202.
61. Chang S, Puryear J, Cairney J. A simple and efficient method for isolating RNA from pine trees. Plant Molecular Biology Reporter. 1993;11:113-6.

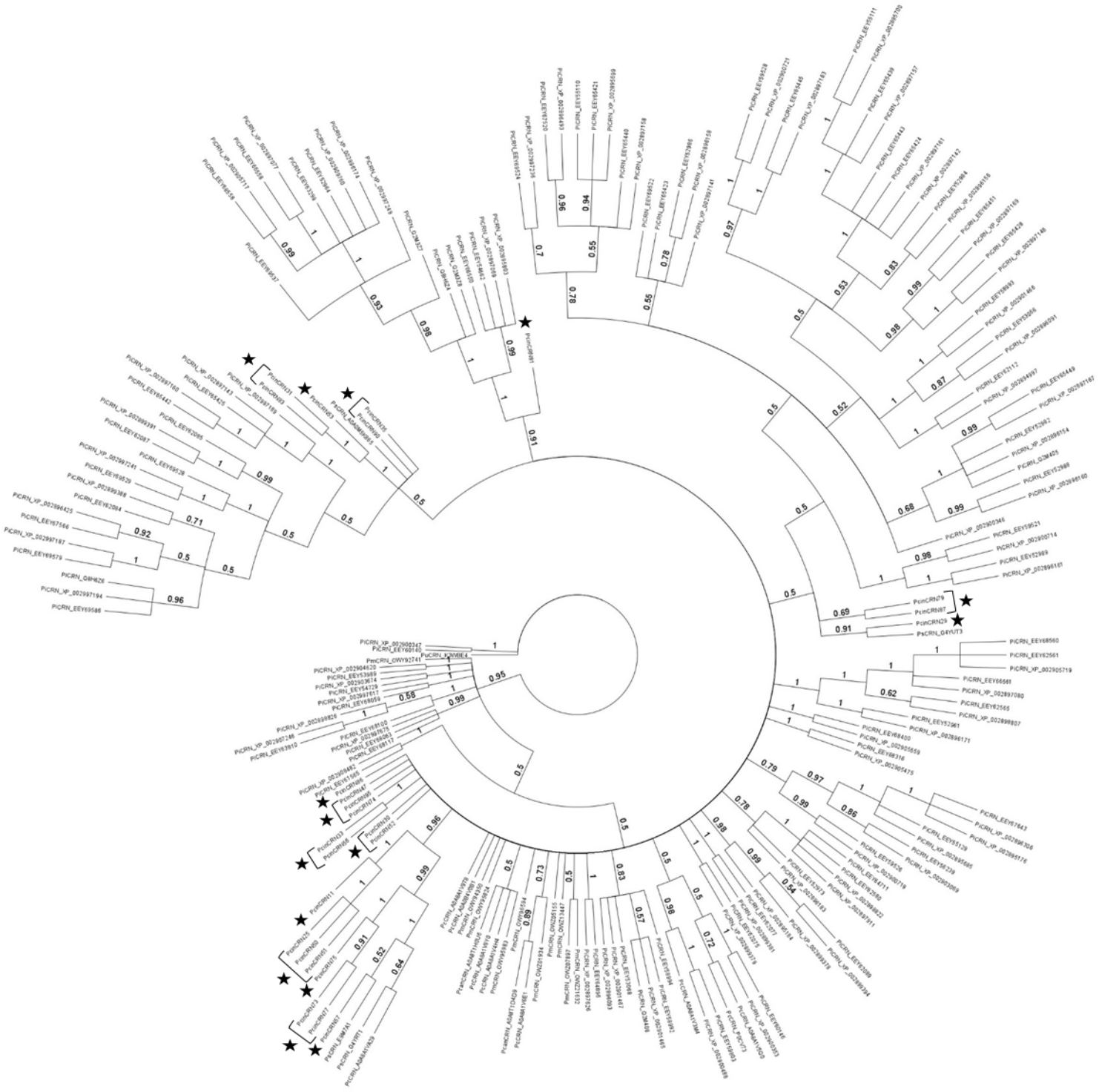

Supplementary Figure 1. Evolutionary relatedness of identified PcinCRNs to CRNs from other *Phytophthora* spp. Alignment of predicted N-terminal regions of putative *Phytophthora cinnamomi* crinkling and necrosis (PcinCRN) effectors with the N-terminal regions of CRNs from other *Phytophthora* spp. resulted in the construction of a phylogenetic tree using Bayesian inference analysis. Support for branches is indicated by posterior probability values, which are displayed for each node to the second significant digit. with a posterior probability cut-off of < 0.5. Putative PcinCRN effectors proteins are indicated with stars. All 25 PcinCRNs were found to have homology to CRNs from other *Phytophthora* spp.

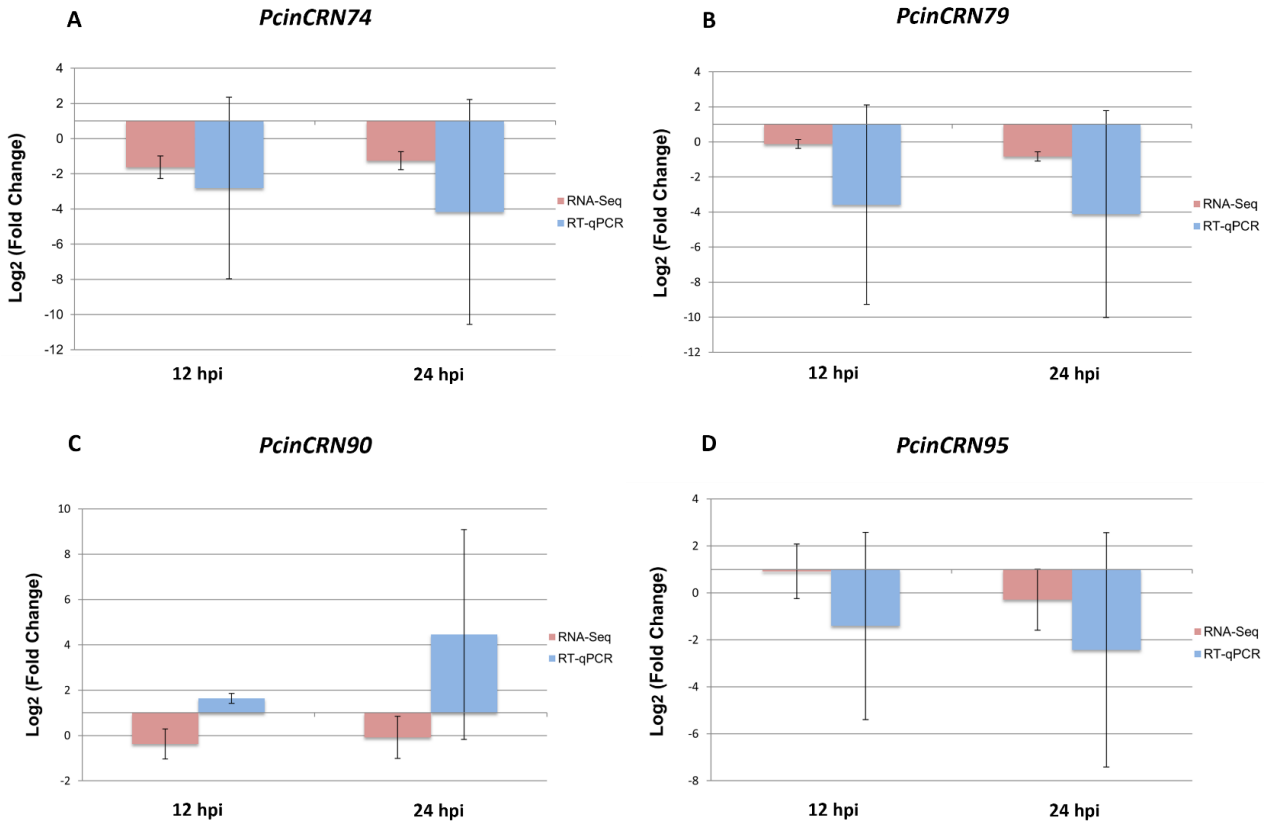

Supplementary Figure 2. Expression validation of selected *Phytophthora cinnamomi crinkling and necrosis (PcinCRN)* effector genes at 12 and 24 hpi compared to mycelial control. Normalized Log2 (Fold Change) for (A) *PcinCRN74*, (B) *PcinCRN79*, (C) *PcinCRN90*, and (D) *PcinCRN95* were calculated using the method described by Pfaffl (2001) (58). The expression of PcinCRNs during infection of R012 avocado rootstock is indicated by vertical bars across two time points using RNA-seq data (red) and RT-qPCR (blue). The samples were compared to *P. cinnamomi* mycelia. SE for each bar is shown.

A

```
                                  20                  40                  60                  80
PcinCRN30_1 MVKLFCAIVG VAGNAFSVRV DESDCVGDLK YAIKKKKPND FKDIDADKLR LFLAKTKGGV WLDGAGAASV ALDERGHPQG 80
PcinCRN30_2 MVKLFCAIVG VAGNAFSVRV DESDCVGDLK YAIKKKKPND FKDIDADKLR LFLAKTKGGV WLDGAGAASV ALDGRGHPQG 80
                                 100                 120
PcinCRN30_1 YLQMDPALWI KYPKHFGANF RPGEGQVHVL VVVPGHVRVD IGETASRALK YKRTYSRP 138
PcinCRN30_2 YLQMDPALWI KYPKHFGANF RPGEGQVHVL VVVPGHVRVD IGETASRALK YKRTYSRP 138
```

B

```
                                  20                  40                  60                  80
PcinCRN81_1 MVLVALTCAL VGNAGVFGVK IDDSAKVSKL KDVVKGKNTS TIKCDAKDLQ LFLAKNDEGR GAWLDGAGAA AVALDERGHP 80
PcinCRN81_2 MVLVALTCAL VGNAGVFGVK IDDSAKVSKL KDVVKGKNTS TIKCDAKDLQ LFLAKNDEGR GAWLDGAGAA AVALDERGHP 80
                                 100                 120                 140
PcinCRN81_1 QGCVQMDPTL SIKNPKHFGD NFQPGEGQVH VLVVVPGHVR VDIGGTASRA LKYKRTYSRP 140
PcinCRN81_2 QGCVQMDPTL SIKNPKHFGD NSQPGEGQVH VLVVVPGHVR VDIGGTASRA LKYKRTYSRP 140
```

Supplementary Figure 3. Schematic comparing PcinCRN30 and PcinCRN81 protein sequences. The confirmed amino acid sequences of the *Phytophthora cinnamomi* crinkling and necrosis (PcinCRN) effectors of **(A)** PcinCRN30_1 and PcinCRN30_2, and **(B)** PcinCRN81_1 and PcinCRN81_2 were aligned using CLC Main Workbench with a gap open cost value of 10,0 and a gap extension cost value of 1,0. Both PcinCRN30 and PcinCRN81 have a single nucleotide polymorphism (SNP) change between their variants, which results in a non-synonymous amino acid change indicated in red.

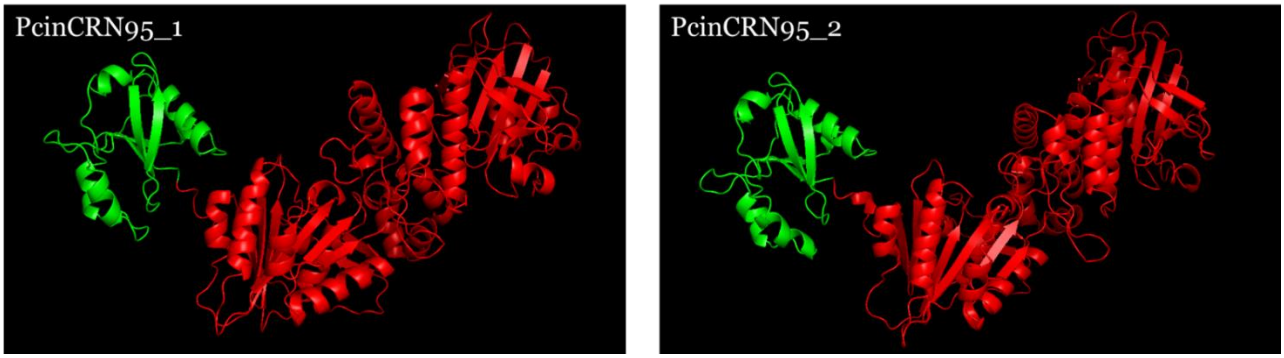

Supplementary Figure 4. Predicted protein structures of the amino acid sequences encoded by the PcinCRN95 alleles using AlphaFold. AlphaFold (28, 29) was used to predict the tertiary structure of *Phytophthora cinnamomi* crinkling and necrosis effector protein 95 (PcinCRN95). On a scale from 0 to 100, AlphaFold generated a per-residue confidence metric titled predicted local distance difference test (pLDDT). A high pLDDT score (> 80) indicates high confidence in the structure of the residue, whereas a low pLDDT score (< 50) may indicate that the residues are in intrinsically disordered protein regions. The predicted tertiary structures were visualised in PyMOL v2.5.5 (Schrödinger, LLC). Green labelled structures represent the N-terminal up until the HVLVXXP motif. Red labelled structures represent the C-terminal. Protein structure of PcinCRN95_1 (pLDDT = 84.27) and PcinCRN95_2 (pLDDT = 84.89) showed no obvious change in tertiary protein folding between them.

E = 83.0% R^2 = 0.996 Slope = -3.881

E = 83.1% R^2 = 0.999 Slope = -3.806

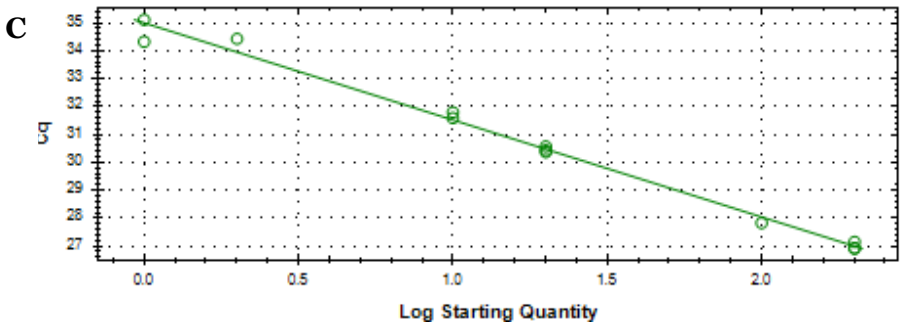

E = 93.9% R^2 = 0.991 Slope = -3.478

Supplementary Figure 5. Standard curves of RT-qPCR reference genes. Standard curves of the reference genes were prepared from a 5-fold dilution series of a cDNA template pool. The (A) *Ubc*, (B) *B-Tubulin* and (C) *WS041*. The log of the starting quantity was plotted against the Cq value for each of the standard wells and a line of best fit was drawn through the data points. The efficiency (E), slope and correlation (R^2) values are indicated.

A

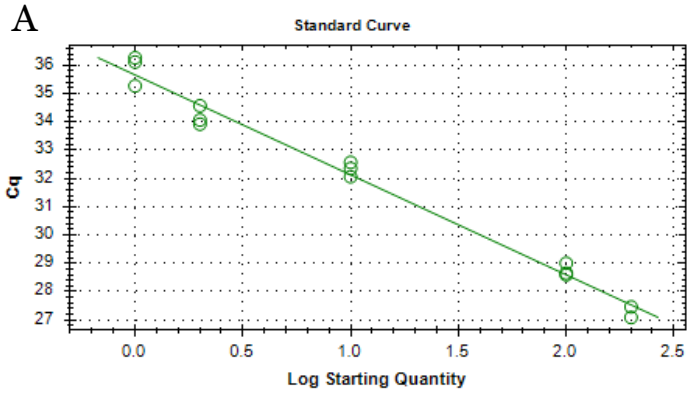

E = 91.8% **R²** = 0.985 **Slope** = -3.535

B

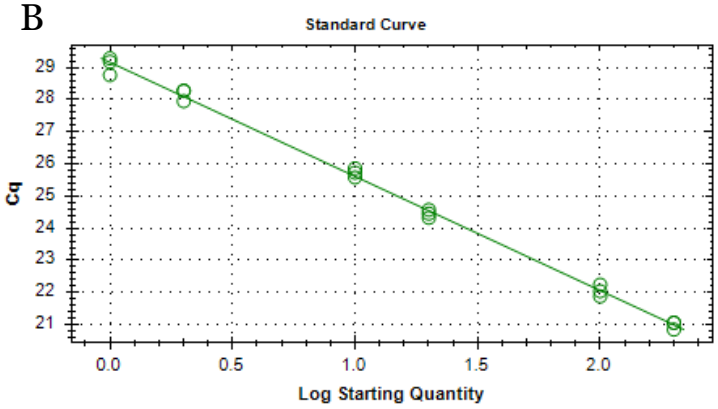

E = 91.3% **R²** = 0.997 **Slope** = -3.551

C

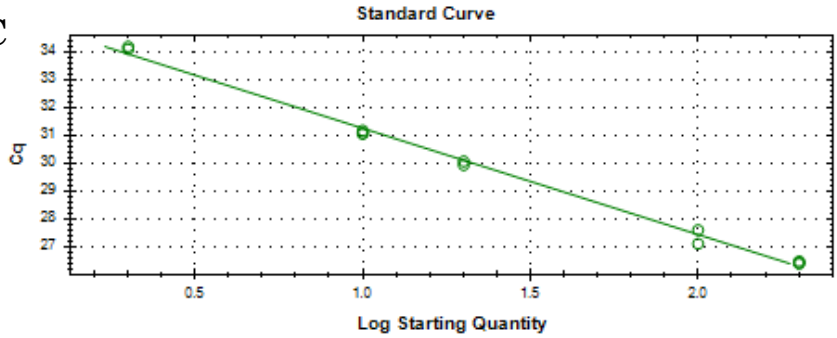

E = 83.0% **R²** = 0.995 **Slope** = -3.811

D

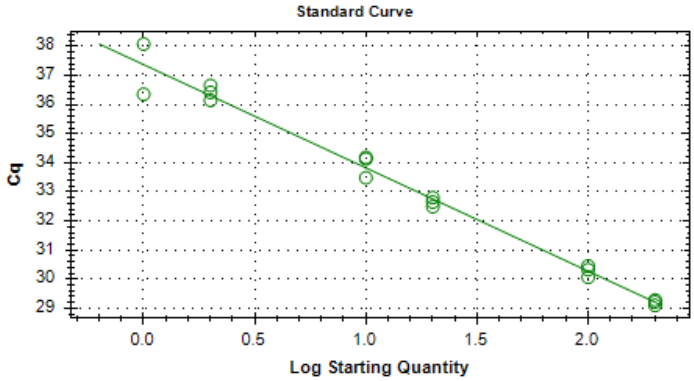

E = 91.3% **R²** = 0.984 **Slope** = -3.550

Supplementary Figure 6. Standard curves of target *PcinCRN* genes for RT-qPCR. Standard curves of the reference genes were prepared from a 5-fold dilution series of a cDNA template pool. (A) *PcinCRN74*, (B) *PcinCRN79*, (C) *PcinCRN90* and (D) *PcinCRN95*. The log of the starting quantity was plotted against the Cq value for each of the standard wells and a line of best fit was drawn through the data points. The efficiency (E), slope and correlation (R^2) values are indicated.

Supplementary Table 1. List of putative *Phytophthora cinnamomi* crinkling and necrosis (PcinCRN) generated from the *Phytophthora cinnamomi* GKB4 transcriptome. A list of 46 putative PcinCRN effector proteins was generated from the *Phytophthora cinnamomi* GKB4 transcriptome using a Hidden Markov model (HMM) profile. The E-values, sequence bit score and bias for all 46 putative are indicated. Putative PcinCRNs with sequence ID jg9519.t1, jg8578.t1, jg11278.t1, jg14023.t1 were excluded from further analysis due to the E-values being <10-3 and the lack of both LXLFLAK and HVLVXXP motifs.

Sequence ID	E-value	Sequence bit score	Bias
PcinCRN79	7.0e-68	229.5	0.7
PcinCRN50	3.7e-64	217.3	0.1
PcinCRN51	1.4e-62	212.1	0.1
PcinCRN77	5.7e-61	206.8	0.5
PcinCRN73	1.8e-60	205.2	0.6
PcinCRN75	6.4e-57	193.5	1.1
PcinCRN87	4.1e-53	181.1	2.5
PcinCRN53	4.5e-52	177.7	1.0
PcinCRN11	1.6e-43	149.7	0.0
PcinCRN30	2.0e-43	149.3	0.0
PcinCRN52	4.4e-43	148.2	0.0
jg9952.t2	9.9e-43	147.1	0.1
PcinCRN95	8.5e-40	137.5	0.0
PcinCRN25	1.4e-38	133.4	0.0
PcinCRN90	1.9e-37	129.8	1.5
PcinCRN35	2.6e-36	126.0	0.0
PcinCRN56	4.2e-34	118.8	3.1
jg4983.t1	2.2e-29	103.4	2.1
PcinCRN57	8.9e-29	101.4	0.1
PcinCRNpartial1	2.1e-28	100.2	0.0
PcinCRN29	9.9e-28	97.9	2.0
PcinCRN33	5.9e-27	95.4	1.9
jg14422.t1	2.4e-26	93.4	0.2
PcinCRN31	2.4e-26	93.4	0.8
PcinCRN81	7.5e-25	88.5	0.2
jg8505.t1	1.8e-21	77.5	0.1
PcinCRN47	6.2e-21	75.7	0.1
PcinCRN83	5.2e-20	72.6	0.8
PcinCRN74	3.6e-19	69.9	0.0
jg14560.t1	4.5e-15	56.5	0.0
jg7432.t2	1.7e-14	54.6	3.4
jg7432.t1	2.1e-14	54.3	3.4
PcinCRN86	1.1e-12	48.6	0.0
jg8953.t1	1.4e-11	45.1	0.0
jg16316.t1	3.2e-11	43.9	0.0
jg5203.t1	1.9e-10	41.4	0.1
jg17230.t1	1.6e-09	38.3	0.0
jg14294.t1	4.8e-09	36.7	0.0
jg13126.t1	5.8e-07	29.9	1.9
jg2719.t1	1.6e-06	28.5	0.2

jg2083.t1	9.1e-06	26.0	0.0
jg14293.t1	5.7e-05	23.4	0.0
jg9519.t1	*0.00013	22.2	0.0
jg8578.t1	*0.00017	21.8	0.1
jg11278.t1	*0.01	16.0	0.0
jg14023.t1	*0.015	15.5	0.0

* The E-value is >10-3 and therefore are not considered as significant hits

Supplementary Table 2: Analysis of all putative PcinCRN sequences identified from the *P. cinnamomi* genome. Table summarizing the CRN architecture of all putative *Phytophthora cinnamomi* crinkling and necrosis (PcinCRN) effectors identified from the *P. cinnamomi CRN* effector proteins from this study and the study by Engelbrecht, et al (2022) (26), where the BLAST2GO method was used to search the same *P. cinnamomi* genome. A PcinCRN was validated as a 'true' Full-length *Phytophthora* CRN if the sequence contains both the LXLFLAK and HVLVXXP motifs and did not contain a trans membrane helix (TMH). A CRN was classified as a partial/CRN-like sequence if it has all characteristic CRN motifs but is truncated. The presence/absence of a signal peptide, TMH, low complexity regions (LCR's), LXLFLAK and HVLVXXP motif are indicated. The classification of the putative PcinCRN is also denoted as either full-length CRN, Partial/CRN-like or not a CRN.

Sequence ID	Amino acid length	Signal peptide	TMH	LXLFLAK motif	HVLVXXP motif	Low Complexity regions (LCR's)	Classification
PcinCRN79	427	Yes	No	Yes	Yes	None	Full length CRN
PcinCRN50	424	Yes	No	Yes[1]	Yes	Terminal LCR	Full length CRN
PcinCRN51	424	No	No	Yes[1]	Yes	None	Full length CRN
PcinCRN77	305	Yes	No	Yes	Yes[1]	None	Full length CRN
PcinCRN73	303	Yes	No	Yes	Yes[1]	None	Full length CRN
PcinCRN75	305	Yes	No	Yes	Yes	None	Full length CRN
PcinCRN87	177	Yes	No	Yes	Yes	Terminal LCR	Full length CRN
PcinCRN53	260	No	No	Yes	Yes	None	Full length CRN
PcinCRN11	423	Yes	No	Yes[1]	Yes	Central & terminal LCR	Full length CRN
PcinCRN30	172	Yes	No	Yes	Yes	Central LCR	Full length CRN
PcinCRN52	170	No	No	Yes	Yes	Central LCR	Full length CRN
jg9952.t2	283	No	Yes	Yes	Yes	N/A	Not a CRN
PcinCRN95	626	No	No	Yes	Yes	Central LCR	Full length CRN
PcinCRN25	417	Yes	No	Yes[1]	Yes	Terminal LCR	Full length CRN
PcinCRN90	130	Yes	No	Yes	Yes[2]	None	Full length CRN
PcinCRN35	305	Yes	No	Yes[1]	Yes[1]	None	Full length CRN
PcinCRN56	131	No	No	Yes	Yes[2]	Central & terminal LCR	Full length CRN
jg4983.t1	80	No	No	Yes	No	None	Not a CRN
PcinCRN57	190	No	No	Yes[1]	Yes[1]	N/A	Full length CRN
PcinCRNpartial1	520	No	No	Yes	Yes	N/A	Partial/CRN-like
PcinCRN29	142	Yes	No	Yes[1]	Yes[2]	None	Full length CRN
PcinCRN33	142	No	No	Yes	Yes[1]	Central LCR	Full length CRN
jg14422.t1	125	No	No	Yes[1]	No	N/A	Not a CRN
PcinCRN31	227	Yes	No	Yes	Yes[2]	Terminal LCR	Full length CRN
PcinCRN81	140	Yes	No	Yes	Yes[2]	Central & terminal LCR	Full length CRN
jg8505.t1	532	No	Yes	Yes[1]	Yes	N/A	Not a CRN
PcinCRN47	478	No	No	Yes	Yes[1]	Central & terminal LCR	Full length CRN
PcinCRN83	216	Yes	No	Yes	Yes[2]	None	Full length CRN
PcinCRN74	349	No	No	Yes	Yes	Central LCR	Full length CRN
jg14560.t1	641	No	No	No	Yes[1]	N/A	Not a CRN
jg7432.t2	2644	No	No	No	No	N/A	Not a CRN
jg7432.t1	2646	No	No	No	No	N/A	Not a CRN

PcinCRN86	133	Yes	No	Yes[1]	Yes[1]	Terminal LCR	Full length CRN
jg8953.t1	490	Yes	No	No	No	N/A	Not a CRN
jg16316.t1	629	No	No	No	Yes	N/A	Not a CRN
jg5203.t1	130	No	No	No	No	N/A	Not a CRN
jg17230.t1	84	No	No	No	No	N/A	Not a CRN
jg14294.t1	106	No	No	Yes[1]	No	N/A	Not a CRN
jg13126.t1	215	No	No	No	No	N/A	Not a CRN
jg2719.t1	130	No	No	No	Yes[1]	N/A	Not a CRN
jg2083.t1	163	No	No	No	No	N/A	Not a CRN
jg14293.t1	600	Yes	No	Yes[1]	No	N/A	Not a CRN
jg6645.t1*	238	No	No	No	No	N/A	Not a CRN
jg6890.t1*	1080	No	No	No	Yes[1]	N/A	Not a CRN
jg17778.t1*	439	Yes	Yes	No	Yes[1]	N/A	Not a CRN
jg19385.t1*	280	No	No	No	No	N/A	Not a CRN
jg19378.t1*	442	No	No	No	No	N/A	Not a CRN
jg19379.t1*	244	Yes	Yes	No	No	N/A	Not a CRN
jg19379.t2*	484	No	No	No	No	N/A	Not a CRN
jg9617.t1*	172	No	No	No	No	N/A	Not a CRN
jg9617.t2*	105	No	No	No	No	N/A	Not a CRN
jg9315.t1*	334	No	Yes	No	No	N/A	Not a CRN
jg10796.t1*	122	No	No	No	No	N/A	Not a CRN
jg13186.t1*	290	No	No	No	No	N/A	Not a CRN
jg6983.t1*	295	No	No	No	Yes[1]	N/A	Not a CRN
jg2628.t1*	424	No	No	No	No	N/A	Not a CRN

* Sequences identified via BLAST2GO method (26); 1 The motif differs by a single amino acid; 2 The sequence was manually annotated in GenomeView2250.

Supplementary Table 3A: Table summarizing the Phytophthora cinnamomi crinkling and necrosis (PcinCRN) effector architecture of all PcinCRNs generated in the current study and in previous studies conducted by (Hardham and Blackman. 2018) and (Engelbrecht et al. 2021). A PcinCRN was validated as a 'true' *Phytophthora* CRN if the sequence contains both the LXLFLAK and HVLVXXP motifs and did not contain a trans membrane helix (TMH). A CRN was classified as a partial/CRN-like sequence if it has all characteristic CRN motifs but is truncated. The presence/absence of a signal peptide, TMH, low complexity regions (LCR's), LXLFLAK and HVLVXXP motif are indicated.

Sequence	Signal peptide	TMH	LXLFLAK motif	HVLVXXP motif	Classification	Reference
PcinCRN79	Yes	No	Yes	Yes	Full length CRN	Current study and (Engelbrecht et al. 2021)
PcinCRN50	Yes	No	Yes[1]	Yes	Full length CRN	Current study and (Engelbrecht et al. 2021)
PcinCRN51	NO	No	Yes[1]	Yes	Full length CRN	Current study and (Engelbrecht et al. 2021)
PcinCRN77	Yes	No	Yes	Yes[1]	Full length CRN	Current study and (Engelbrecht et al. 2021)
PcinCRN73	Yes	No	Yes	Yes[1]	Full length CRN	Current study and (Engelbrecht et al. 2021)
PcinCRN75	Yes	No	Yes	Yes	Full length CRN	Current study and (Engelbrecht et al. 2021)
PcinCRN87	Yes	No	Yes	Yes	Full length CRN	Current study and (Engelbrecht et al. 2021)
PcinCRN53	NO	No	Yes	Yes	Full length CRN	Current study and (Engelbrecht et al. 2021)
PcinCRN11	Yes	No	Yes[1]	Yes	Full length CRN	Current study and (Engelbrecht et al. 2021)
PcinCRN30	Yes	No	Yes	Yes	Full length CRN	Current study and (Engelbrecht et al. 2021)
PcinCRN52	NO	No	Yes	Yes	Full length CRN	Current study and (Engelbrecht et al. 2021)
jg9952.t2	No	Yes	Yes	Yes	Not a CRN	Current study and (Engelbrecht et al. 2021)
PcinCRN95	NO	No	Yes	Yes	Full length CRN	Current study and (Engelbrecht et al. 2021)
PcinCRN25	Yes	No	Yes[1]	Yes	Full length CRN	Current study and (Engelbrecht et al. 2021)
PcinCRN90	Yes	No	Yes	Yes[2]	Full length CRN	Current study and (Engelbrecht et al. 2021)
PcinCRN35	Yes	No	Yes[1]	Yes[1]	Full length CRN	Current study and (Engelbrecht et al. 2021)
PcinCRN56	NO	No	Yes	Yes[2]	Full length CRN	Current study and (Engelbrecht et al. 2021)

jg4983.t1	No	No	Yes	No	Not a CRN	Current study and (Engelbrecht et al. 2021)
PcinCRN57	No	No	Yes[1]	Yes[1]	Full length CRN	Current study and (Engelbrecht et al. 2021)
PcinCRNpartial1	No	No	Yes	Yes	Partial/CRN-like	Current study
PcinCRN29	Yes	No	Yes[1]	Yes[2]	Full length CRN	Current study and (Engelbrecht et al. 2021)
PcinCRN33	NO	No	Yes	Yes[1]	Full length CRN	Current study and (Engelbrecht et al. 2021)
jg14422.t1	No	No	Yes[1]	No	Not a CRN	Current study and (Engelbrecht et al. 2021)
PcinCRN31	Yes	No	Yes	Yes[2]	Full length CRN	Current study and (Engelbrecht et al. 2021)
PcinCRN81	Yes	No	Yes	Yes[2]	Full length CRN	Current study and (Engelbrecht et al. 2021)
jg8505.t1	No	Yes	Yes[1]	Yes	Not a CRN	Current study
PcinCRN47	NO	No	Yes	Yes[1]	Full length CRN	Current study
PcinCRN83	Yes	No	Yes	Yes[2]	Full length CRN	Current study and (Engelbrecht et al. 2021)
PcinCRN74	NO	No	Yes	Yes	Full length CRN	Current study and (Engelbrecht et al. 2021)
jg14560.t1	No	No	No	Yes[1]	Not a CRN	Current study
jg7432.t2	No	No	No	No	Not a CRN	Current study
jg7432.t1	No	No	No	No	Not a CRN	Current study
PcinCRN86	Yes	No	Yes[1]	Yes[1]	Full length CRN	Current study and (Engelbrecht et al. 2021)
jg8953.t1	Yes	No	No	No	Not a CRN	Current study and (Engelbrecht et al. 2021)
jg16316.t1	No	No	No	Yes	Not a CRN	Current study and (Engelbrecht et al. 2021)
jg5203.t1	No	No	No	No	Not a CRN	Current study and (Engelbrecht et al. 2021)
jg17230.t1	No	No	No	No	Not a CRN	Current study and (Engelbrecht et al. 2021)
jg14294.t1	No	No	Yes[1]	No	Not a CRN	Current study
jg13126.t1	No	No	No	No	Not a CRN	Current study and (Engelbrecht et al. 2021)
jg2719.t1	No	No	No	Yes[1]	Not a CRN	Current study and (Engelbrecht et al. 2021)
jg2083.t1	No	No	No	No	Not a CRN	Current study and (Engelbrecht et al. 2021)
jg14293.t1	Yes	No	Yes[1]	No	Not a CRN	Current study and (Engelbrecht et al. 2021)

jg6645.t1	No	No	No	No	Not a CRN	(Engelbrecht *et al.* 2021)
jg6890.t1	No	No	No	Yes[1]	Not a CRN	(Engelbrecht *et al.* 2021)
jg17778.t1	Yes	Yes	No	Yes[1]	Not a CRN	(Engelbrecht *et al.* 2021)
jg19385.t1	No	No	No	No	Not a CRN	(Engelbrecht *et al.* 2021)
jg19378.t1	No	No	No	No	Not a CRN	(Engelbrecht *et al.* 2021)
jg19379.t1	Yes	Yes	No	No	Not a CRN	(Engelbrecht *et al.* 2021)
jg19379.t2	No	No	No	No	Not a CRN	(Engelbrecht *et al.* 2021)
jg9617.t1	No	No	No	No	Truncated	(Engelbrecht *et al.* 2021)
jg9617.t2	No	No	No	No	Truncated	(Engelbrecht *et al.* 2021)
jg9315.t1	No	Yes	No	No	Not a CRN	(Engelbrecht *et al.* 2021)
jg10796.t1	No	No	No	No	Not a CRN	(Engelbrecht *et al.* 2021)
jg13186.t1	No	No	No	No	Not a CRN	(Engelbrecht *et al.* 2021)
jg6983.t1	No	No	No	Yes[1]	Not a CRN	(Engelbrecht *et al.* 2021)
jg2628.t1	No	No	No	No	Not a CRN	(Engelbrecht *et al.* 2021)
PHYCI_99711	Yes	No	Yes	Yes	Full length CRN	(Hardham and Blackman. 2018)
PHYCI_98916	Yes	No	Yes	Yes	Full length CRN	(Hardham and Blackman. 2018)
PHYCI_93895	Yes	No	Yes	Yes	Full length CRN	(Hardham and Blackman. 2018)
PHYCI_82897	Yes	Yes	No	No	Not a CRN	(Hardham and Blackman. 2018)
PHYCI_75608	Yes	No	Yes	No	Not a CRN	(Hardham and Blackman. 2018)
PHYCI_68121	Yes	No	Yes	No	Not a CRN	(Hardham and Blackman. 2018)
PHYCI_557374	Yes	No	No	Yes	Not a CRN	(Hardham and Blackman. 2018)
PHYCI_251494	Yes	No	Yes	No	Not a CRN	(Hardham and Blackman. 2018)
PHYCI_213501	Yes	No	No	No	Not a CRN	(Hardham and Blackman. 2018)
PHYCI_148758	Yes	No	No	No	Not a CRN	(Hardham and Blackman. 2018)
PHYCI_115716	Yes	No	Yes	Yes	Full length CRN	(Hardham and Blackman. 2018)
PHYCI_141767	Yes	No	Yes	Yes	Full length CRN	(Hardham and Blackman. 2018)
PHYCI_105597	Yes	No	Yes	Yes	Full length CRN	(Hardham and Blackman. 2018)
PHYCI_111648	Yes	No	Yes	Yes	Full length CRN	(Hardham and Blackman. 2018)
PHYCI_64923	No	No	No	No	Not a CRN	(Hardham and Blackman. 2018)
PHYCI_62387	No	Yes	No	No	Not a CRN	(Hardham and Blackman. 2018)
PHYCI_68122	No	No	Yes	Yes[1]	Full length CRN	(Hardham and Blackman. 2018)
PHYCI_79900	No	No	Yes	No	Not a CRN	(Hardham and Blackman. 2018)

PHYCI_90916	No	No	Yes	Yes	Full length CRN	(Hardham and Blackman. 2018)
PHYCI_88963	No	Yes	Yes	Yes	Not a CRN	(Hardham and Blackman. 2018)
PHYCI_229518	No	Yes	Yes	No	Not a CRN	(Hardham and Blackman. 2018)
PHYCI_227703	No	Yes	No	No	Not a CRN	(Hardham and Blackman. 2018)
PHYCI_173318	No	No	No	No	Truncated	(Hardham and Blackman. 2018)
PHYCI_136542	No	No	Yes	No	Truncated	(Hardham and Blackman. 2018)
PHYCI_116790	No	No	No	No	Not a CRN	(Hardham and Blackman. 2018)
PHYCI_196376	No	No	Yes	No	Truncated	(Hardham and Blackman. 2018)
PHYCI_189960	No	No	No	No	Truncated	(Hardham and Blackman. 2018)
PHYCI_169888	No	No	No	No	Truncated	(Hardham and Blackman. 2018)
PHYCI_167517	No	No	Yes	Yes	Partial/CRN-like	(Hardham and Blackman. 2018)
PHYCI_124970	No	No	Yes	No	Truncated	(Hardham and Blackman. 2018)
PHYCI_87750	No	No	Yes	Yes	Partial/CRN-like	(Hardham and Blackman. 2018)
PHYCI_63173	No	No	No	Yes	Not a CRN	(Hardham and Blackman. 2018)
PHYCI_211579	No	No	No	No	Not a CRN	(Hardham and Blackman. 2018)
PHYCI_497768	No	No	No	No	Not a CRN	(Hardham and Blackman. 2018)
PHYCI_261700	No	No	Yes	No	Not a CRN	(Hardham and Blackman. 2018)
PHYCI_251677	No	No	No	No	Not a CRN	(Hardham and Blackman. 2018)
PHYCI_93350	No	No	No	Yes	Not a CRN	(Hardham and Blackman. 2018)
PHYCI_94491	No	No	Yes	No	Not a CRN	(Hardham and Blackman. 2018)
PHYCI_145054	No	No	Yes	Yes	Full length CRN	(Hardham and Blackman. 2018)
PHYCI_142491	No	No	Yes	No	Not a CRN	(Hardham and Blackman. 2018)
PHYCI_112955	No	No	No	No	Not a CRN	(Hardham and Blackman. 2018)
PHYCI_111548	No	No	No	No	Not a CRN	(Hardham and Blackman. 2018)

Supplementary Table 3B: Table summarizing the *Phytophthora cinnamomi* crinkling and necrosis (PcinCRN) effector results generated in the current study and in previous studies conducted by (Hardham and Blackman. 2018) and (Engelbrecht et al. 2021). The number of putative PcinCRNs identified before exclusion criteria are indicated, followed by the number of validated as a 'true' *Phytophthora* CRN if the sequence contains both the LXLFLAK and HVLVXXP motifs and did not contain a trans membrane helix (TMH). A CRN was classified as a partial/CRN-like sequence if it has all characteristic CRN motifs but is truncated.

	Putative CRN sequences identified	**Validated full-length CRNs**	**Validated partial CRNs or CRN-like**
pBLAST (Hardham and Blackman. 2018)	49	10	2
BLAST2GO (Engelbrecht, *et al.* 2021)	49	24	0
HMMer (Current research)	46	25	1